Structure-Activity Relationship Studies of 2-Phenylbenzimidazoles and Related Organometallic Complexes as Antiplasmodial Agents

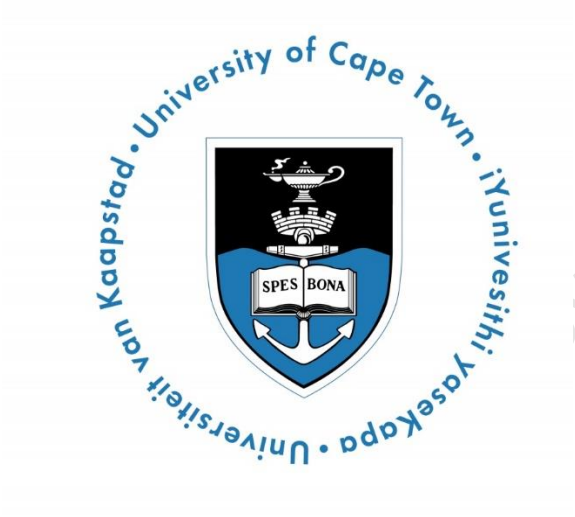

Laa-iqa Rylands

Department of Chemistry

University of Cape Town

December 2017

Structure-Activity Relationship Studies of 2-Phenylbenzimidazoles and Related Organometallic Complexes as Antiplasmodial Agents

A dissertation submitted to the University of Cape Town in fulfilment of the requirements for the degree of

Master of Science

by

Laa-iqa Rylands

Supervisor: Assoc. Prof. Gregory S. Smith

Co-supervisor: Prof. Kelly Chibale

Department of Chemistry

University of Cape Town

Rondebosch, 7701

Cape Town

South Africa

December 2017

Declaration

I know the meaning of plagiarism and declare that "***Structure-activity relationship studies of 2-phenylbenzimidazole ligands and related organometallic complexes as antiplasmodial agents"*** is my original work and to the best of my knowledge has not been presented for the award of any degree at any university. I declare that all of the work in this document, except for that which is properly acknowledged, is my own.

SIGNATURE: Signed by candidate

DATE: December 2017

Acknowledgements

I would not have been able to complete this thesis without the help of the following people:

First and foremost, I would like to thank my supervisors, Assoc. Prof. Gregory S. Smith and Prof. Kelly Chibale. I thank Assoc. Prof. Gregory S. Smith for all his support, guidance, encouragement and patience throughout the course of this project. I also thank Prof. Kelly Chibale for his advice and encouragement.

A special thanks to the Organometallic Research Group (Cody, Diteboho, Dylan, Nadia, Nikechukwu, Shepherd and Tameryn), for all the support, laughter and fun chats in and out of the lab. I would especially like to thank Dr Tameryn Stringer for the useful discussion and advise, it is truly appreciated. I would also like to thank Dr Shankari Nair, Dr Muneebah Adams and Marwaan Rylands.

I would like to acknowledge the following people for their assistance and analytical expertise: Pete Roberts (NMR, UCT), Gianpiero Binincasa (Elemental Analysis, UCT), Charney Anderson (Elemental Analysis, University of Stellenbosch), Dr Marietjie Stander (Mass spectrometry, University of Stellenbosch), Dr Hong Su (X-ray crystallography analysis, UCT), Dr Malkeet Kumar and Dr Preshendren Govender for help with LC-MS. Sincere thanks to Nina Lawrence (Clinical Pharmacology, H3D) for the solubility tests; Dr Dale Taylor (Clinical Pharmacology, UCT) and Dr Tameryn Stringer for screening the synthesised compounds for antiplasmodial activity and for performing the cytotoxicity studies as well as for taking the time to perform the β-haematin assays.

I would like to sincerely thank the Harry Crossley Research Foundation and the National Research Foundation (NRF) for their financial support. I am truly grateful.

Finally, thanks to all my family and friends who have supported and encouraged me throughout my studies. I thank my husband, Marwaan for his love, support and encouragement, always.

Thank you all!

Conference Contributions

June 2017 – Poster Presentation:

Structure-Activity Studies of 2-Phenylbenzimidazole based Organometallic Complexes as Antiplasmodial Agents, presented at the Inorganic Chemistry Conference 2017 & Carman Physical Chemistry Symposium of the South African Chemical Institute Western Cape, 25 – 29 June 2017, Kleinmond, South Africa.

August 2017 – Poster Presentation:

Structure-Activity Studies of 2-Phenylbenzimidazole based Organometallic Complexes as Antiplasmodial Agents, presented at the 10th annual UCT Postgraduate Student Council (PGSC) Symposium, titled "Science through an African lens", 7 – 8 August 2017, Cape Town, South Africa.

August 2017 – Poster Presentation:

Structure-Activity Studies of 2-Phenylbenzimidazoles and related Organometallic Complexes as Antiplasmodial Agents, presented at the International Conference for Young Chemists (ICYC 2017), 16 – 19 August 2017, Georgetown, Penang, Malaysia.

Abstract

Malaria remains a huge public health concern, affecting millions of people from all around the world. The widespread resistance by *Plasmodium* parasites to previously effective quinoline-based drugs and the emerging resistance to current antimalarial therapies, stresses the urgent need for the exploration and development of diverse new classes of compounds. Amongst other requirements, these diverse new compound classes should target resistant strains in particular. In this regard, benzimidazoles have been identified as promising potential drug candidates, displaying potent antiplasmodial activity. Furthermore, benzimidazoles can be chemically transformed into metal-containing organometallic complexes that elevate generally flat benzimidazoles to the third dimension. To date, examples of metal-containing benzimidazoles are extremely limited, with only two reported as having antiplasmodial activity. Thus, we report the syntheses of a series of substituted 2-phenylbenzimidazole ligands, from the cyclo-condensation of *o*-phenylenediamines and benzaldehyde, as well as the synthesis of Ru(II) and Ir(III) cyclometallated benzimidazole complexes. All of the compounds synthesised were fully characterised by ^{1}H and $^{13}C\{^{1}H\}$ Nuclear Magnetic Resonance (NMR) Spectroscopy, Elemental Analysis and Mass Spectrometry.

The synthesised 2-phenylbenzimidazoles and metal complexes were screened *in vitro* against the chloroquine-sensitive NF54 strain and selected complexes were screened against the chloroquine-resistant K1 strain of *P. falciparum*. In addition, selected compounds were also tested against the Chinese Hamster Ovarian (CHO) mammalian cell-line to evaluate their selectivity.

The 2-phenylbenzimidazoles generally displayed weak to moderate antiplasmodial activity against the chloroquine-sensitive NF54 strain, where IC_{50} values ranged from 3.27 – 32.97 µM. Furthermore, it was demonstrated that the antiplasmodial activities of the 2-phenylbenzimidazoles increased significantly upon metal complexation, using Ru and Ir metals. In general, the antiplasmodial activity of the Ru(II) complexes were significantly better compared to the Ir(III) complexes. The cyclometallated benzimidazole complexes were much more active across both parasite strains ($0.12 < IC_{50} < 4.31$), compared to the corresponding ligands tested. The unsubstituted Ru(II) and Ir(III) cyclometallated benzimidazole complexes were found to possess the most potent antiplasmodial activity against the NF54 strain,

displaying IC_{50} values of 0.12 and 0.19 μM, respectively. In most cases, the resistance indices obtained for the select compounds tested were significantly lower compared to chloroquine, which suggested that the compounds are not cross-resistant with chloroquine. Furthermore, cytotoxicity studies indicated that the synthesised compounds had low cytotoxicity and were selective towards the malaria parasites. Additional studies which involved testing the aqueous solubility of selected compounds in PBS buffer at pH 6.5 showed that the introduction of water-solubilising groups improved the compounds solubility significantly. Preliminary mechanistic studies suggested that the synthesised benzimidazoles may have a different mode of action to chloroquine as the compounds did not inhibit β-haematin formation at the maximum concentration of 500 μM.

Abbreviations

ACT	Artemisinin-based combination therapy
Ar	Aromatic
bs	Broad singlet (NMR)
$CDCl_3$	Deuterated chloroform
CHO	Chinese Hamster Ovarian
Cp*	1,2,3,4,5-Pentamethylcylopentadienyl
CQ	Chloroquine
CQR	Chloroquine-resistant
CQS	Chloroquine-sensitive
d	Doublet (NMR)
dd	Doublet of doublets
DCM	Dichloromethane
DMF	Dimethylformamide
EA	Elemental analysis
EI	Electron impact
ESI	Electronspray ionisation
EtOAc	Ethyl acetate
EtOH	Ethanol
Eq.	Equivalent(s)
EWG	Electron withdrawing group
h	Hour(s)
HSQC	Heteronuclear single quantum coherence
Hz	Hertz
IC_{50}	50% Inhibition concentration
IR	Infrared
J	Coupling constant
m	Multiplet (NMR); Medium intensity (IR)
Me	Methyl
MeOH	Methanol
$MgSO_4$	Magnesium sulfate

min	Minute(s)
Mp	Melting point
MS	Mass spectrometry
m/z	Mass to charge ratio (MS)
nd	Not determined
NMR	Nuclear magnetic resonance
NP-40	Nonyl phenoxypolyethoxyethanol
Pet. ether	Petroleum ether
PT	Proton transfer
ppm	Parts per million
q	Quartet (NMR)
R_f	Retention factor
RI	Resistance Index
ROS	Reactive oxygen species
rt	Room temperature
s	Singlet (NMR); Strong intensity (IR)
SD	Standard deviation
SE	Standard error
SI	Selectivity index
S_NAr	Nucleophilic Aromatic substitution
t	Triplet (NMR)
TFA	Trifluoroacetic acid
TLC	Thin layer chromatography
TMS	Tetramethylsilane
t_R	Retention time

Contents

Chapter 1: Introduction

1.1 Malaria

1.1.1 History and Prevalence

Malaria is a mosquito-borne infectious disease caused by parasitic protozoa of the genus *Plasmodium*. Five different *Plasmodium* species have been identified to infect humans, namely; *Plasmodium falciparum* (*P. falciparum)*, *P. vivax, P. ovale*, *P. malariae* and *P. knowlesi*.[1, 2] The most severe and fatal of the five species is *P. falciparum*, which constitutes close to 90% of all reported malaria cases. Malaria remains infamous as one of the top three killers among communicable diseases. It is largely prevalent in the tropical areas of sub-Saharan Africa, Southeast Asia and Latin America (Figure 1.1), where conditions are ideal for mosquitos to survive and multiply.[3, 4]

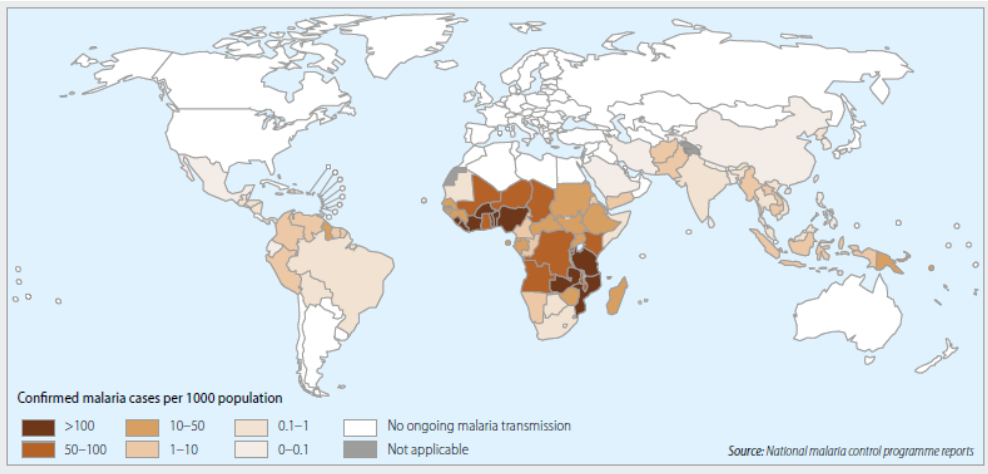

Figure 1.1: Global distribution of malaria cases.[3]

In 2016, the World Health Organisation (WHO) estimated 216 million cases of malaria; and a resultant 445 000 deaths of which are mostly pregnant women and children under the age of five.[5] Despite the general decrease, in mortality and morbidity rates associated with malaria (in recent years), malaria continues to negatively impact developing countries both socially and economically.[5, 6]

The term malaria was first derived from the Italian term *mala'aria* which translates to bad air, due to its early association with swamps and marshes. Throughout recorded history it has been one of the major health problems faced by humanity, in fact reference to this disease dates as far back as 2700 BC in China, as well as Greece and ancient Egypt.[7] Despite early

documentation on malaria, scientists only began to understand this disease towards the end of the 19th century. The discovery that the cause of malaria is a protozoan was first made in 1880 by Nobel Prize winner, Charles Louis Alphonse Laveran.[8] Later, in 1897, Ronald Ross, a British officer in the Indian Medical Service, discovered that transmission of malaria was caused by mosquitos. The complete parasite life cycle was also established by Ronald Ross, who later in 1902 was also awarded a Nobel Prize.[9, 10]

1.1.2 Biology of the disease

The severity associated with malaria is a result of the complex molecular and cellular events that take place during the parasite's life cycle (Figure 1.2). It is necessary to look at the life cycle of the parasite in order to understand some of the current antimalarial chemotherapies. The parasite's life cycle is dependent on two hosts: a vector host and human host for sexual reproduction and asexual reproduction, respectively, which are essential for the parasite to survive and propagate.[11]

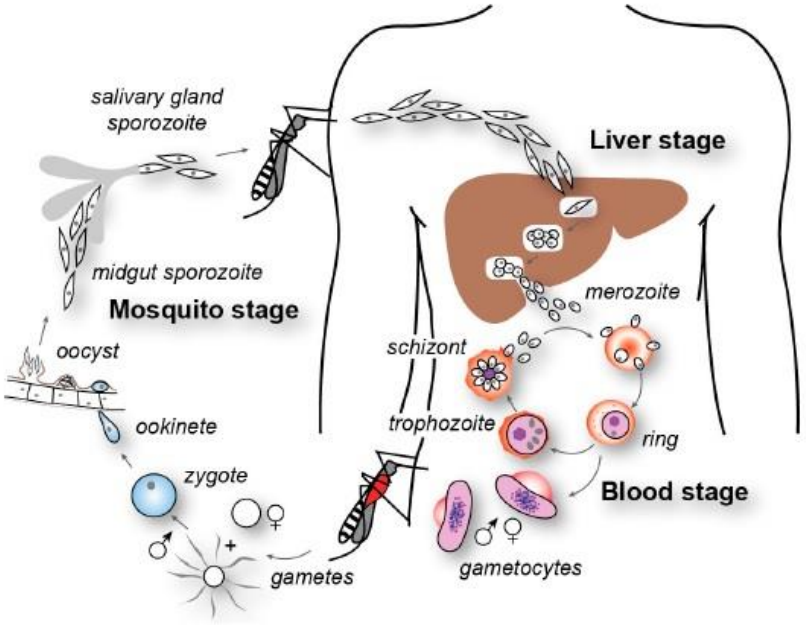

Figure 1.2: Life cycle of the malaria parasite.[12]

Unicellular parasites called sporozoites are found in the salivary glands of an infected female *Anopheles* mosquito. When a human is bitten by an infected mosquito, saliva containing these sporozoites are injected into the bloodstream of the human host. The exo-erythrocytic stage is initiated when the sporozoites enter the host's liver and invade hepatocytes. At this stage,

the parasite may either stay dormant as hypnozoites causing relapses weeks or months later particularly in malaria caused by *P. vivax*; or they may multiply and mature into schizonts. Mature schizonts eventually rupture, releasing tens of thousands of merozoites per liver cell, back into the host's bloodstream. The intra-erythrocytic stage begins once the merozoites invade the red blood cells and develop into ring forms and trophozoites, which later mature into schizonts. The red blood cells then rupture, resulting in merozoites and toxins being released into the bloodstream. At this point, clinical symptoms of malaria such as fever, headache, chills, diarrhoea and anaemia transpire. The merozoites released may then invade more red blood cells or a small portion may develop into male and female gametocytes. Further transmission of the parasite results when the infected host is bitten by an uninfected female *Anopheles* mosquito. Sexual reproduction occurs within the mosquito when the male and female gametocytes fuse and develop into ookinetes which then migrate into the midgut of the mosquito. In the external midgut, formation and maturation of oocysts occur. Rupturing of these mature oocysts results in the release of thousands of sporozoites, which migrate to the mosquito's salivary glands, recommencing the cycle.[11, 13]

1.1.3 Prevention and Treatment

Owing to the complex nature of the multiple stages of the parasite's lifecycle, the implementation of several preventative and chemotherapeutic strategies is required in order to control and eliminate malaria.

Since there is no effective vaccination available, a first-line approach is to reduce the number of infectious mosquitos by vector control. Vector control may be achieved through the use of insecticide-treated nets (ITNs) or indoor residual spraying (IRS).[14] The WHO recently reported a decrease in the number of malaria cases between 2001 and 2015, is largely a result of malaria control interventions such as ITNs and IRS.[15] This strategy, however, has been hampered due to the widespread development of resistance to insecticides by the malaria parasite.[5]

Chemotherapy has historically played a key role in controlling and treating malaria. Over many years, several families of antimalarial drugs, which aim to target the lifecycle and multiple mechanisms of survival of the parasite, have been developed.[11, 16] Since the exo-

erythrocytic/liver stage is the first site where replication of the parasite occurs, it is an ideal stage for drugs to target. However, during the exo-erythrocytic stage, no malaria-like symptoms are evident. Consequently, treatment during this stage is understandably challenging, as patients are often unaware that they are infected. The intra-erythrocytic/blood stage of the lifecycle, where symptoms are evident, is therefore the main target site of many antimalarial drugs. A general strategy in the development of antimalarial drugs involves the identification of important biological pathways that are either specific to the parasite or that have sufficient differences from the host. Major organelles involved in parasite growth and survival include: the parasite food vacuole, apicoplast and mitochondrion, all of which are considered to be prime targets for potential antimalarial drugs.[11] The design and synthesis of an antimalarial drug which targets all stages of the parasite's life cycle is in fact key for the elimination and eradication of this disease.

It is for this reason that an international consortium sequenced the complete genome of *P. falciparum*.[17] Subsequent proteomic studies based on the sequenced genome are now providing researchers with new potential drug and vaccine targets and also providing a better understanding of the parasites sophisticated molecular and cellular biology as well as its biochemistry.[18, 19] The field of proteomics has also proved to be valuable with respect to investigations into the mechanism(s) of action of current and new antiplasmodial drugs.[20, 21]

1.1.4 Quinoline and non-quinoline based antimalarial drugs

Over many years, significant strides have been made regarding the development of antimalarial drugs, which are currently being used. Despite current trends in drug discovery, most of the currently used antimalarial drugs were in fact developed from natural products. Examples of such compounds include, but are not limited to, quinine and artemisinin.

Quinine, a major alkaloid of the *Cinchona* plant and initially used by natives in South America to reduce fever, was first isolated in 1820.[22] Later, through systematic modification of quinine, an array of quinoline antimalarial drugs with diverse substitutions around the quinoline ring were discovered. Chloroquine, a synthetic 4-aminoquinoline, was first chemically synthesised in 1934 and quickly became the drug of choice for treating malaria.[23] The success of

chloroquine was due to it being cheap, very effective, and of relatively low toxicity.[11, 24, 25] In most parts of the world however, chloroquine and some of its derivatives shown in Figure 1.3, have now become virtually ineffective due to the increase in resistant parasites.[25]

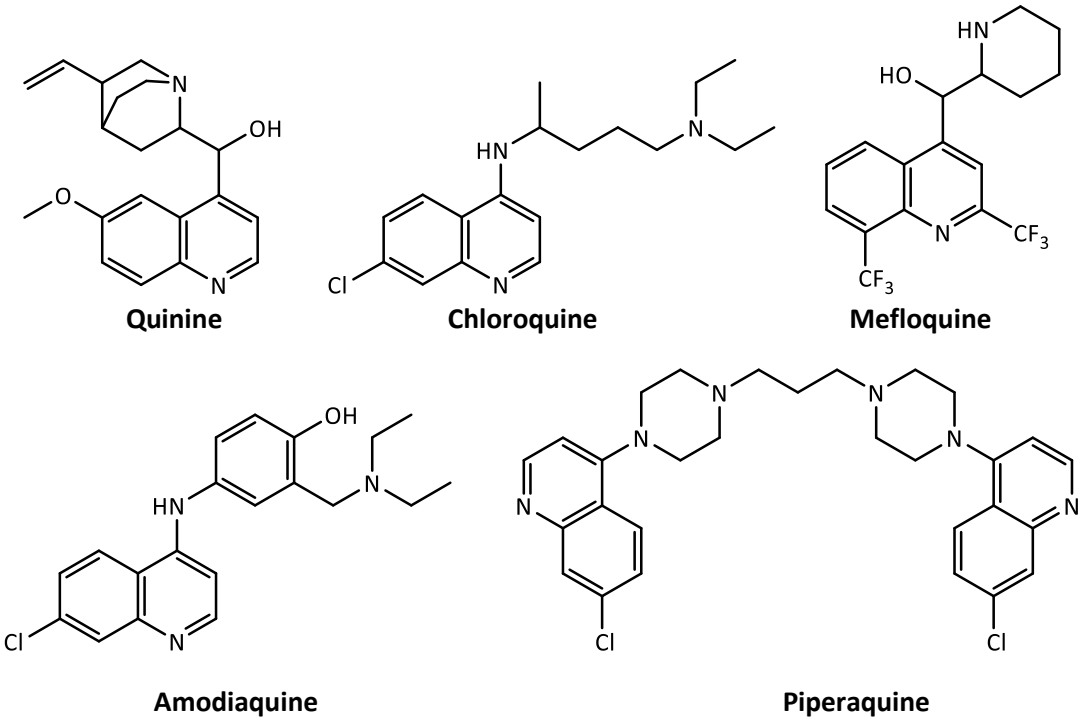

Figure 1.3: Selected quinoline-based antimalarial drugs

By understanding the mechanism of drug action and the process associated with resistance, it becomes possible to unveil biological details that will lead to circumvention of drug resistance. The mechanism of action of quinoline-based antimalarial drugs has been well documented.[23, 26] There is a general consensus that chloroquine along with, quinine, amodiaquine and mefloquine, inhibit haemozoin formation, a detoxification process specific to the parasite which occurs during the intra-erythrocytic stage of the parasites lifecycle.[27] Haemozoin is an insoluble material produced by the parasite. It has been reported that the survival of the parasite is dependent on its ability to form haemozoin. Formation of haemozoin prevents oxygen radical-mediated damage to the parasite. Thus, an attractive approach in drug development is to inhibit haemozoin formation or its synthetic counter-part, β-haematin. The quinoline methanols (quinine), 4-aminoquinolines (chloroquine, amodiaquine, and piperaquine) and the aryl alcohols (mefloquine) all form part of a group of drugs which are able to prevent the conversion of haematin (ferriprotoporphyrin IX) to haemozoin, which is achieved by these drugs forming complexes with haem through π-π

stacking of their planar aromatic groups.[28] It is widely accepted that the site of action of chloroquine is within the acidic food vacuole of the malaria parasite, where haemoglobin is actively degraded by the parasite.[29] Chloroquine diffuses across the vacuolar membrane against a pH-gradient, as a neutral species. However, once inside the food vacuole, protonation of the nitrogen atoms occur, preventing the resultant species from crossing the membrane again. This then leads to the accumulation of chloroquine within the food vacuole. The accumulated chloroquine may then form a complex with haematin *via* π-π stacking with the porphyrin ring system, resulting in further accumulation of the drug.[30] The accumulation of toxic haematin and chloroquine-haematin adducts inevitably leads to parasite death and erythrocyte lysis, due to the inhibition of haemozoin formation and key enzymes.[30]

Artemisinin, a sesquiterpene lactone containing an endoperoxide bridge, was first isolated in 1970 from the Chinese plant, *Artemisia annua*. In 1983, the first complete chemical synthesis of artemisinin was reported.[31] However, it was thought to be too expensive for commercial pharmaceutical production. Semi-synthetic artemisinin derivatives, artemether, artesunate and dihydroartemisinin were developed soon after the discovery of artemisinin. Artemisinin-based drugs have been reported to be active against the asexual (exo-erythrocytic and intra-erythrocytic) stages inside the host and the sexual stage (targeting gametocytes).[31]

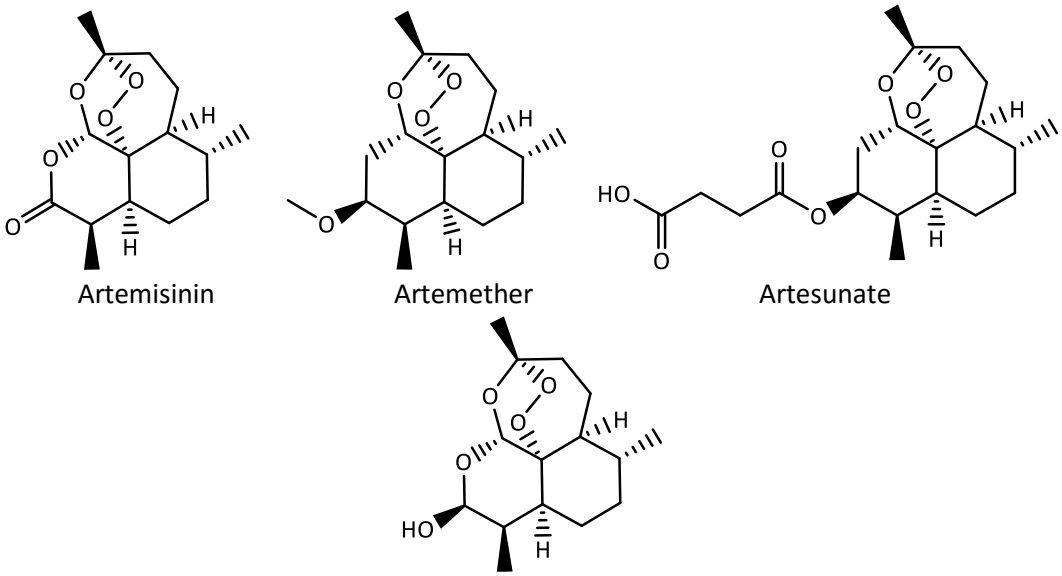

Figure 1.4: Artemisinin and derivatives

The site and mechanism of action of artemisinins remain unclear. However, structure-activity relationship (SAR) studies recently revealed that the presence of the endoperoxide bridge is

essential for antimalarial activity.[31] It is reported that the endoperoxide bridge generates oxidative stress.[31, 32] Oxidative stress is induced by reactive oxygen species (ROS). The generation of oxidative stress can trigger programmed cell death as a result of ROS causing irreparable damage to cell structures such as DNA, lipids and proteins. It has been reported that the *Plasmodium* parasite possesses internal defence mechanisms against ROS.[33] However, cell damage may occur if a given drug is able to sufficiently increase cellular oxidative potential, resulting in the parasites internal defence mechanisms being incapacitated.[33] Artemisinin-based drugs may therefore act by impairing parasite redox homeostasis. There are many other proposed ACT drug targets, some of which include a *Pf*ATP6 enzyme, the *P. falciparum* ortholog of mammalian sarcoendoplasmic reticulum Ca^{21}-ATPases (SERCAs), translational controlled tumor protein, and haem.[21, 34]

Although artemisinin-based drugs are known to act faster than any other currently available antimalarial, the fact that artemisinins have a short half-life is of concern as there is increased risk of recrudescence or resistance. Thus, the current recommended treatment for malaria is artemisinin-based combination therapy (ACTs), which involves the use of a combination of artemisinin derivatives with other antimalarial drugs, possessing a longer half-life. The most frequently used ACTs are: artemether-lumefantrine, artesunate-amodiaquine, artesunate-mefloquine and dihydroartemisin-piperaquine.[32]

1.1.5 Challenges in treating malaria

The rise in resistance against current antimalarial drugs is of notable concern. Over the last 60 years, the parasite has managed to develop resistance to antimalarial drugs at a pace that exceeds the rate at which new antimalarial drugs were and are being developed. By definition, drug resistance occurs when the parasite is able to survive, and even multiply, despite the administration of a drug in doses, which are equal to or higher than the usual recommended dose, but are within the limits of tolerance of the subject.[35] Resistance occurs generally through spontaneous mutations. In some cases, resistance may occur due to a single mutation, whereas in other cases, multiple mutations are required to lead to drug resistance.

In recent years, our understanding of molecular mechanisms associated with drug resistance in *P. falciparum* has advanced substantially. For instance, polymorphisms in a gene called the *P. falciparum* chloroquine resistant transporter gene (*pf*crt), was discovered to cause reduced

susceptibility to quinoline and quinoline-like antimalarial drugs.[36] *Pf*crt is localised at the membrane of the parasite's acidic food vacuole and when this gene undergoes a key mutational change, key interactions with protonated quinoline antimalarials, that ensures their concentration in the food vacuole is maintained, are lost. This results in the drugs leaking out of the parasites digestive vacuole, thus rendering these drugs virtually ineffective.[37, 38]

Resistance of *P. falciparum* to chloroquine has been reported as a gradual process. The emergence of chloroquine resistance was first reported in 1957, at the Thai-Cambodian border.[39] Later, in 1960, chloroquine-resistant strains were reported in Venezuela and Colombia and in 1976 in Papua New Guinea. Finally, in 1978, chloroquine resistance emerged in Africa and by 1983 cases of chloroquine resistance was reported in Sudan, Uganda, Zambia and Malawi.[35] Resistance to mefloquine (including other chloroquine derivatives) and alternative drugs introduced to treat chloroquine resistant strains, developed in some cases relatively rapidly over recent years. Decreased sensitivity of *P. falciparum* to artemisinins were recently reported in Southeast Asia, causing great alarm as ACTs are currently the most effective antimalarial treatment.[34, 35] These reports of decreased efficacy and the known emergence of resistance to current drugs drive the need to develop new antimalarials which are effective against resistant strains.

A possible solution to overcoming drug resistance may be to explore pharmacophores such as benzimidazoles for instance, which are structurally different to that of antimalarials currently in use.

New drugs, however, are not so simple to develop. A general challenge often faced when a lead compound has been developed is that it rarely passes Phase I clinical trials, due to poor physicochemical/pharmacokinetic properties. It is therefore necessary that physicochemical properties be optimised as early as possible in the drug design and development process.

A promising drug candidate should have a good ADMET profile, in order for it to be an efficient and effective drug. ADMET is an abbreviation for absorption, distribution, metabolism, excretion and toxicity. Solubility is often the first step in drug absorption processes. In fact, this physicochemical parameter is often linked to metabolism and bioavailability.[40] There has been numerous reports of potential drug candidates having failed drug development phases due to poor solubility. Recent applications of combinatorial chemistry and high-throughput

screening (HTS) systems has led to a change in the profile of many compound libraries. These compound libraries include compounds of higher hydrophobicity and higher molecular weights, resulting in a profile of lower solubility. Thus, improving the aqueous solubility of a compound continues to be a major and common issue in medicinal chemistry.[41]

There are many strategies which can be employed in order to improve solubility. A classical approach is to introduce water solubilising groups into a molecule, such as, sulfones, sulfoxides, hydroxyls, tetrazoles or trifluoromethanes. Le Manach and co-workers recently reported several strategies which could improve aqueous solubility;[42] replacement of phenyl rings with pyridyl rings was aimed at reducing lipophilicity and introduction of water-solubilising H-bonding groups such as hydroxyl containing amides and piperazine sulfones resulted in an improvement in solubility. A significant increase in solubility was also observed upon replacement of a sulfone group with a sulfoxide.[42] An alternative approach for improving aqueous solubility is by the disruption of molecular planarity and symmetry. Disruption of molecular planarity and symmetry may be achieved through the removal of aromaticity, the increase of dihedral angle, substitution of benzylic positions or the twisting of fused rings.[41]

1.2 Benzimidazoles

1.2.1 Structure/Synthesis

The imidazole nucleus (Figure 1.5, a) is present in a number of important biological building blocks, such as histidine, histamine and purine. Benzimidazole (Figure 1.5, b), also known as benziminazole and 1,3-benzodiazole, is a benzo-fused derivative of imidazole and is well-established in literature as an important biologically active nitrogen heterocycle.[43, 44]

a **b**

Figure 1.5: a) Imidazole and **b)** Benzimidazole

Over many years, this compound class has become known to medicinal chemists as a privileged scaffold due to its versatile heterocyclic moiety displaying a vast array of biological

activities.[43] Interest in benzimidazole chemistry however, was initiated, in the 1950s, by the discovery that the 5,6-dimethylbenzimidazole moiety is an integral component of vitamin B_{12}.[45] Since then, numerous efforts have been made in order to produce libraries of these compounds. In fact, the synthesis of many other drugs and anthelmitics such as albendazole, mebendazole and thiabendazole was a result of the optimisation of substituents around the benzimidazole nucleus.[46]

In 1872, the very first benzimidazole (2,5 or 2,6-dimethylbenzimdiazole) was synthesised by Hobrecker, through the reduction of 2-nitro-4-methylacetanilide.[47] Ladenburg later obtained the same compound by refluxing 2,4-diamino toluene with acetic acid.[48] In very early literature, these compounds were called 'anhydrobases' due to their synthesis involving the loss of water.[45] In the past years, several synthetic methods involving the synthesis of benzimidazoles have been developed. However, the most classical and common method of synthesising benzimidazoles involves the cyclo-condensation of *o*-phenylenediamine with aldehydes, carboxylic acids or their derivatives (nitriles, amidates, orthoesters), under harsh conditions, using strong acids such as hydrochloric acid, polyphosphoric acid (PPA) or *p*-toluenesulfonic acid (Scheme 1.1). By using milder reagents, for example Lewis acids, both the yield and purity of the reaction can be improved.[49, 50]

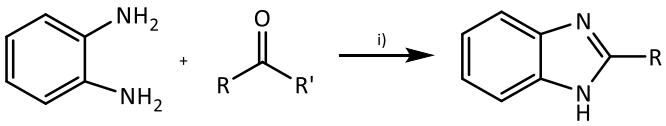

Scheme 1.1: General scheme for the synthesis of benzimidazole, where R = Alkyl/Aryl; R'= OH, H, CN, NH_2, OR'' or OCO_2R. **Reagent**: i) strong acids/ mild reagents/ oxidative reagent/ different catalyst.

The synthesis of benzimidazoles *via* the abovementioned method, requires an oxidative reagent to generate the benzimidazole nucleus. Various oxidative reagents previously employed, include; nitrobenzene, benzoquinone, sodium metabisulfite, mercuric oxide, lead tetraacetate, iodine, copper(II) acetate, indium perfluorooctane sulfonates, ytterbium perfluorooctane sulfonates, and even air.[49]

1.2.2 Antiparasitic activity

The benzimidazole scaffold is undoubtedly a useful structural motif, which may be used for the development of molecules with both pharmaceutical and biological interest. Several compounds recently synthesised, containing the benzimidazole moiety, have been reported to display interesting biological activity as antitumor agents, antiretrovirals and antimalarials.[44, 51-53]

The first of many compounds containing the benzimidazole moiety, and displaying lethal parasitic effects in man, was mebendazole, a benzimidazole carbamate derivative (Figure 1.6a).[54, 55] There are now more than twenty benzimidazole derivatives currently available and used as anthelmintic drugs, examples include; albendazole (Figure 1.6b) and thiabendazole (Figure 1.6c). In 2011, Sawant and Kawade reported the synthesis and biological evaluation of 2-phenylbenzimidazole-1-acetamide derivatives for anthelmintic activity.[56] In comparison to albendazole (the standard), compound **d** (Figure 1.6d) was the most potent with regard to paralysing and killing helminths.[56] This SAR study also concluded that substitution of R with an electron-withdrawing polar group, increased the potency of the compound significantly.[56]

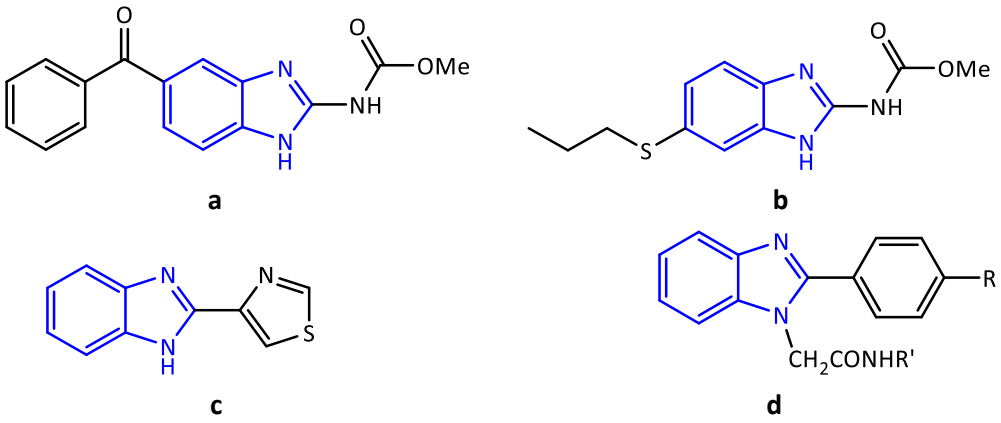

Figure 1.6: Anthelmintic compounds, **a)** mebendazole, **b)** albendazole, **c)** thiabendazole and **d)** 2-phenylbenzimidazole-1-acetamide derivative, where R= NO_2 and R'= Et.

A library of pyrido[1,2- *a*]benzimidazoles were recently synthesised and screened for antimalarial properties, by Ndakala *et al.*[51] They report the synthesis of a pyrido[1,2-*a*]benzimidazole compound (Figure 1.7a), which exhibited antiplasmodial activity comparable to that of chloroquine (IC_{50} = 0.17 – 0.20 µM) in the chloroquine-sensitive NF54 strain.[51] More recently, Singh *et al.* reported further SAR studies on the lead antimalarial compound

previously reported by Ndakala *et al*.[57] They concluded that a key factor to improving *in vitro* activity against *P. falciparum* is through substitution on the benzimidazole phenyl. Furthermore, the synthesised compounds displayed significantly better *in vivo* activity in the mouse *P. berghei* model and against gametocytes.[57]

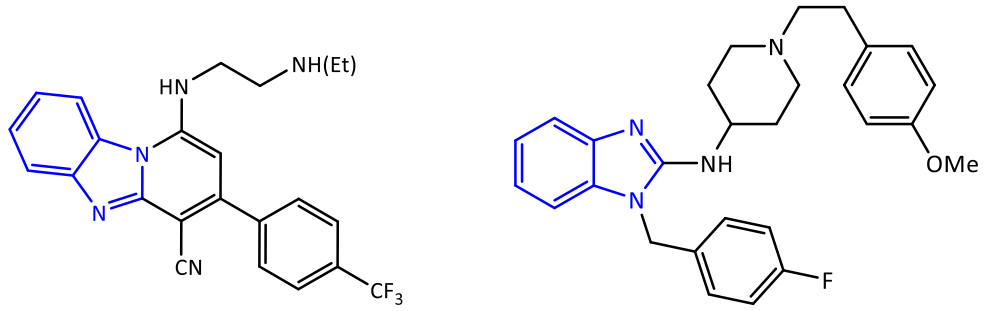

a **b**

Figure 1.7: a) Anti-malarial pyrido[1,2-*a*]benzimidazole (IC_{50}: *Pf*NF54= 0.11 µM; *Pf*K1= 0.12 µM) and **b)** Astemizole.

Roman *et al.* reported on the screening of a library of existing drugs, for inhibitors of *P. falciparum*.[58] This screen led to the identification of astemizole, a drug that inhibits the proliferation of three parasite strains, which differ in chloroquine sensitivity. Astemizole (Figure 1.7b) contains a benzimidazole scaffold and is known as a non-sedating, selective H_1-histamine receptor antagonist.[58] They concluded that the benzimidazole core is an essential structural prerequisite for the exhibition of antiplasmodial activity. The substitution of various groups at positions 1 and 2 proved to have significant effects on their antiplasmodial activity. Replacement of the fluoro- group of astemizole with a trifluoromethyl group resulted in the antiplasmodial activity surpassing that of astemizole.[58]

The above-mentioned selected examples of compounds containing the benzimidazole scaffold, confirms that this pharmacophore is worthy of further exploration.

1.2.3 Proposed mode(s) of action of benzimidazole drugs

Several benzimidazole containing compounds have been prepared and demonstrated significant antimalarial activity. However, the modes of action of these benzimidazole compounds remain unclear.

Recently, a series of piperazine-based compounds were synthesised and upon linkage to a benzimidazole core (Figure 1.8), the compound displayed a chloroquine-like mechanism, concerning accumulation in the acidic food vacuole and inhibition of β-haematin formation.[59]

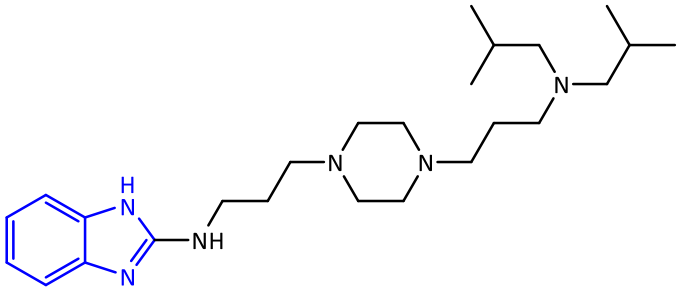

Figure 1.8: A compound containing the benzimidazole core, displaying a chloroquine-like mechanism

In addition, Saify *et al.* recently reported the synthesis of benzimidazole-acetophenone compounds, whereby various substitutions were made on the acetophenone ring.[60] These compounds displayed antiplasmodial activity and proved to be plasmepsin inhibitors (Figure 1.9a).[60] Plasmepsins are aspartic acid proteases which are produced by the *P. falciparum* parasite. There are ten plasmepsins which have been identified in the genome of *P. falciparum*. Four of these plasmepsins (plasmepsin-I, plasmepsin-II, plasmepsin-III and plasmepsin-IV/HAP) have been identified to participate in haemoglobin degradation.[61] Ligand docking studies with plasmepsin-II, carried out by Saify *et al.*, predicted binding of the benzimidazole compounds at the centre of the extended substrate-binding cleft.[60]

Another known target site for antimalarial drugs, is the *Plasmodium* mitochondrial electron transport chain (ETC), which is believed to contain five hydrogenases; namely NADH: ubiquinone oxidoreductase (*Pf*NDH2), succinate: ubiquinone oxidoreductase, glycerol-3-phosphate dehydrogenase, the malate quinone oxidoreductase (MQO) and dihydroorotate dehydrogenase (DHODH).[62] Although the function of these dehydrogenases to the ETC is not completely understood, *Pf*NDH2 and MQO were identified as dehydrogenases, specific to the parasites mitochondria. The molecular structure of the parasites DHODH were also found to be different to that of the human homolog and it is said to be involved in *de novo* pyrimidine biosynthesis, which is an essential source of energy for the parasites survival.[62, 63] It is for this reason that this organelle remains a target site for many antimalarial drugs.

In 2011, Skerlj *et al.* reported on the synthesis and SAR studies of a series of 5-(2-methylbenzimidazol-1-yl)-*N*-alkylthiophene-2-carboxamides.[64] These benzimidazole derivatives were found to be potent inhibitors against DHODH of the *P. falciparum* parasite and displayed good activity against the *P. falciparum* 3D7 strain (Figure 1.9b).[64] Later in 2015, Abdullah *et al.* also reported on the synthesis of benzimidazole analogues displaying inhibitory effects against DHODH.[65]

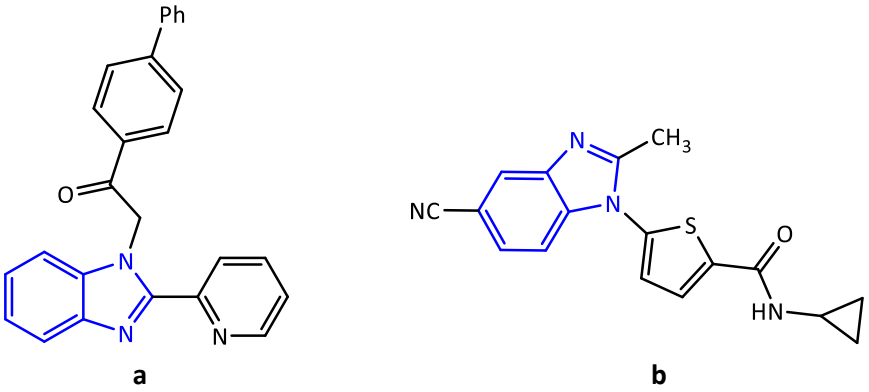

Figure 1.9: a) Plasmepsin inhibitor **b)** DHODH inhibitor

From literature, organic compounds containing the benzimidazole moiety clearly display multifaceted modes of action in the malaria parasite. Multiple modes of action coupled to the incorporation of chemical/structural diversity, may provide new drug leads and aid in combating resistance. In this regard, investigation of metal-based benzimidazoles is of interest.

1.3 Metals in Medicine

1.3.1 Metal-based drugs

Despite the field of bioinorganic chemistry being relatively new, there is now a significant number of metal-based drugs currently in clinical trials. It is well-known that transition metals play essential roles in biological and biomedical processes.[66] Consequently, there are many cases in medicine, where organic compounds do not have a purely organic mode of action. The activation or biotransformation of these organic compounds are often reliant on metal ions. Through the synthesis of metal coordination complexes, biological and chemical diversity, which is distinct from that of organic drugs, can be achieved. Synthetic diversity is generated not only by varying the metal ion, but through variation of its oxidation state and

the ligands to which the metals are coordinated, as well as from the different coordination geometries of the metal.[66, 67] In addition, organometallic species are relatively lipophilic compared to purely organic compounds and are capable of binding to biological targets.[68] Organometallic compounds are therefore considered as promising alternatives in medicinal chemistry.

One of the first examples of a metallodrug used in medicine was Salvarsan, an arsenic-based antimicrobial agent, which was developed in 1912 by Paul Ehrlich.[69] Preceding World War II, Salvarsan was known as the standard drug for the treatment of syphilis, after which it was replaced by penicillin.[70] For many years the structure of Salvarsan was debatable. Salvarsan was assumed to have an As=As double bond (as shown in Figure 1.10a). However, it was recently discovered through extensive mass spectral analysis that salvarsan consists of single As-As bonds. Salvarsan was also found to consist of a mixture of cyclic species (Figure 1.10b and 1.10c).[71]

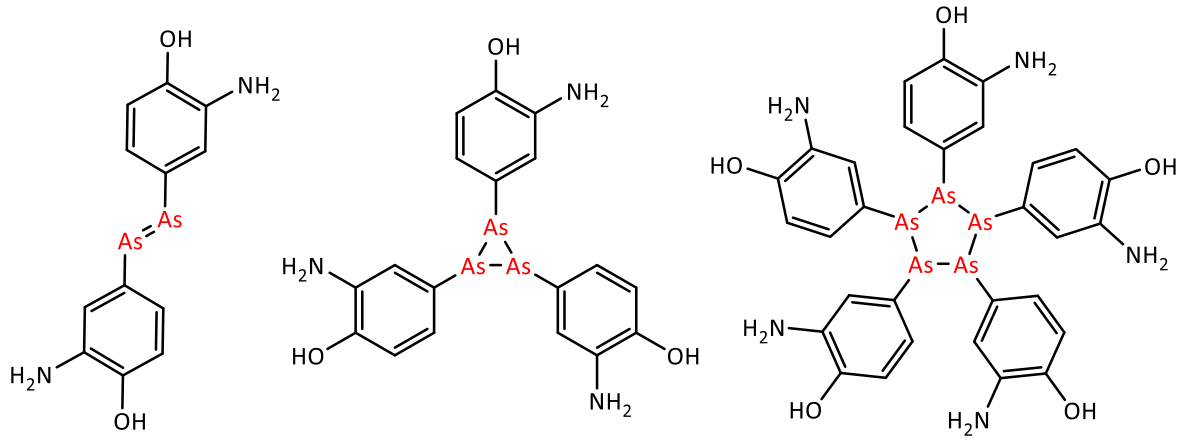

a **b** **c**

Figure 1.10: a) Initial proposed structure of Salvarsan. **b)** and **c)** cyclic species as models for Salvarsan

The discovery of Salvarsan is often regarded as the beginning of modern chemotherapy and the development of metallodrugs. However, the serendipitous discovery of the anticancer drug cisplatin in 1965, led to a huge surge of interest in the field of bioinorganic medicinal chemistry.[72] Platinum-based drugs; cisplatin, carboplatin and oxaliplatin (Figure 1.11), have since become leading compounds in cancer chemotherapy.

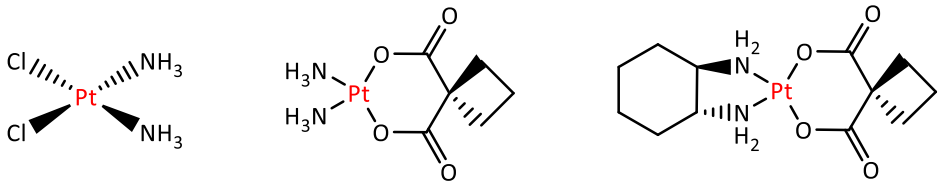

a **b** **c**

Figure 1.11: Platinum anticancer therapy agents: **a)** cisplatin, **b)** carboplatin and **c)** oxaliplatin

Despite the success of these platinum-based drugs as anticancer agents, their use is often accompanied by undesirable side effects such as neurotoxicity. Other limitations of these traditional platinum-based drugs include; sensitivity to mechanisms of resistance, their inactivation by small biomolecules such as glutathione and efflux out of the cell.[68] A wide range of transition-metal drug candidates are therefore currently under consideration for future development in order to overcome these limitations.

A transition metal that has recently received immense attention is ruthenium. The synthesis of ruthenium-based drugs allows for access of various oxidation states [Ru(II), Ru(III) and Ru(IV)]. These ruthenium complexes are generally lower in toxicity, which may be due to their ability to mimic iron.[68] Although no commercially available ruthenium-based drugs currently exist, ruthenium compounds have recently provided promising alternatives to platinum-based drugs. As a result of the increase in research efforts in this field, two ruthenium coordination complexes (Figure 1.12) have reached clinical trials for cancer chemotherapy, namely; NAMI-A (developed by Alessio, Mestroni, Sava, and co-workers) and KP1019 (developed by Keppler and co-workers).[73-75]

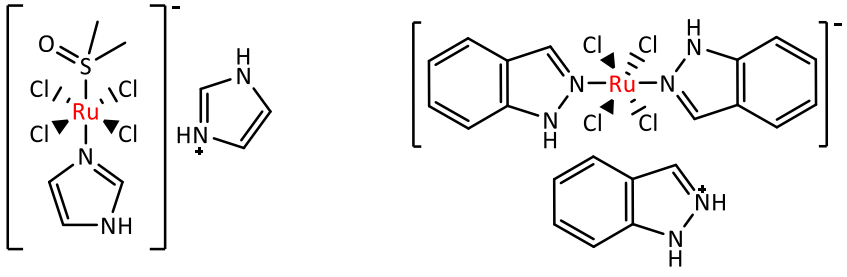

a **b**

Figure 1.12: Ruthenium anticancer therapy agents: **a)** NAMI-A and **b)** KP1019

More recently the transition metals, iridium and rhodium, have provided fascinating alternatives to both platinum and ruthenium metallodrugs. Although these group 9 metals

were initially regarded as chemically inert, it was discovered that upon complexation to a suitable auxiliary ligand, the reactivity and biological activity may be unlocked.[76] The use of arene ligands such as pentamethylcyclopentadienyl (Cp*) for example has been reported to aid in stabilisation of the Ir(III) or Rh(III) metal center.[76]

During the last decade, the synthesis and anticancer activity of Ru(II), Os(II), Ir(III) and Rh(III) arene complexes have been well-documented.[77-80] The success of metallodrugs in cancer chemotherapy has therefore spurred further research interest in the use of coordination complexes in other areas such as anti-inflammatories, antifungal and antimalarial agents.[81]

1.3.2 Metalloantimalarials

The design and development of many metalloantimalarial compounds have been encouraged through the successful synthesis of a vast array of metal compounds displaying antitumor, antiarthritic and antibacterial properties. It has been reported that metal compounds show pronounced selectivity for selected biomolecules of parasites compared to that of the host's.[82]

The successful modification of chloroquine with metal-containing fragments has led to the development of other metalloantimalarials. RhCl(COD)CQ, a compound synthesised by Sanchez-Delgado *et al.*, was one of the first organometallic complexes which was evaluated as an antiplasmodial agent.[83] Sanchez-Delgado *et al*, also reported on the synthesis and antimalarial evaluation of ruthenium(II) chloroquine $[RuCQCl_2]_2$ and gold(I) chloroquine $[Au(PPh_3)CQ]PF_6$ (Figure 1.13). These metal complexes were found to be active against *P. berghei* and against chloroquine-resistant FcB1 and FcB2 *P. falciparum* strains. The authors concluded that the ruthenium complexes exhibited *in* vitro and *in vivo* activity against the rodent strain *P. berghei* and a 94% reduction of parasitaemia was observed.[83] Coordination of ruthenium and gold significantly enhanced the activity of the parent drug, suggesting that metal coordination may be worthwhile exploring in malaria chemotherapy.[83, 84]

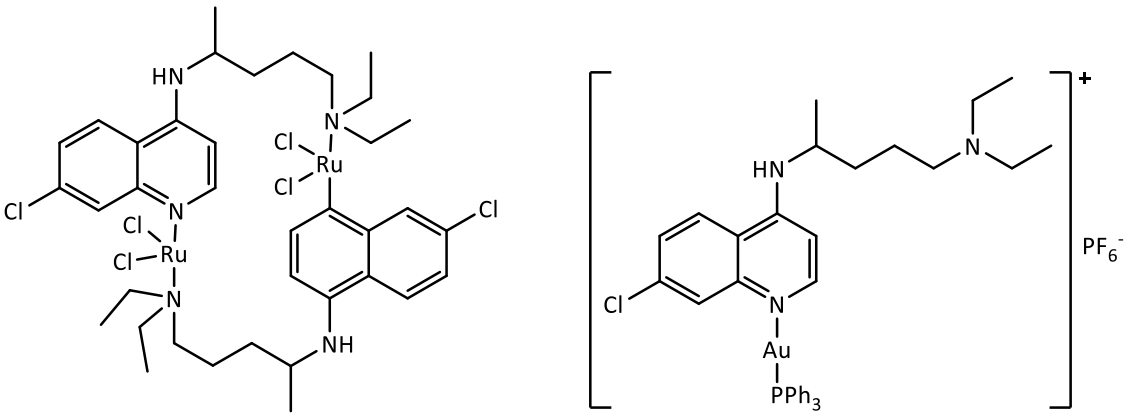

Figure 1.13: a) $[RuCQCl_2]_2$ and **b)** $[Au(PPh_3)CQ]PF_6$

In addition, ferroquine, a successful metallodrug, has demonstrated excellent activity against malarial parasites, both *in vitro* and *in vivo*. Ferroquine is classified as a 4-aminoquinoline which contains a quinoline nucleus and a ferrocenyl group in its side chain. Excellent activity against chloroquine-resistant strains has also been displayed by this metalloantimalarial.[82, 85]

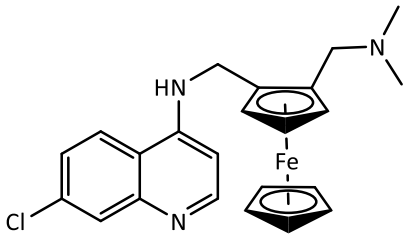

Figure 1.14: Bioorganometallic drug candidate, ferroquine, under phase II clinical trials

Following the success of ferroquine, several other analogues were synthesised. SAR studies revealed that the ferrocene moiety does not show any efficacy on its own. But when this moiety was covalently linked to the 4-aminoquinoline and the alkyl amine moieties, the potency of chloroquine was enhanced.[86] On the other hand, Smith and co-workers have reported on the synthesis and anti-parasitic activity of a series of chelating (*N,S*-) cationic Ru(II)-arene complexes based on thiosemicarbazone scaffolds.[87] The antiplasmodial activity of the *p*-cymene Ru(II) thiosemicarbazone complexes were significantly higher compared to the free thiosemicarbazone ligands.[87]

These findings further provide data in support of the now proven hypothesis that incorporation of a transition metal onto a known pharmacophore may be a useful strategy in drug design and development.

1.4 Transition-metal based benzimidazoles

Despite many reports on metal-based benzimidazoles displaying good anticancer activity, there is currently, very little research on transition-metal based benzimidazoles which display antimalarial activity. According to a recent literature search, there are only two known examples of metal-based benzimidazoles which have been synthesised and evaluated for antiplasmodial activity.[88, 89]

Copper(II) nanohybrid solids [$LCu(CH_3COO)_2$ and $LCuCl_2$] were recently synthesised using bis(benzimidazole)diamide as the capping ligand. The Cu(II) coordination complexes displayed antiplasmodial activity comparable to chloroquine, where IC_{50} values ranged from 0.048 – 0.059 µM against the *P. falciparum* chloroquine-sensitive (MRC 2) strain.[88]

More recently, a study which involved the conjugation of ferrocene and rhenium to a benzimidazole scaffold and the antimalarial evaluation showed promising results against the chloroquine-sensitive (3D7) and chloroquine-resistant (W2) strain.[89]

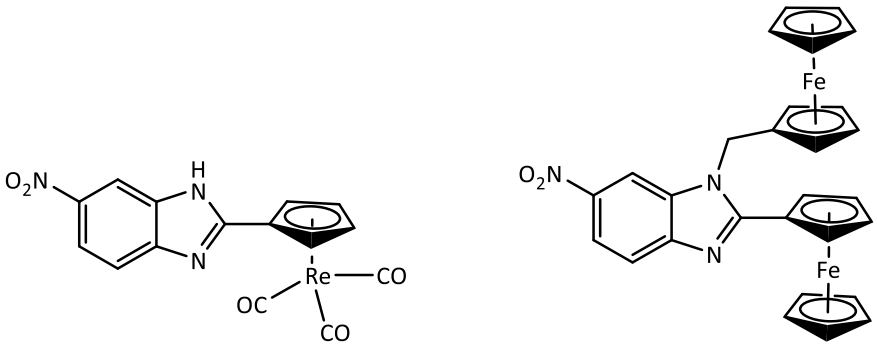

Figure 1.15: a) Cyrrhetrenyl and **b)** ferrocenyl benzimidazole complexes

The cyrhetrenyl compound displayed better activity (IC_{50} = 10.4 – 26.5 µM) in both strains, compared to its ferrocenyl analogue (IC_{50} =23.9 – 48.0 µM). Increased antiplasmodial activity was also demonstrated through substitution of a nitro group in the 5-position of the benzimidazole.[89]

1.5 Research Rationale and Motivation

The increasing rise in resistant strains against antimalarial drugs, which has previously been known to be effective, remains a huge global concern. Thus, there is an urgent need to develop novel and effective anti-malarial drugs that are chemically and structurally diverse.

Over the past decade, the field of bioorganometallic medicinal chemistry has provided promising alternatives to traditional organic drugs. There are many examples which demonstrate the advantages of using metals (such as PGMs) in drug design and development. For example, Ru(II) or Ir(III) metal complexes have been reported to display lower toxicity. In addition, the synthesis of a cyclometallated complex may aid in stabilising the metal complex and may introduce chemical diversity. Furthermore, enhanced activity is often observed upon metal complexation onto a particular pharmacophore.

As already mentioned, the benzimidazole pharmacophore has been well-documented to display diverse biological activities. However, there is very little research on metal-based benzimidazoles and their antiplasmodial activity. This project therefore aims to explore/investigate SAR studies of cyclometallated Ru(II) and Ir(III) benzimidazole complexes as antiplasmodial agents.

2. Aims and Objectives

The aim of the project was to design and prepare a series of benzimidazole-based compounds for antiplasmodial evaluation.

More specifically, the research project had two main points of focus; the first was to prepare a series of structurally related 2-phenylbenzimidazoles and to assess the effect of structural diversity on their activity as antiplasmodial agents. The second focus point was to investigate the effects of converting the purely organic 2-phenylbenzimidazoles to Ru and Ir cyclometallated complexes on activity. The specific objectives of this project are outlined below;

(i) The synthesis and characterisation of 2-phenylbenzimidazole ligands;

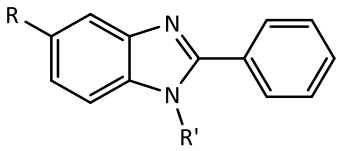

Where, R = H, F, Cl, CF_3, CH_3, OMe, SO_2Me, CN, $CONH_2$
R' = CH_3 or $CH_2CH_2CH_3$

(ii) The functionalisation of previously synthesised 2-phenylbenzimidazole with water-solubilising H-bonding groups towards improving solubility;

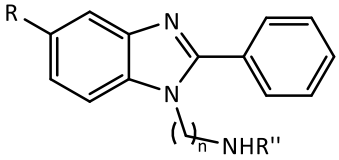

Where, R is selected as the most active substituent

R''= 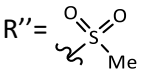

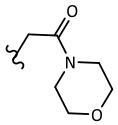

(iii) The synthesis and characterisation of organometallic complexes containing platinum group metals (Ru and Ir) of the most active ligands;

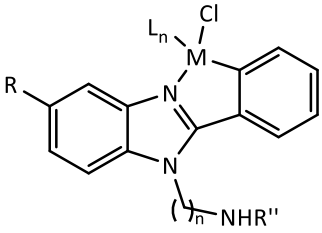

Where, M= Ru and L_n= *p*-cymene or
M= Ir and L_n= Cp*

(iv) The antiplasmodial activity and cytotoxicity evaluation of all synthesised benzimidazole ligands and organometallic complexes;

(v) The determination of solubility of the synthesised compounds according to the screening cascade.

References

1. R. G. Ridley and A. T. Hudson, *Expert. Opin. Ther. Pat.*, 1998, **8**, 121-136.
2. J. Crawley, C. Chu, G. Mtove and F. Nosten, *Lancet*, 2010, **375**, 1468-1481.
3. The World Health Organisation, *World Malaria Report*, 2014. http: //www.who.int/malaria/publications/world_malaria_report_2014/en/ (accessed Feb 15 2016).
4. J. A. Patz, T. K. Graczyk, N. Geller and A. Y. Vittor, *Int. J. Parasitol.*, 2000, **30**, 1395-1405.
5. The World Health Organisation, *World Malaria Report*, 2017. http: //www.who.int/malaria/publications/world-malaria-report-2017/report/en/ (accessed Dec 10, 2017)
6. The World Health Organisation, *World Malaria Report*, 2005. http: //www.who.int/malaria/publications/atoz/9241593199/en/ (accessed Feb 15, 2016).
7. F. E. Cox, *Clin. Microbiol. Rev.*, 2002, **15**, 595-612.
8. A. Laveran, *Traité des fièvres palustres: avec la dsecription des microbes du paludisme*, Paris, 2 edn., 1884.
9. P. Manson-Bahr, *Proc. R. Soc. Med.*, 1961, **54**, 91-100.
10. F. E. G. Cox, *Parasit. Vectors*, 2010, **3**, 5.
11. P. F. Salas, C. Herrmann and C. Orvig, *Chem. Rev.*, 2013, **113**, 3450-3492.
12. A. F. Cowman, D. Berry and J. Baum, *J. Cell Biol.*, 2012, **198**, 961-971.
13. L. H. Miller, D. I. Baruch, K. Marsh and O. K. Doumbo, *Nature*, 2002, **415**, 673-679.
14. R. Kigozi, S. M. Baxi, A. Gasasira, A. Sserwanga, S. Kakeeto, S. Nasr, D. Rubahika, G. Dissanayake, M. R. Kamya, S. Filler and G. Dorsey, *PLoS One*, 2012, **7**, e42857.
15. O. World Health, *World Malaria Report 2015*, 2015.
16. M. Schlitzer, *ChemMedChem*, 2007, **2**, 944-986.

17. M. J. Gardner, N. Hall, E. Fung, O. White, M. Berriman, R. W. Hyman, J. M. Carlton, A. Pain, K. E. Nelson, S. Bowman, I. T. Paulsen, K. James, J. A. Eisen, K. Rutherford, S. L. Salzberg, A. Craig, S. Kyes, M. S. Chan, V. Nene, S. J. Shallom, B. Suh, J. Peterson, S. Angiuoli, M. Pertea, J. Allen, J. Selengut, D. Haft, M. W. Mather, A. B. Vaidya, D. M. Martin, A. H. Fairlamb, M. J. Fraunholz, D. S. Roos, S. A. Ralph, G. I. McFadden, L. M. Cummings, G. M. Subramanian, C. Mungall, J. C. Venter, D. J. Carucci, S. L. Hoffman, C. Newbold, R. W. Davis, C. M. Fraser and B. Barrell, *Nature*, 2002, **419**, 498-511.

18. L. Florens, M. P. Washburn, J. D. Raine, R. M. Anthony, M. Grainger, J. D. Haynes, J. K. Moch, N. Muster, J. B. Sacci, D. L. Tabb, A. A. Witney, D. Wolters, Y. Wu, M. J. Gardner, A. A. Holder, R. E. Sinden, J. R. Yates and D. J. Carucci, *Nature*, 2002, **419**, 520-526.

19. J. Wang, L. Gaob, Y. Lee, K. A. Kalesh, Y. S. Ong, J. Lim, J.-E. Jee, H. Sune, S. S. Lee, Z.-C. Hua and Q. Lin, *Pharmacol. Ther.*, 2016, **162**, 10-22.

20. S. E. Lindner, K. E. Swearingen, A. Harupa, A. M. Vaughan, P. Sinnis, R. L. Moritz and S. H. I. Kappe, *Mol. Cell Proteomics*, 2013, **12.5**, 1127-1143.

21. H. M. Ismail, V. Barton, M. Phanchana, S. Charoensutthivarakul, M. H. L. Wong, J. Hemingway, G. A. Biagini, P. M. O'Neill and S. A. Ward, *Proc. Natl. Acad. Sci. U S A*, 2016, **113**, 2080-2085.

22. J. Achan, A. O. Talisuna, A. Erhart, A. Yeka, J. K. Tibenderana, F. N. Baliraine, P. J. Rosenthal and U. D'Alessandro, *Malar. J.*, 2011, **10**, 144.

23. K. Kaur, M. Jain, R. P. Reddy and R. Jain, *Eur. J. Med. Chem.*, 2010, **45**, 3245-3264.

24. C. Biot, W. Castro, C. Y. Botte and M. Navarro, *Dalton Trans.*, 2012, **41**, 6335-6349.

25. M. Schlitzer, *Arch. Pharm. Chem. Life Sci.*, 2008, **341**, 149-163.

26. J. N. Burrows, K. Chibale and T. N. Wells, *Curr. Top. Med. Chem.*, 2011, **11**, 1226-1254.

27. J. M. Combrinck, T. E. Mabotha, K. K. Ncokazi, M. A. Ambele, D. Taylor, P. J. Smith, H. C. Hoppe and T. J. Egan, *ACS Chem. Biol.*, 2012, **8**, 133-137.

28. M. Mungthin, P. G. Bray, R. G. Ridley and S. A. Ward, *Antimicrob. Agents Chemother.*, 1998, **42**, 2973-2977.

29. A. Yayon, Z. I. Cabantchik and H. Ginsburg, *EMBO J.*, 1984, **3**, 2695-2700.

30. S. R. Vippagunta, A. Dorn, H. Matile, A. K. Bhattacharjee, J. M. Karle, W. Y. Ellis, R. G. Ridley and J. L. Vennerstrom, *J. Med. Chem.*, 1999, **42**, 4630-4639.

31. L. H. Miller and X. Su, *Cell*, 2011, **146**, 855-858.

32. E. Fernández-Álvaro, W. Hong, G. Nixon, P. O'Neill and F. Calderon, *J. Med. Chem.*, 2016, **59**, 5587-5603.
33. P. Sobolewski, I. Gramaglia, J. A. Frangos, M. Intaglietta and H. van der Heyde, *Infect. Immun.*, 2005, **73**, 6704-6710.
34. P. M. O'Neill, V. E. Barton and S. A. Ward, *Molecules*, 2010, **15**, 1705-1721.
35. C. Severini and M. Menegon, *J. Glob. Antimicrob. Resist.*, 2015, **3**, 58-63.
36. A. B. S. Sidhu, D. Verdier-Pinard and D. A. Fidock, *Science*, 2002, **298**, 210-213.
37. R. L. Summers, A. Dave, T. J. Dolstra, S. Bellanca, R. V. Marchetti, M. N. Nash, S. N. Richards, V. Goh, R. L. Schenk, W. D. Stein, K. Kirk, C. P. Sanchez, M. Lanzer and R. E. Martin, *Proc. Natl. Acad. Sci. U S A*, 2014, **111**, 1759-1767
38. M. Jida, C. P. Sanchez, K. n. Urgin, K. Ehrhardt, S. Mounien, A. Geyer, M. Elhabiri, M. Lanzer and E. Davioud-Charvet, *ACS Infect. Dis.*, 2017, **3**, 119-131.
39. T. Harinasuta, P. Suntharasamai and C. Viravan, *The Lancet*, 1965, **286**, 657-660.
40. H. van de Waterbeemd and E. Gifford, *Nature*, 2003, **2**, 192-204.
41. M. Ishikawa and Y. Hashimoto, *J. Med. Chem.*, 2011, **54**, 1539-1554.
42. C. L. Manach, T. Paquet, D. G. l. Cabrera, Y. Younis, D. Taylor, L. Wiesner, N. Lawrence, S. Schwager, D. Waterson, M. J. Witty, S. Wittlin, L. J. Street and K. Chibale, *J. Med. Chem.*, 2014, **54**, 8839-8848.
43. B. Narasimhan, D. Sharma and P. Kumar, *Med Chem Res*, 2012, **21**, 269-283.
44. K. Shah, S. Chhabra, S. K. Shrivastava and P. Mishra, *Med. Chem. Res.*, 2013, **22**, 5077-5104.
45. J. B. Wright, *Chem. Rev.*, 1951, **48**, 397-541.
46. Y. Bansal and O. Silakari, *Bioorg. Med. Chem.*, 2012, **20**, 6208-6236.
47. F. Hobrecker, *Ber. Dtsch. Chem. Ges.*, 1872, **5**, 920.
48. A. Ladenburg, *Ber. Dtsch. Chem. Ges.* , 1875, **8**, 677.
49. R. S. Keri, A. Hiremathad, S. Budagumpi and B. M. Nagaraja, *Chem. Biol. Drug. Des.*, 2015, **86**, 19-65.
50. L. C. R. Carvalho, E. Fernandes and M. M. B. Marques, *Chem. Eur. J.*, 2011, **17**, 12544-12555.
51. A. J. Ndakala, R. K. Gessner, P. W. Gitari, N. October, K. L. White, A. Hudson, F. Fakorede, D. M. Shackleford, M. Kaiser, C. Yeates, S. A. Charman and K. Chibale, *J. Med. Chem.*, 2011, **54**, 4581-4589.

52. G. Yadav and S. Ganguly, *Eur. J. Med. Chem.*, 2015, **97**, 419-443.

53. M. Wang, X. Han and Z. Zhou, *Expert Opin. Ther. Patents*, 2015, **25**, 595-612.

54. G. Navarrete-Vazquez, R. Cedillo, A. Hernandez-Campos, L. Yepez, F. Hernadez-Luis, J. Valdez, R. Morales, R. Cortes, M. Hernandez and R. Castillo, *Bioorg. Med. Chem. Lett.*, 2001, **11**, 187-190.

55. D. Rathore, T. F. McCutchan, M. Sullivan and S. Kumar, *Expert. Opin. Investig. Drugs*, 2005, **14**, 871-883.

56. R. Sawant and D. Kawade, *Acta Pharmaceut*, 2011, **61**, 353-361.

57. K. Singh, J. Okombo, C. Brunschwig, F. Ndubi, L. Barnard, C. Wilkinson, P. M. Njogu, M. Njoroge, L. Laing, M. Machado, M. Prudêncio, J. Reader, M. Botha, S. Nondaba, L. Birkholtz, S. Lauterbach, A. Churchyard, T. L. Coetzer, J. N. Burrows, C. Yeates, P. Denti, L. Wiesner, T. J. Egan, S. Wittlin and K. Chibale, *J. Med. Chem.*, 2017, **60**, 1432-1448.

58. G. Roman, I. E. Crandall and W. A. Szarek, *ChemMedChem.*, 2013, **8**, 1795-1804.

59. R. Deprez-Poulain and P. Melnyk, *Comb. Chem. High Throughput Screen*, 2005, **8**, 39-48.

60. Z. S. Saify, M. K. Azim, W. Ahmad, M. Nisa, D. E. Goldberg, S. A. Hussain, S. Akhtar, A. Akram, A. Arayne, A. Oksman and I. A. Khan, *Bioorg. Med. Chem. Lett.*, 2012, **22**, 1282-1286.

61. R. Banerjee, J. Liu, W. Beatty, L. Pelosof, M. Klemba and D. E. Goldberg, *Proc. Natl. Acad. Sci. U S A*, 2002, **99**, 990-995.

62. G. L. Nixon, C. Pidathala, A. E. Shone, T. Antoine, N. Fisher, P. M. O'Neill, S. A. Ward and G. A. Biagini, *Future Med. Chem.*, 2013, **13**, 1573-1591.

63. A. Singh, M. Maqbool, M. Mobashir and N. Hoda, *Eur. J. Med. Chem.*, 2017, **125**, 640-651.

64. R. T. Skerlj, C. M. Bastos, M. L. Booker, M. L. Kramer, J. Robert H. Barker, C. A. Celatka, T. J. O'Shea, B. Munoz, A. B. Sidhu, J. F. Cortese, S. Wittlin, P. Papastogiannidis, I. Angulo-Barturen, M. B. Jimenez-Diaz and E. Sybertz, *ACS Med. Chem. Lett.*, 2011, **2**, 708-713.

65. I. Abdullah, C. F. Chee, Y.-K. Lee, S. S. R. Thunuguntla, K. S. Reddy, K. Nellore, T. Antony, J. Verma, K. W. Munb, S. Othman, H. Subramanya and N. A. Rahman, *Bioorg. Med. Chem.*, 2015, **23**, 4669-4680.

66. N. P. E. Barry and P. J. Sadler, *ACS Nano*, 2013, **7**, 5654-5659.

67. Z. J. Guo and P. J. Sadler, *Angew. Chem. Int. Ed.*, 1999, **38**, 1513-1531.

68. N. Cutillas, G. S. Yellol, C. de Haro, C. Vicente, V. Rodríguez and J. Ruiz, *Coord. Chem. Rev.*, 2013, **257**, 2784-2797.

69. P. Ehrlich and A. Bertheim, *Eur. J. Inorg. Chem.*, 1912, **45**, 756-766.

70. K. Dralle Mjos and C. Orvig, *Chem. Rev.*, 2014, **114**, 4540−4563.

71. N. C. Lloyd, H. W. Morgan, B. K. Nicholson and R. S. Ronimus, *Angew. Chem. Int. Ed.*, 2005, **44**, 941-944

72. P. J. Rosenthal, *J. Exp. Biol.*, 2003, **206**, 3735-3744.

73. G. Sava, E. Alessio, A. Bergamo and G. Mestroni, in *Topics in Biological Inorganic Chemistry*, eds. M. J. Clarke and P. J. Sadler, Springer-Verlag, Berlin, 1999, vol. 1, p. 143.

74. A. Bergamo, S. Zorzet, B. Gava, A. Sorc, E. Alessio, E. Iengo and G. Sava, *Anticancer Drugs*, 2000, **11**, 665-672.

75. C. G. Hartinger, S. Zorbas-Seifried, M. A. Jakupec, B. Kynast, H. Zorbas and B. K. Keppler, *J. Inorg. Biochem.*, 2006, **100**, 891-904.

76. C. Leung, H. Zhong, D. Chan and D. Ma, *Coord. Chem. Rev.*, 2013, **257**, 1764-1776.

77. A. Habtemariam, M. Melchart, R. Fernandez, S. Parsons, I. D. Oswald, A. Parkin, F. P. Fabbiani, J. E. Davidson, A. Dawson, R. E. Aird, D. I. Jodrell and P. J. Sadler, *J. Med. Chem.*, 2006, **49**, 6858-6868.

78. Y. Fu, A. Habtemariam, A. M. Pizarro, S. H. van Rijt, D. J. Healey, P. A. Cooper, S. D. Shnyder, G. J. Clarkson and P. J. Sadler, *J. Med. Chem.*, 2010, **53**, 8192-8196.

79. C. Scolaro, A. Bergamo, L. Brescacin, R. Delfino, M. Cocchietto, G. Laurenczy, T. J. Geldbach, G. Sava and P. J. Dyson, *J. Med. Chem.*, 2005, **48**, 4161-4171.

80. P. Govender, T. Riedel, P. J. Dyson and G. S. Smith, *Dalton Trans.*, 2016, **45**, 9529-9539.

81. B. S. Sekhon and N. Bimal, *J. Pharm. Educ. Res.*, 2012, **3**, 52-63.

82. M. Navarro, C. Gabbiani, L. Messori and D. Gambino, *Drug Discov. Today*, 2010, **15**, 1070-1078.

83. R. A. Sanchez-Delgado, M. Navarro, H. Pe´rez and J. A. Urbina, *J. Med. Chem.*, 1996, **39**, 1095-1099.

84. M. Navarro, H. Perez and R. A. Sanchez-Delgado, *J. Med. Chem.*, 1997, **40**, 1937-1939.

85. R. W. Brown and C. J. T. Hyland, *Med. Chem. Commun.*, 2015, **6**, 1230-1243.

86. C. Biot, Wassim Daher, C. M. Ndiaye, P. Melnyk, B. Pradines, N. Chavain, A. Pellet, L. Fraisse, L. Pelinski, C. Jarry, J. Brocard, J. Khalife, I. Forfar-Bares and D. Dive, *J. Med. Chem.*, 2006, **49**, 4707-4714.

87. M. Adams, Y. Li, H. Khot, C. De Kock, P. J. Smith, K. Land, K. Chibale and G. S. Smith, *Dalton Trans.*, 2013, **42**, 4677-4685.

88. S. C. Mohapatra, H. Kumar Tiwari, M. Singla, B. Rathi, A. Sharma, K. Mahiya, M. Kumar, S. Sinha and S. Singh Chauhan, *J. Biol. Inorg. Chem.*, 2010, **15**, 373-385.

89. P. Toro, A. H. Klahn, B. Pradines, F. Lahoz, A. Pascual, C. Biot and R. Arancibia, *Inorg. Chem. Commun.*, 2013, **35**, 126-129.

Chapter 2: Synthesis and characterisation of 2-phenylbenzimidazole ligands and cyclometallated Ru(II)/Ir(III) benzimidazole complexes

2.1. Introduction

It is well-documented that minor structural changes, such as variation of substituents, of a potential drug candidate can significantly influence the overall efficacy of a compound.[1, 2] Therefore, one of the aims was to assess the effects of such changes on the 2-phenylbenzimidazole core and investigate how these changes relate to the observed antimalarial activity. 2-Phenylbenzimidazoles were chosen specifically because of their known ability to readily form stable metal complexes through cyclometallation, which enabled an investigation into the effects of metal complexation on bioactivity.

With regard to antimalarial drugs, several research articles have reported on the synthesis and promising antimalarial activity of various metals complexed to chloroquine.[3-5] There is clear evidence, as demonstrated in these papers, that the introduction of a metal can be advantageous.[3-5] Indeed, exploring the effect of metal complexation and whether or not it generally enhances the antiplasmodial activity of a molecule was one of the major driving forces for this research project. A summary of the proposed chemical modifications of the 2-phenylbenzimidazole is outlined in Figure 2.1 below.

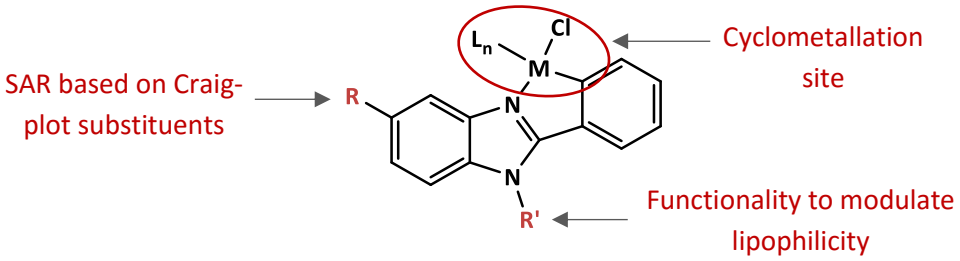

Figure 2.1: Proposed SAR studies

Several reports state that substitution at position-5 of the benzimidazole core results in enhanced antiplasmodial activity.[6-8] The synthesis described in this chapter was thus aimed at producing a series of compounds, where the effects of varying the R substituent at

position-5 of the benzimidazole moiety was investigated. Substituents were chosen based on the Craig Plot (Figure 2.2).

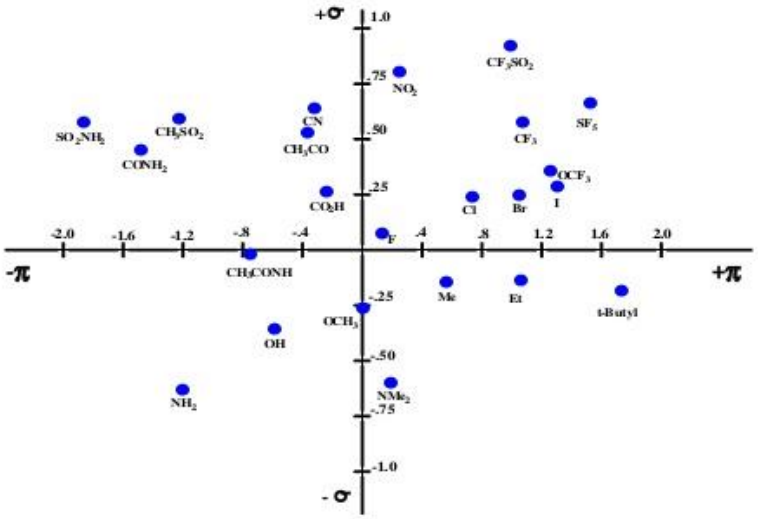

Figure 2.2: The Craig Plot

The Craig plot is often used in rational drug design, whereby variation of substituents allows for the probing of the electronics and steric effects of a compound. For example, often the size or bulkiness of a particular drug may influence its ability to approach and interact with a binding site. Bulky substituents may either hinder the drug from binding or may somehow aid in positioning the drug for maximum binding, thus increasing the activity of the drug. The Craig plot has a y- and x-axis. The y- and x- axis is represented by the σ- and π-constants, respectively. A positive π-constant indicates that the substituent is more hydrophobic, whereas a positive σ-constant indicates the substituent is electron-withdrawing.

The Craig plot continuously informs drug-design in the sense that if groups in a particular quadrant are observed to have a positive effect on activity then subsequent design will involve making more compounds where R groups are chosen from the more active quadrant. The aim was therefore to efficiently and expediently synthesise compounds from the various quadrants. For this reason, a general synthetic sequence that would allow access to functionally diverse 2-phenylbenzimidazoles was considered. The sequence would incorporate the desired functional group (FG) by choosing an appropriate starting material and would then also have to tolerate and conserve different FG's (electronically and sterically) through the entire synthesis. The synthetic sequence chosen would also allow for further

modification of the benzimidazole moiety, where the effect of the chain length could be investigated, where R' (Figure 2.1) is either a methyl or propyl group. Additionally, the introduction of water-solubilising groups via R', was also explored in order to evaluate the effects on aqueous solubility.

In this chapter, the synthesis and characterisation of novel 2-phenylbenzimidazoles and cyclometallated Ru(II) and Ir(III) benzimidazole complexes are described. As already mentioned, the rationale for synthesising these benzimidazole-based compounds concerns the fact that the benzimidazole moiety is a known pharmacophore, highly cited in literature for displaying interesting biological activities.[6, 9, 10] Furthermore, the concept of incorporating a metal onto a known pharmacophore or an existing drug has become increasingly popular.[11,12]

2.2. Synthesis of 2-phenylbenzimidazoles and corresponding intermediates

The synthesis of the *N*-methyl and *N*-propyl 2-phenylbenzimidazole ligands (**35** – **50**) involved three synthetic steps: 1) Nucleophilic aromatic substitution (S_NAr) of methylamine or *n*-propylamine with either an *ortho*- substituted fluoro- or chloro- nitrobenzene, followed by 2) the reduction of the nitro- moiety to the amine functionality, and lastly 3) a condensation cyclisation reaction to afford the desired benzimidazole ligand. The overall synthetic scheme is outlined below (Scheme 2.1) and the syntheses and characterisation of these compounds are described subsequently.

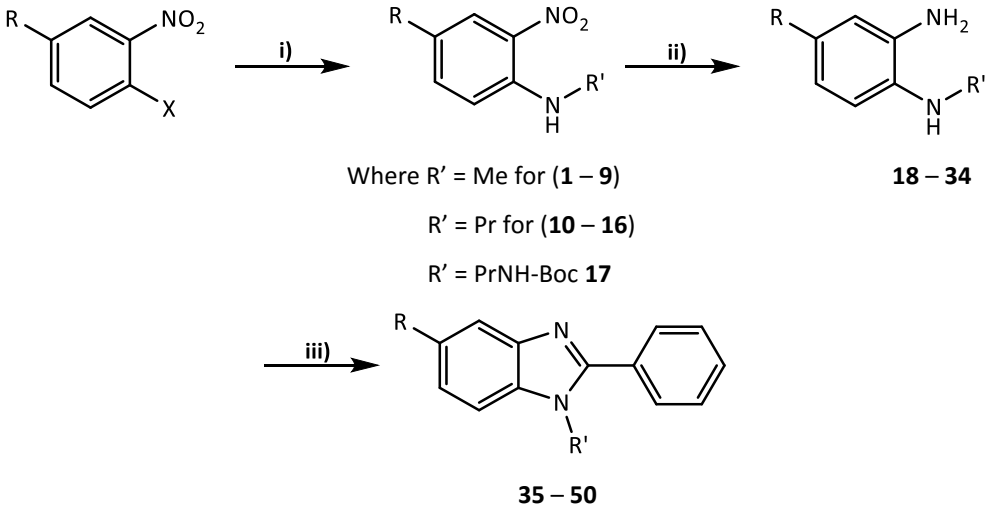

Scheme 2.1: Synthesis of intermediates and 2-phenylbenzimidazoles. Reagents and conditions: **i)** $MeNH_2$/ DCM/ K_2CO_3/ rt or *n*-$PrNH_2$/ DMF/ rt or *N*-Boc-1,3-propanediamine/ DMF/ rt; **ii)** Zn/ NH_4Cl/ MeOH/ rt; **iii)** Benzaldehyde/ TFA/ $MgSO_4$/ EtOH/ rt.

There are several methods which describe the synthesis of benzimidazoles. However, the most common methodology involves the condensation of 1,2-diaminobenzenes with aromatic aldehydes.[13, 14] Thus, the first step towards the synthesis of the 2-phenylbenzimidazole ligands involved forming a nitroaniline derivative, which could easily be reduced to the required 1,2-diaminobenzene.

2.2.1. Synthesis of nitroanilines (1 – 16)

The synthesis of the *N*-methyl nitroaniline derivatives (**1** – **9**) and the *N*-propyl nitroaniline derivatives (**10** – **16**) involved a S_NAr reaction, whereby an excess amount of methylamine or

n-propylamine was reacted with various substituted nitrobenzene compounds containing either a fluoro- or chloro- atom *ortho*- to the nitro- moiety (Scheme 2.2).

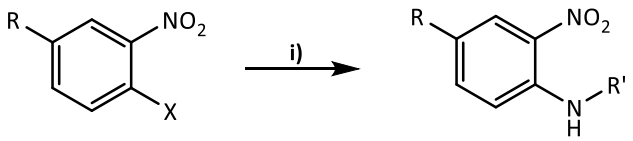

1 – 16

Scheme 2.2: Synthesis of nitroaniline compounds, where X = Cl or F; Where R' = Me and R = H (**1**), Cl (**2**), OCH_3 (**3**), CN (**4**), CH_3 (**5**), CF_3 (**6**), SO_2CH_3 (**7**), $CONH_2$ (**8**), or F (**9**); Where R' = Pr and R = H (**10**), Cl (**11**), CH_3 (**12**), CN (**13**), SO_2CH_3 (**14**), OCH_3 (**15**), CF_3 (**16**). Reagents and conditions: **i)** $MeNH_2$/ DMF/ rt or *n*-$PrNH_2$/ DMF/ rt

In most cases the reaction conditions for the synthesis of the nitroaniline compounds involved dissolving the nitrobenzene starting material in a polar aprotic solvent such as DMF, adding two equivalents of the desired amine and allowing the reaction to stir for 24 h at room temperature. However, in certain cases where compounds were previously reported, literature methods were followed. These methods varied in terms of solvent choice, reaction temperature and/or the addition of a base.

A nucleophilic aromatic substitution reaction (S_NAr) is described as a reaction, where the addition of a nucleophile to an aromatic ring, is followed by the elimination of a leaving group (Scheme 2.3). The alkyl amine, which acts as both nucleophile and base, attacks the aromatic carbon bearing the halogen, resulting in the formation of a negatively charged intermediate Meisenheimer complex. The Meisenheimer complex formed, is stabilised through resonance by the electron withdrawing nitro- group. Subsequent elimination of the halogen results in the production of the nitroaniline compound. The addition of two equivalents of alkyl amine is usually necessary as the second equivalent of amine acts as a base to neutralise the HCl or HF formed from the reaction.

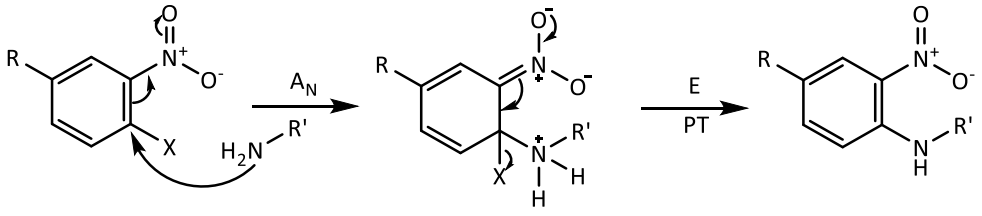

Scheme 2.3: Proposed mechanism for the Nucleophilic Aromatic Substitution (S_NAr) reaction.

In general, the synthesis of the nitroaniline compounds proceeded easily, as almost complete conversion of starting material was observed under mild reaction conditions. However, as expected the nitroaniline bearing the electron-donating methoxy substituent was found to be less reactive toward substitution than its EWG counterparts. As a result of this, the methoxy analogue was prepared in a sealed vessel at 100 °C.

Reaction progress was monitored by thin layer chromatography (TLC). In most cases after 24 h, TLC analysis of the reaction revealed almost complete conversion of the starting material to a more polar product. However, the reaction time involving the synthesis of the methoxy analogue, was increased to 48 h, for reasons previously discussed. In general, purification of the nitroaniline compounds was achieved by either column chromatography or recrystallisation methods. In some cases, the product could not be purified by column chromatography, despite the optimisation of solvent ratios and flow rates. Consequently, the crude material was used and purified in the next step, as was the case for compounds **2** and **11**. The synthesised nitroaniline derivatives were generally isolated as either orange/yellow solids or oils in good to excellent yields (48 – 99%).

Analysis of the ^{1}H NMR spectra of compounds **1** – **16,** supported the successful synthesis of these compounds. Evidence of substitution of the methylamine or *n*-propylamine group is given by the broad singlet, which appears in the aromatic region of the ^{1}H NMR spectra and is assigned to the proton of the secondary amine, H_h. The appearance of a distinct doublet, with a *J*-value of 5.2 Hz, in the aliphatic region, integrating for three protons is assigned to the methyl of the methylamine. The resonance, H_g is observed as a doublet due to its coupling to the proton of the secondary amine, H_h. With respect to the synthesis of the nitroaniline compounds bearing a propyl chain, the appearance of three distinct signals observed as a triplet, multiplet and triplet, in the aliphatic region is assigned to the propyl chain and confirmed the successful substitution of the propylamine.

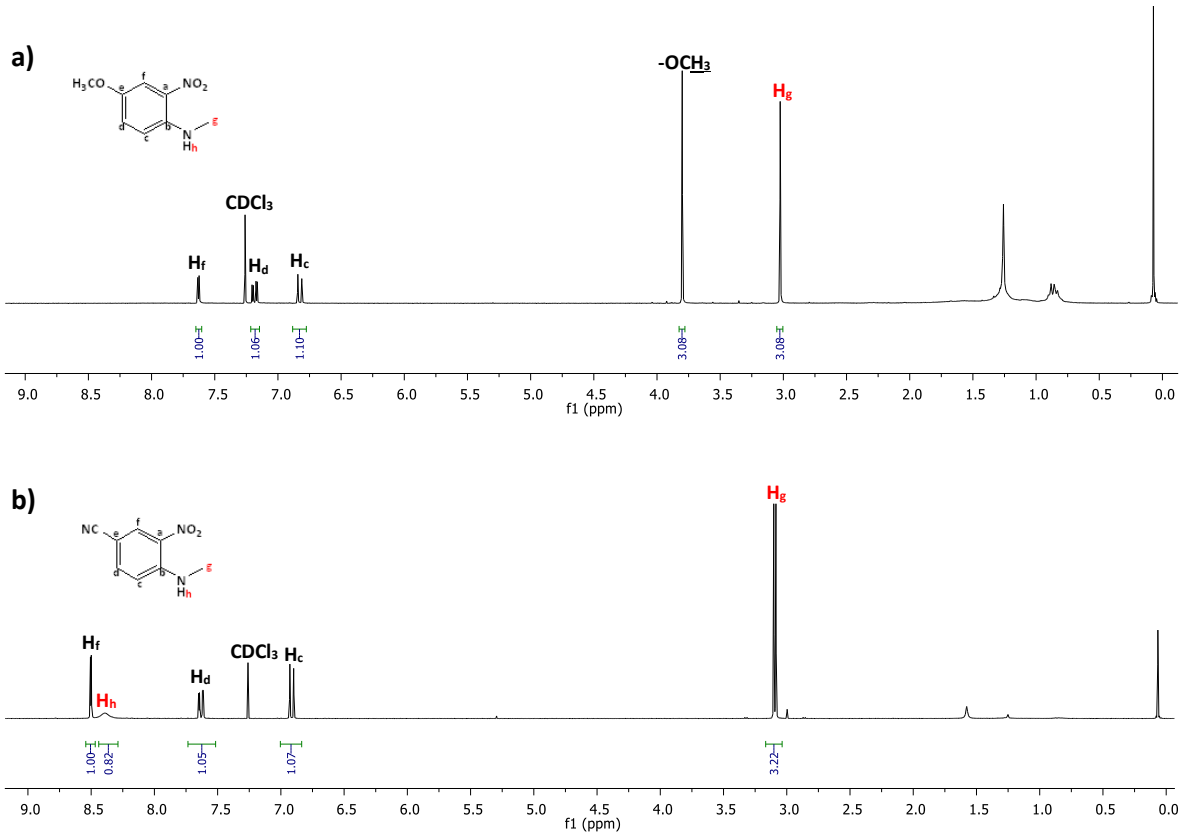

Figure 2.3: ^{1}H NMR spectra of nitroaniline compounds **a) 3** and **b) 4** in $CDCl_3$.

In the aromatic region of the ^{1}H NMR spectra of the synthesised nitroaniline compounds, three distinct peaks are observed. The proton signal H_f, for the compound containing the electron-withdrawing nitrile group, is observed more downfield compared to the proton signal H_f of the electron-donating methoxy analogue (Figure 2.3). This clearly shows how the electronic effects influence the relative shifts of the aromatic protons.

In all instances, the aromatic protons of the nitroanilines were observed as a doublet (H_f), doublet of doublets (H_d) and a doublet (H_c) except the fluoro- analogue, which gave a very interesting splitting pattern (Figure 2.4a). This is due to the protons coupling to the spin-active fluorine atom.

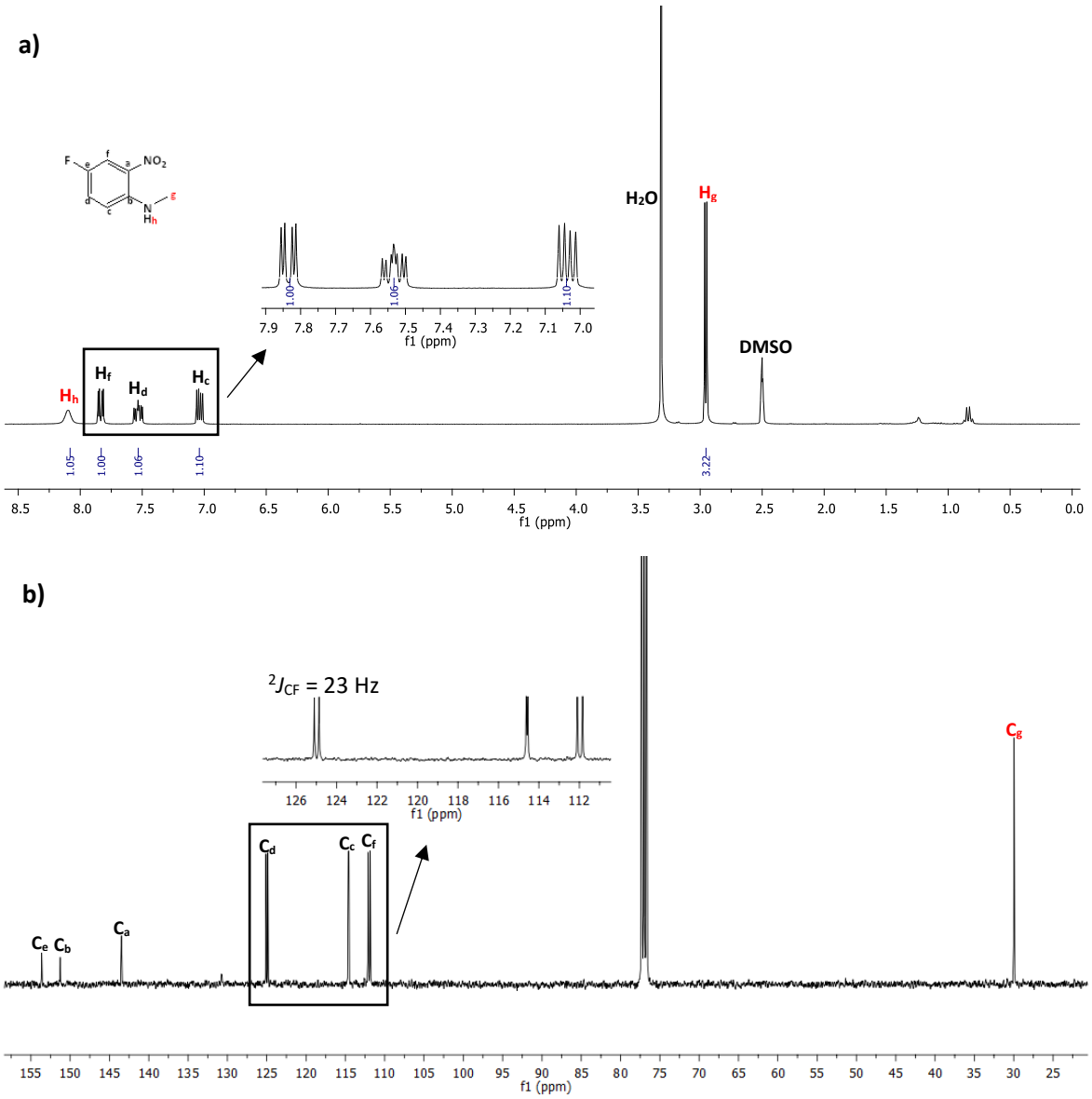

Figure 2.4: a) ^{1}H NMR spectrum of **9** in DMSO-d_6 and **b)** ^{13}C NMR spectrum of **9** in $CDCl_3$.

As a result of the $^{13}C\{^{1}H\}$ NMR spectra not being ^{19}F decoupled, fluorine coupling can also be observed in the 1D $^{13}C\{^{1}H\}$ NMR. In the $^{13}C\{^{1}H\}$ NMR spectra of compound **9** (Figure 2.4b), three distinct doublets are observed. The doublets, observed at 124 and 111 ppm in the $^{13}C\{^{1}H\}$ NMR spectrum, display *J*-values in the range of 23 – 26 Hz which is typical for that observed for a $^{2}J_{CF}$ coupling.

The $^{13}C\{^{1}H\}$ NMR spectra of the nitroaniline compounds synthesised (**1** – **16**), generally show six signals in the aromatic region, of which three signals appear as relatively less intense quaternary signals (C_a, C_b and C_e), confirming that the compound is tri-substituted.

Furthermore, the ESI mass spectra of compounds **1** – **16** all displayed a molecular ion peak which corresponds to the base peak, further confirming that the desired compounds were obtained.

2.2.2. Synthesis of 1,2-diamines (18 – 33)

The synthesis of the 1,2-diamine compounds (**18** – **33**) involved the reduction of the nitro-group of previously prepared nitroanilines, to the amino moiety. The synthesis was achieved *via* a Zinc/ammonium chloride reduction, wherein the synthesised nitroaniline compounds were reacted with 10 equivalents of ammonium chloride and 20 equivalents of zinc dust (Scheme 2.4). TLC analysis indicated that the reaction was complete after 30 – 45 mins. The diamines were then purified using column chromatography and, in general, isolated as dark brown oils or solids in good yields (34 – 98%).

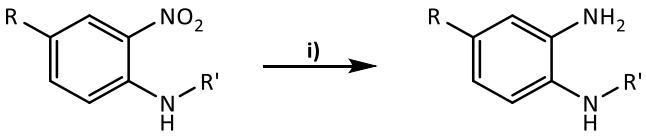

18 – **33**

Scheme 2.4: Synthesis of the 1,2-diamine compounds, Where R' = Me and R = H (**18**), Cl (**19**), OCH_3 (**20**), CN (**21**), CH_3 (**22**), CF_3 (**23**), SO_2CH_3 (**24**), $CONH_2$ (**25**), F (**26**); or Where R' = Pr and R = H (**27**), Cl (**28**), CH_3 (**29**), CN (**30**), SO_2CH_3 (**31**), OCH_3 (**32**), CF_3 (**33**). Reagents and conditions: **i)** Zn/ NH_4Cl/ MeOH/ rt

Compounds **18** – **33** were analysed by ^{1}H NMR spectroscopy, which confirmed that the nitro-moiety was successfully reduced to the amine functionality. A representative example of the ^{1}H NMR spectrum of the reduced amine (compound **22**) is shown in Figure 2.5b. The ^{1}H NMR spectrum of **22** illustrates that upon reduction to the amine moiety, there is a general upfield shift of the aromatic proton resonances.

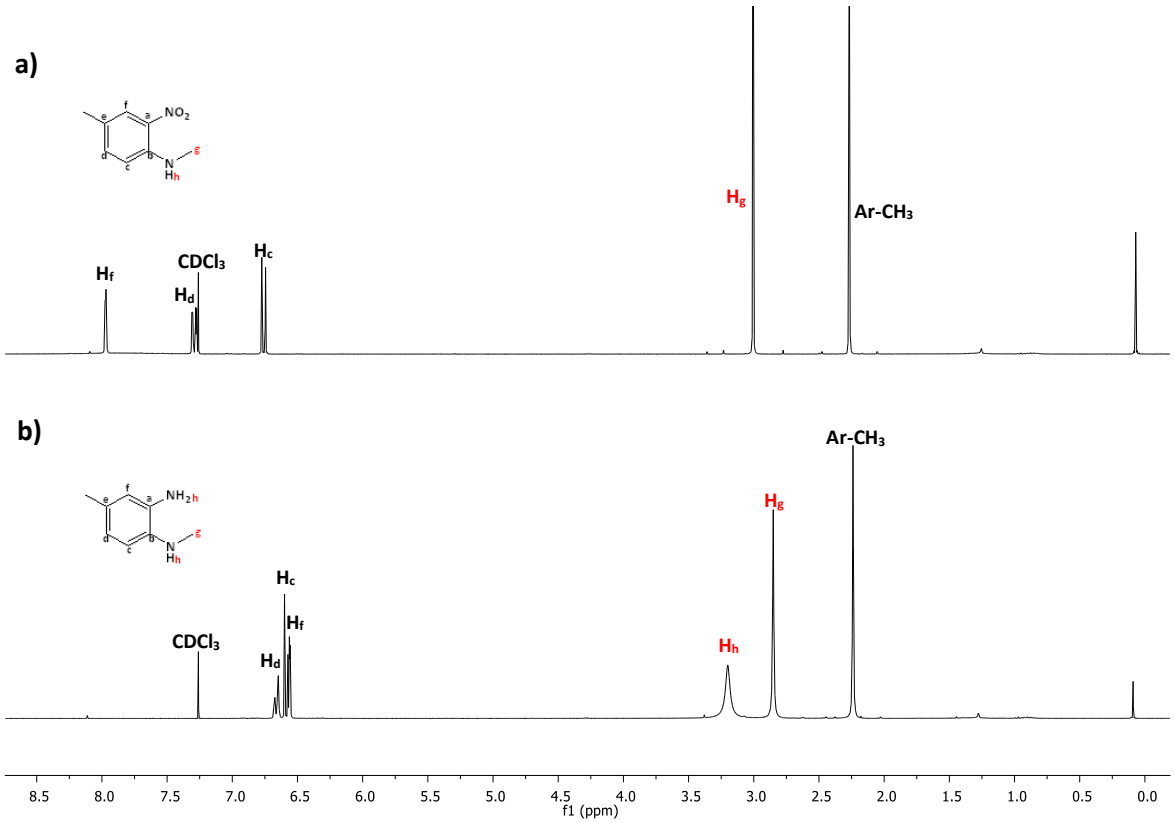

Figure 2.5: ^{1}H NMR spectrum of **a) 5** and **b) 22** in $CDCl_3$.

The signals for the aromatic proton resonances in the product spectrum appear to converge, which may be due to the aromatic protons experiencing similar electronic effects as expected from a 1,2-substituted benzenediamine. No significant change was observed in the aliphatic region of the product spectrum. However, the appearance of a broad singlet at 3.40 ppm, integrating for three protons are assigned to the primary and secondary amine protons of **22**, thus confirming the presence of the primary arylamine.

$^{13}C\{^{1}H\}$ NMR spectroscopy was used to further corroborate the successful synthesis of the 1,2-diamine compounds where the number of expected signals was observed in each spectrum. In the ESI mass spectra of **18** – **33**, a molecular ion peak ($[M]^{+}$) was generally observed, which corresponds to the base peak. Elemental analysis further confirmed the composition of the 1,2-diamine compounds as the data obtained was found to be consistent with expected values.

2.2.3. Synthesis of 2-phenylbenzimidazoles (35 – 50)

The synthesis of the 2-phenylbenzimidazole ligands (**35** – **50**) involved a cyclo-condensation reaction whereby the synthesised 1,2-diamines (**18** – **33**) were reacted with 1.2 equivalents of benzaldehyde and a catalytic amount of TFA (Scheme 2.5).

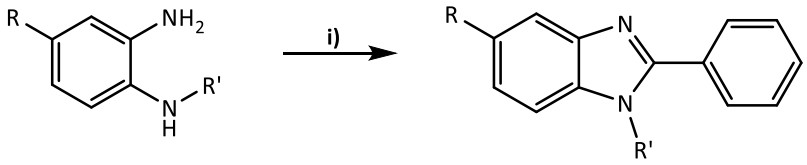

35 – **50**

Scheme 2.5: Synthesis of the 2-phenylbenzimidazoles, Where R' = Me and R = H (**35**), Cl (**36**), OCH_3 (**37**), CN (**38**), CH_3 (**39**), CF_3 (**40**), SO_2CH_3 (**41**), $CONH_2$ (**42**), F (**43**); or Where R' = Pr and R = H (**44**), Cl (**45**), CH_3 (**46**), CN (**47**), SO_2CH_3 (**48**), OCH_3 (**49**), CF_3 (**50**). Reagents and conditions: **i)** Benzaldehyde/ TFA/ $MgSO_4$/ EtOH/ rt.

There are many research articles which describe the synthesis and biological evaluation of benzimidazoles.[15, 16] However, the mechanism for the cyclo-condensation reaction by which benzimidazoles are formed from *o*-phenylenediamines is not well-described in literature. Insight into the mechanism of this reaction was provided by a recently reported article where the proposed mechanism involving the synthesis of 2-arylsubstituted benzimidazoles was reported.[17] The reported mechanisms occur *via* a sequence of reactions and was catalysed using either ammonium acetate or tosylic acid.[17, 18] The proposed mechanism for the cyclo-condensation reaction performed in this study is illustrated in Scheme 2.6.

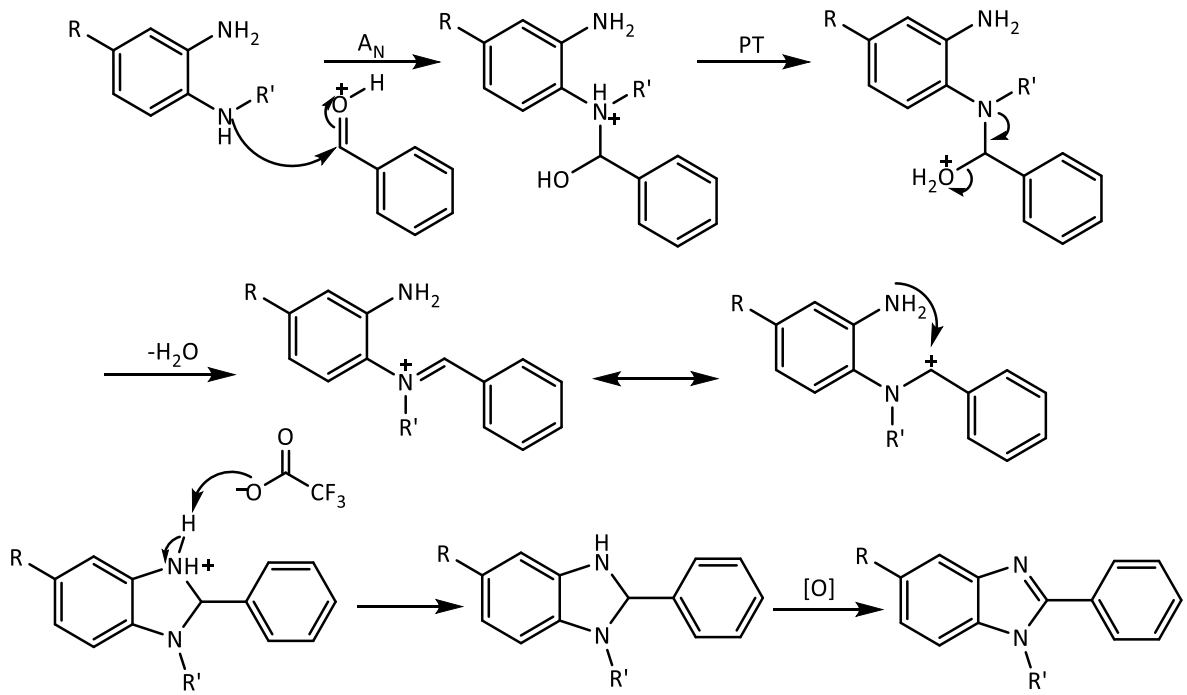

Scheme 2.6: Proposed mechanism for the cyclo-condensation reaction.

Based on the reported mechanisms, the first step in this reaction is a nucleophilic addition promoted by acid catalysis. The secondary amine of the synthesised 1,2-diamine acts as the nucleophile and benzaldehyde acts as the electrophile. The addition of a catalytic amount of TFA is necessary for the protonation of benzaldehyde, resulting in an increase in the electrophilicity of benzaldehyde.

The rate at which the aryl amines react is based on the basicity of the amine. It is well known that more substituted amines are generally more basic, for example, NEt_3 (pKa = 10.8) is more basic compared to NH_3 (pKa = 9.25), and since basicity and nucleophilicity generally follow the same trend, it is proposed that the secondary amine is more reactive towards the carbonyl. Furthermore, it is only addition of the secondary amine onto the carbonyl that results in the formation of the required iminium intermediate. In this way, the nucleophilic diamino complex condenses with the benzaldehyde to form a reactive iminium intermediate, which further undergoes intramolecular nucleophilic addition to afford dihydrobenzimidazole.

Finally, it is proposed in literature that the oxidation of the dihydrobenzimidazole precursor results in the formation of the benzimidazole moiety. It has been reported that oxidation can either be facilitated by an organocatalyst or via air.[18] The mechanism described involves molecular oxygen reacting with the dihydrobenzimidazole to afford hydrogen peroxide and the oxidised benzimidazole. This is achieved through a single electron transfer (SET) mechanism where oxygen heterolytically abstracts the benzimidazole NH to form two radical products ($N^{\cdot}$ and $O^{\cdot}$), which further react when the oxygen radical anion abstracts the second ring proton (C-2 of the ring) to form peroxide and the aromatised benzimidazole.[19] Therefore, for the synthesis of the 2-phenylbenzimidazoles in this study, the reaction flask was left open to air.

The reactions were monitored using TLC analysis. In general, TLC analysis indicated the consumption of starting material and the appearance of two new spots, one of which was slightly more polar than the starting material and the other relatively non-polar. After 24 h, there was no change in the distribution of the two spots with respect to a change in their relative intensities. The reaction was therefore stopped and column chromatography was used to isolate what was believed to be two separate products. The more non-polar product was isolated, albeit the ^{1}H NMR spectrum obtained was too complicated to resolve and no further time was invested in elucidating the identity of the compound. The more polar and major product from the reaction was the 2-phenylbenzimidazole. The 2-phenylbenzimidazoles (**35** – **50**) were all successfully isolated in good yields (37 – 69%) and characterised by spectroscopic techniques.

The ^{1}H NMR spectra of the 2-phenylbenzimidazole compounds (**35** – **50**) show the presence of additional peaks in the aromatic region, which integrate for five protons and are assigned to the protons of the phenyl ring. In total, there are eight protons in the aromatic region and the aromatic resonances appear more downfield, compared to the starting material. In addition, as observed in the Figure 2.6 for compound **36**, the absence of the broad signal at approximately 3.1 ppm further support the absence of the 1,2-diamine functionality.

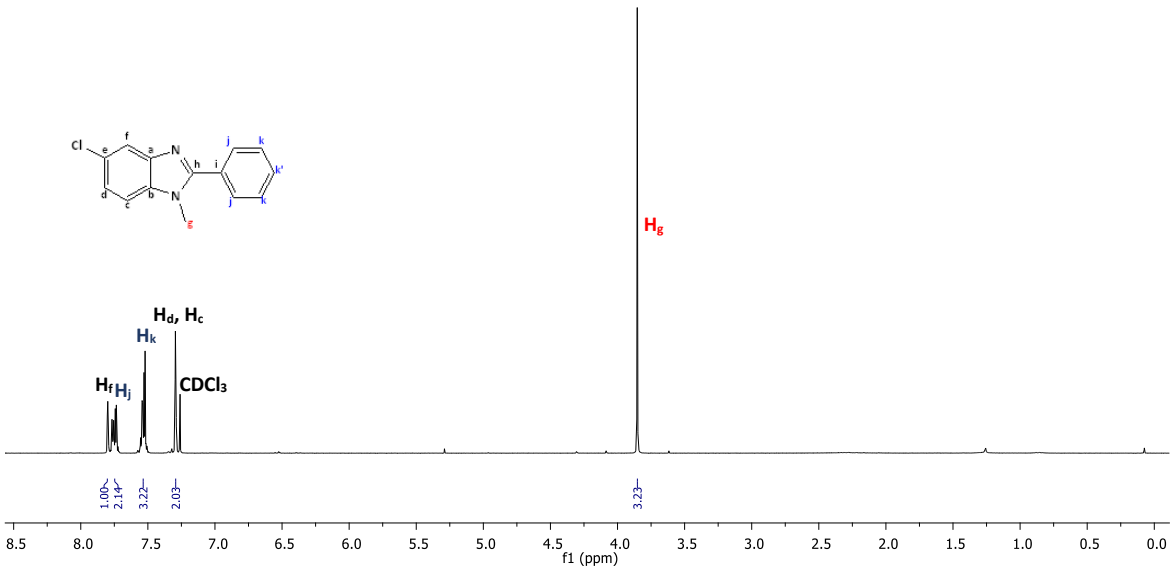

Figure 2.6: ^{1}H NMR spectrum of **36** in $CDCl_3$.

The $^{13}C\{^{1}H\}$ NMR spectral data for compounds (**35** – **50**) further supports the formation of the benzimidazole ring. The number of signals observed in the $^{13}C\{^{1}H\}$ NMR spectra agrees with the number of carbon atoms present in the compounds. Infrared (IR) analysis of the 2-phenylbenzimidazoles (**35** – **50**) was carried out by using attenuated total reflectance (ATR). In the IR spectra, a weak absorption band is observed between 1627 – 1595 cm^{-1}, corresponding to the stretching frequency of the C=N bond. The appearance of the C=N stretch suggests that the benzimidazole ring was obtained due to the C=N stretch being absent in the starting material.

ESI mass spectrometry data was obtained for the 2-phenylbenzimidazoles. Generally a base peak corresponding to either $[M]^+$, $[M-H]^+$ or $[M+H]^+$ was observed, further supporting the integrity of the benzimidazole ligands. The 2-phenylbenzimidazole ligands were also analysed by elemental and LC-MS analyses. From the data obtained, it was found that the 2-phenylbenzimidazole ligands were analytically pure and could be evaluated for antiplasmodial activity.

2.2.4. Synthesis of 2-phenylbenzimidazoles functionalised with water-solubilising H-bonding groups (53 – 54)

Prior to the synthesis of compounds **53** and **54**, results from the biological evaluation of the substituted *N*-methyl and *N*-propyl 2-phenylbenzimidazoles (**35** – **50**), later discussed in Chapter 3 (*vide infra*), provided a criteria for the choice of a methyl group as the R substituent and the propyl chain as the preferred linker.

The synthesis of the benzimidazole ligands containing the water-solubilising groups, involved five synthetic steps (Scheme 2.7). The first three steps were carried out using the same synthetic procedures as described previously in section 2.2.3, for the synthesis of the 2-phenylbenzimidazole ligands containing either a methyl or propyl chain. The fourth step involved deprotection of the terminal amine and then finally, from the synthesised benzimidazole bearing the free amine (**52**), the synthesis of the sulfonamide (**53**), involved a S_NAc reaction and the synthesis of **54** involved a basic S_N2 reaction.

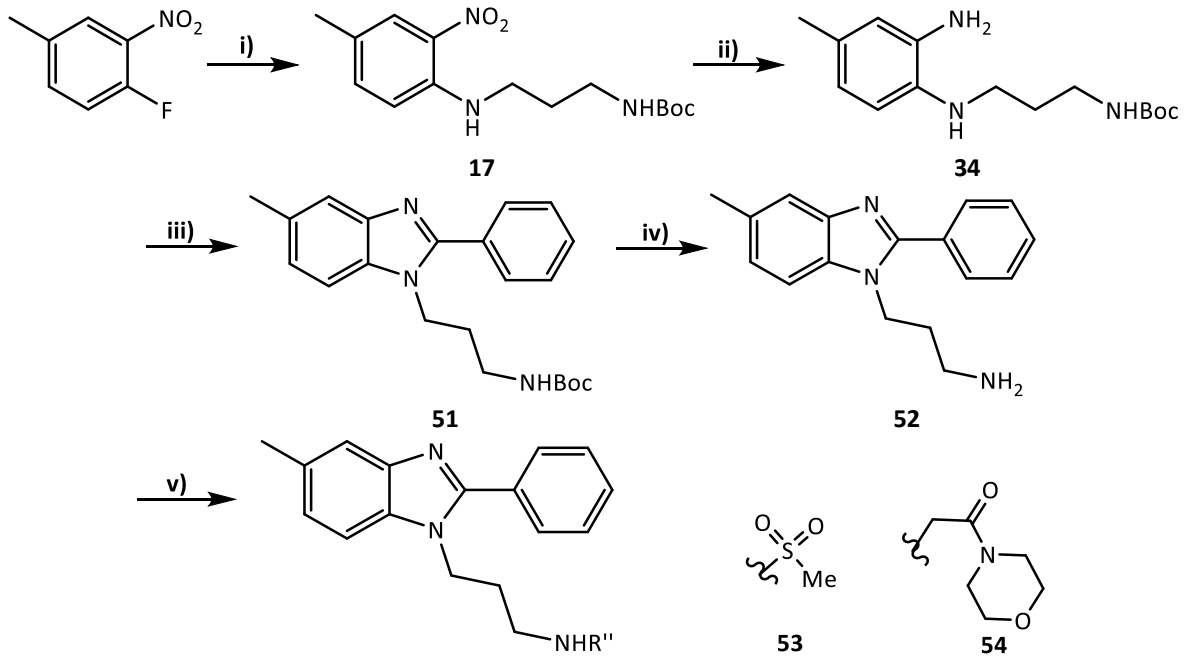

Scheme 2.7: Synthesis of the benzimidazole ligands functionalised with water solubilising H-bonding groups. Reagents and conditions: **i)** 1.1 eq. *N*-Boc-1,3-propanediamine/ DMF/ rt/ 24 h **ii)** Zn/ NH_4Cl/ MeOH/ rt/ 30 min **iii)** benzaldehyde/ TFA/ $MgSO_4$/ EtOH/ rt/ 24 h **iv)** TFA/ DCM/ rt/ 2 h **v)** Compound **53**: MsCl/ NEt_3/ DCM/ 2 h/ 0 °C. Compound **54:** 4-(chloroacetyl)morpholine/ K_2CO_3/ MeCN/ 4 h/ 0 °C.

Preceding the synthesis of the nitroaniline compound **17**, *N*-Boc-1,3-propanediamine was firstly synthesised by the addition of one equivalent of Boc anhydride in 90 mL $CHCl_3$ to an excess amount of 1,3-diaminopropane (60 equivalents). The ^{1}H NMR spectrum of the product confirmed that only one of the primary amines were selectively protected. Successful synthesis of this precursor was further supported by similar shifts observed in the ^{1}H NMR spectrum of the same compound previously reported in literature.[20]

The synthesis of **17** involved the reaction of 1-fluoro-2-nitrotoluene with the synthesised Boc-protected diamine. The reaction was monitored using TLC analysis, which revealed the formation of a more polar product. A base was not added to the reaction and despite the formation of HF in the reaction, the ^{1}H NMR spectrum indicated that the Boc functionality was still intact.

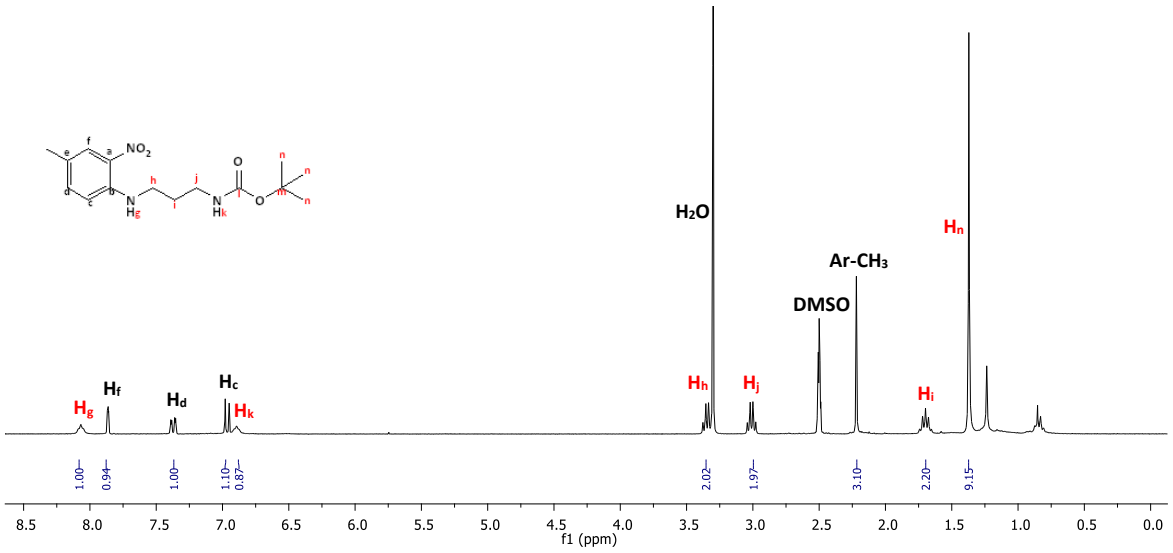

Figure 2.7: ^{1}H NMR spectrum of **17** in DMSO-d_6.

Figure 2.7 displays the ^{1}H NMR spectrum of **17**. The two broad singlets in the aromatic region are assigned to the two secondary amines (H_g and H_k). Due to the electron-withdrawing nitro-group, the proton representing the amine directly attached to the aromatic ring appears to be more deshielded. The singlet at 1.38 ppm integrates for a total of nine protons and is representative of the *t*-butyl group. The two peaks at 3.36 and 3.03 ppm are assigned to the methylene protons adjacent to the secondary amines. These peaks appear as distinct quartets due to coupling of the protons of the amine and those of the neighbouring methylene group.

As previously discussed, it is evident from the ^{1}H NMR spectrum (Figure 2.8b) that the nitro-group was successfully reduced to the amine moiety. Upon reduction of the nitro- moiety, the aromatic protons shifted upfield and seem to converge due to the effects of the 1,2-diamine substituted ring. The introduction of a broad singlet at 4.38 ppm, integrating for two protons, further confirmed the presence of a primary amine. Successful cyclisation of **34** is evidenced by the observed resonances in the aromatic region of the ^{1}H NMR spectrum of **51** (Figure 2.8c), which integrate for a total of eight protons. The absence of the two broad singlets assigned to the primary amine and secondary amine directly attached to the ring further confirms the successful synthesis of the benzimidazole ring.

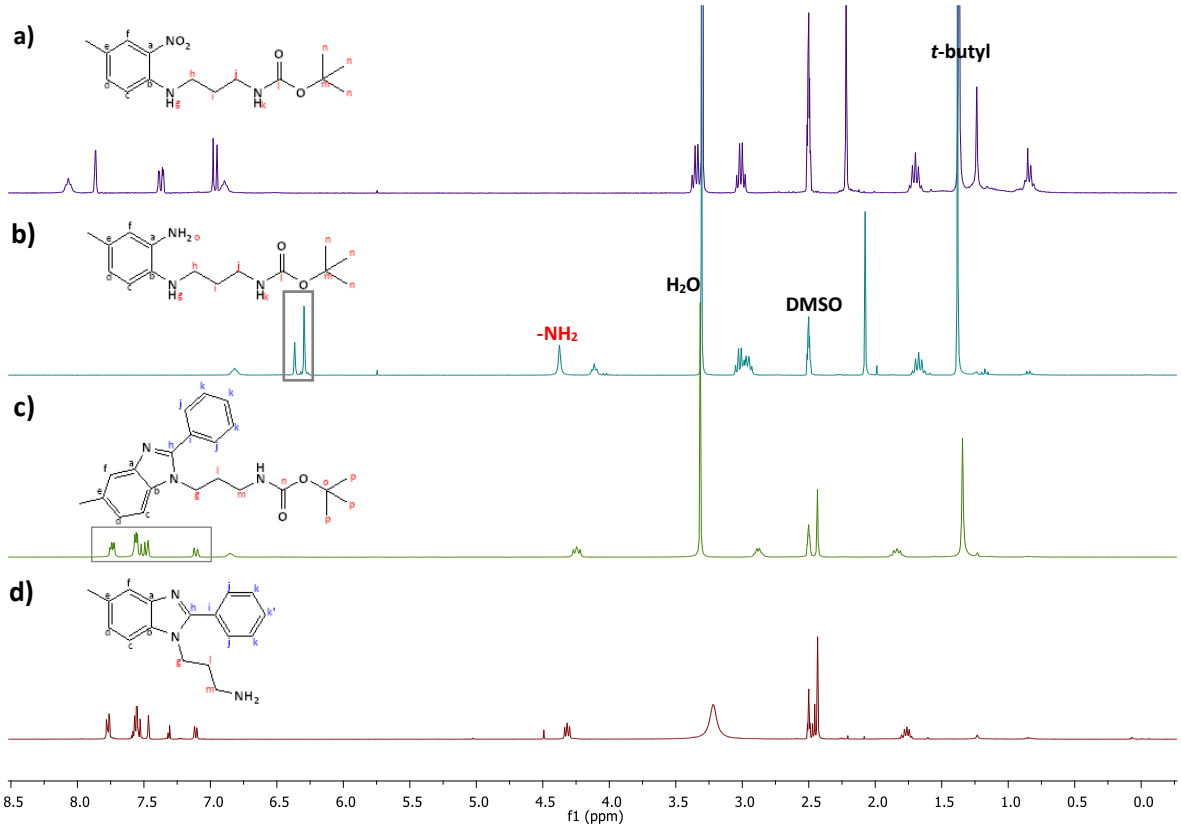

Figure 2.8: ^{1}H NMR spectra of **a) 17**, **b) 34**, **c) 51** and **d) 52** in DMSO-d_6.

Deprotection of the Boc group was obtained by reacting **52** with an excess amount of TFA. After 2 h, TLC analysis showed the consumption of starting material and the formation of a new more polar product spot. The product was isolated as a light brown oil in excellent yield (97%). The ^{1}H NMR spectrum (Figure 2.8d) confirmed that the deprotection was successful. The distinct singlet assigned to the *t*-butyl group initially observed at 1.38 ppm, was no longer present in the product spectrum. ESI mass spectrometry further supports the formation of

compound **52**, where a base peak at *m/z* 265.0131 corresponding to the molecular weight of the compound, was observed.

The synthesis of the benzimidazole containing the sulfonamide group involved a SNAc reaction where the synthesised benzimidazole functionalised with a free amine (**52**) was reacted with one equivalent of methanesulfonyl chloride and 1.1 equivalents of triethylamine in DCM (Scheme 2.8).

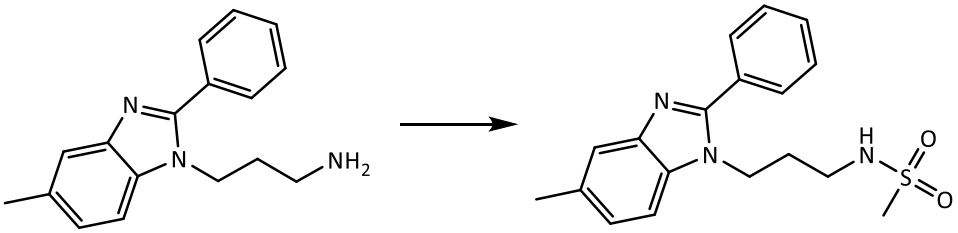

Scheme 2.8: Synthesis of **53**. Reagents and conditions: **i)** MsCl/ NEt_3/ DCM/ 2 h/ 0 °C.

After 24 h, TLC analysis indicated the formation of a new product. However, isolation of the product formed proved to be challenging due to the solubility of the product. After the crude material was washed with ammonium chloride and extracted with EtOAc, there was still product present in the aqueous layer. The aqueous layers were then collected and reduced *in vacuo.* The crude residue was then purified using column chromatography to afford the desired compound as a light brown oil in very poor yield (6%).

In the ^{1}H NMR spectrum (Figure 2.9), a sharp singlet is observed at 2.79 ppm which integrates for three protons. This key peak confirmed the successful substitution of the methyl sulfonyl moiety onto the 2-phenylbenzimidazole ligand. A broad singlet is also observed at 4.18 ppm which is assigned to the secondary amine of the sulfonamide. Further support that the sulfonamide was obtained is given by LC-MS data, which showed a molecular ion peak of m/z 393.9 (t_R = 2.36 min) for this compound.

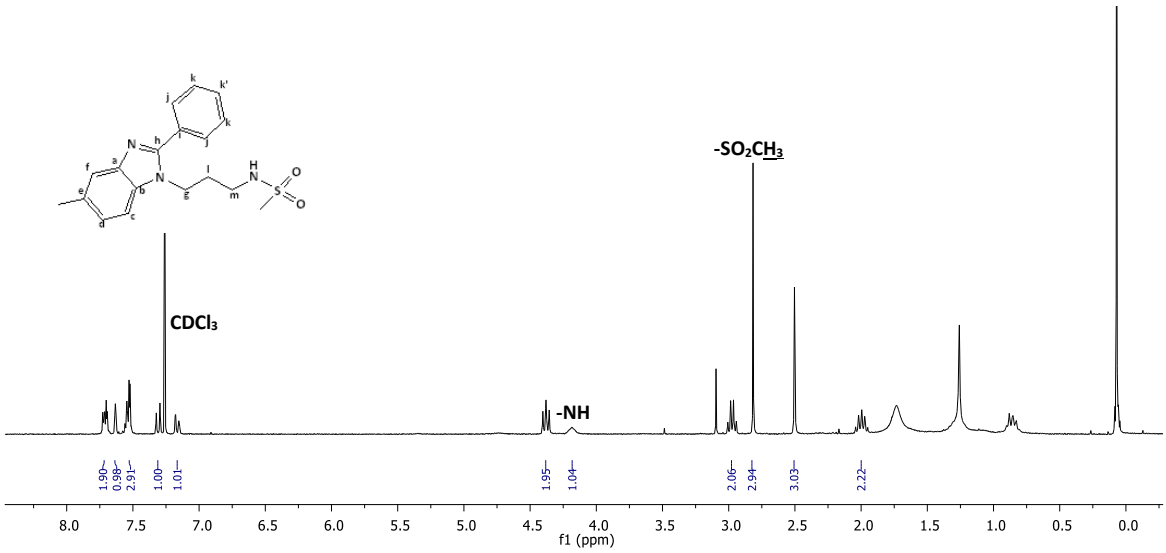

Figure 2.9: ^{1}H NMR spectrum of **53** in $CDCl_3$.

The synthesis of **54** involved an *N*-alkylation of the benzimidazole ligand (**52**) bearing the free amine moiety with 4-(chloroacetyl)morpholine (Scheme 2.9). Compound **52** was dissolved in acetonitrile, thereafter 1.05 equivalents of K_2CO_3 and 4-(chloroacetyl)morpholine was added to the reaction flask at 0 °C. Upon addition of 4-(chloroacetyl)morpholine, the reaction mixture turned cloudy. After 4 h, the reaction was allowed to warm to rt.

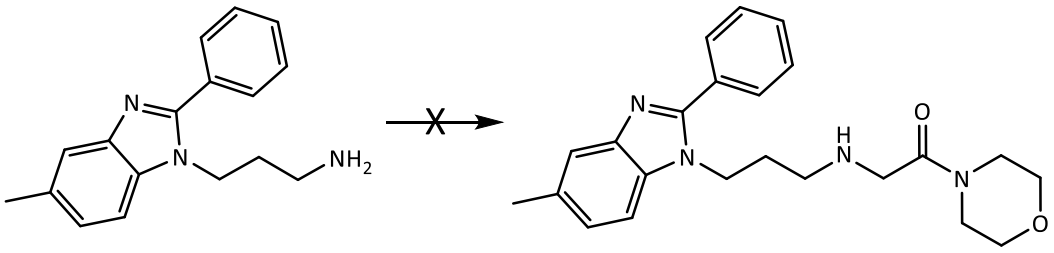

Scheme 2.9: Synthesis of **54**. Reagents and conditions: **i)** 4-(chloroacetyl)morpholine/ K_2CO_3/ MeCN/ 4 h/ 0 °C.

TLC analysis using a solvent system of 1:9 MeOH:EtOAc, showed the formation of two new product spots. The crude material was then purified using column chromatography. Unfortunately, only one of the products were isolated due to the other product being very polar. A light brown oil was obtained in moderate yield (38%).

In the ^{1}H NMR spectrum of **54** (Figure 2.10), there is evidence to suggest that the desired product was not obtained. In fact, the spectrum suggests the formation of a benzimidazole ligand which is doubly substituted with the morpholine moiety. Two broad peaks are

observed between 3.42 and 3.61 ppm and integrate for a total of sixteen protons. A sharp singlet is also observed at 3.36 ppm and integrates for four protons.

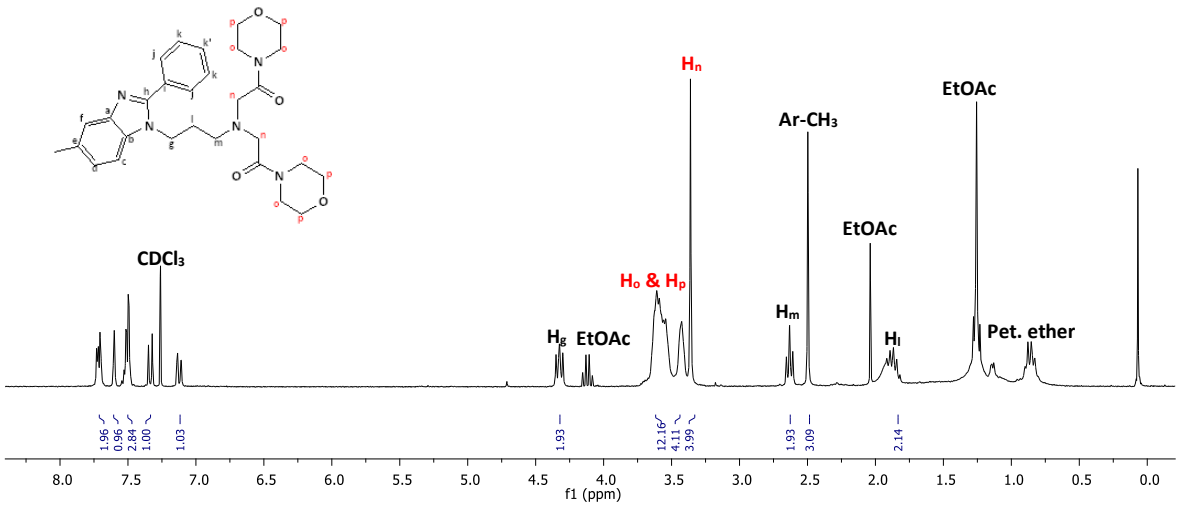

Figure 2.10: ^{1}H NMR spectrum of **54** in $CDCl_3$.

Further proof of the formation of this unexpected product can be observed from LC-MS, where a molecular ion peak is observed and corresponds to the base peak. The antiplasmodial activity and solubility of the isolated compound was also evaluated since it was still much more polar than the first series of 2-phenylbenzimidazole ligands.

3.2. Synthesis of Ru(II) and Ir(III) cyclometallated benzimidazole complexes (55 – 68)

The cyclometallation of the selected 2-phenylbenzimidazole ligands was achieved via sodium acetate mediated C-H activation (Scheme 2.10). The synthesis of these complexes was conducted as follows:

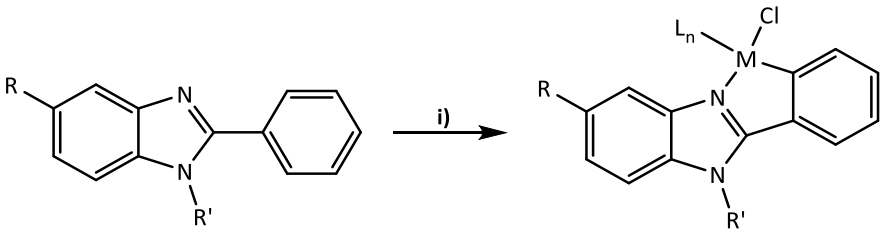

55 – 68

Scheme 2.10: Synthesis of the cyclometallated benzimidazole complexes, where M = Ru, L_n = *p*-cymene and R' = Me; R = H (**55**), Cl (**56**), CH_3 (**57**), CF_3 (**58**), SO_2CH_3 (**59**) or where M = Ir and L_n = Cp* and R' = Me; R = H (**60**). Where M = Ru, L_n = *p*-cymene and R' = Pr; R = H (**61**), Cl (**62**), CH_3 (**63**), CF_3 (**64**) or where M = Ir and L_n = Cp* and R' = Pr; R = H (**65**), Cl (**66**), CH_3 (**67**), CF_3 (**68**). Reagents and conditions: **i)** Metal dimer/ NaOAc/ DCM/ rt.

Selected substituted 2-phenylbenzimidazole ligands were dissolved in DCM and 1.2 equivalents of NaOAc added to the reaction flask. After 10 min of stirring, 0.5 equivalents of either dichloro(*p*-cymene)ruthenium(II) dimer or pentamethylcyclopentadienyliridium(III) dimer was added to the reaction flask. The dichloro(*p*-cymene)ruthenium(II) dimer and pentamethylcyclopentadienyliridium(III) dimer were previously synthesised and used without further purification.[21, 22]

Generally, the synthesis of cyclometallated complexes is achieved via intramolecular C-H activation in the presence of a suitable base. To activate the C-H bond, harsh reaction conditions and a strong base are typically required.[23, 24] However, the discovery made by the Davies group in 2003, has led to a new efficient method for C-H activation.[25] The reported method involved the cyclometallation of nitrogen donor ligands (amines, imines and oxazolines) with $[MCl_2Cp^*]_2$ (M = Ir/Rh) or $[RuCl_2$-(*p*-cymene)$]_2$, which occurred at room temperature and was promoted by sodium acetate.[25]

Although the detailed mechanism and the role(s) of the acetate is not clear, experimental and theoretical studies conducted by Davies *et al.,* have resulted in the identification of key intermediates. A vacant site is needed for C-H activation to occur. It is therefore proposed that initially the loss of an anion (Cl^-) is necessary.[25] Density functional theory calculations performed by Davies *et al.* on the cyclometallation of dimethylbenzylamine with $[Pd(OAc)_2]$, suggested that the reaction proceeds *via* an agostic C-H complex, where the acetate was found to stabilise the agostic intermediate through hydrogen bonding.[26] A low-energy pathway was also proposed, which involved intramolecular H-bonding to the acetate functionality.[27] Based on literature, a proposed transition state for this study is illustrated in Figure 2.11.

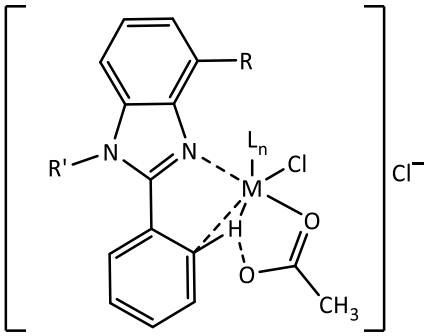

Figure 2.11: Proposed transition state of C-H activation mechanism resulting in the formation of a cyclometallated complex, where L_n = *p*-cymene or Cp*

The proposed pathway in literature was reported to occur via a single, low-energy six-membered transition state, involving the proximal acetate arm being displaced by the incoming C-H bond. The H is transferred to the dissociated acetate arm and the acetate is coordinated through the carbonyl oxygen.[27]

The synthesis of the Ru(II) and Ir(III) cyclometallated benzimidazole complexes (**55** – **68**) did not require any harsh reaction conditions. The ruthenium and iridium complexes were isolated as green or yellow solids in good to excellent yields (41 – 98%) and were stable at room temperature. The structures of these complexes were confirmed by spectroscopic analysis.

Analysis of the ^{1}H NMR spectra of the metal complexes (**55** – **68**), confirmed the successful synthesis of the cyclometallated complexes. The ^{1}H NMR spectrum of the *N*-methyl (methyl substituted) Ru benzimidazole complex **57** (Figure 2.12b) is shown below. As a result of metal coordination onto the phenyl ring, the aromatic signals which previously integrated for eight protons, now integrate for a total of seven protons. In addition, the resonances in the aromatic region of the ^{1}H NMR spectrum of the metal complex appear to be more distinct compared to the aromatic resonances observed in the ^{1}H NMR spectrum of the benzimidazole ligand (Figure 2.12a).

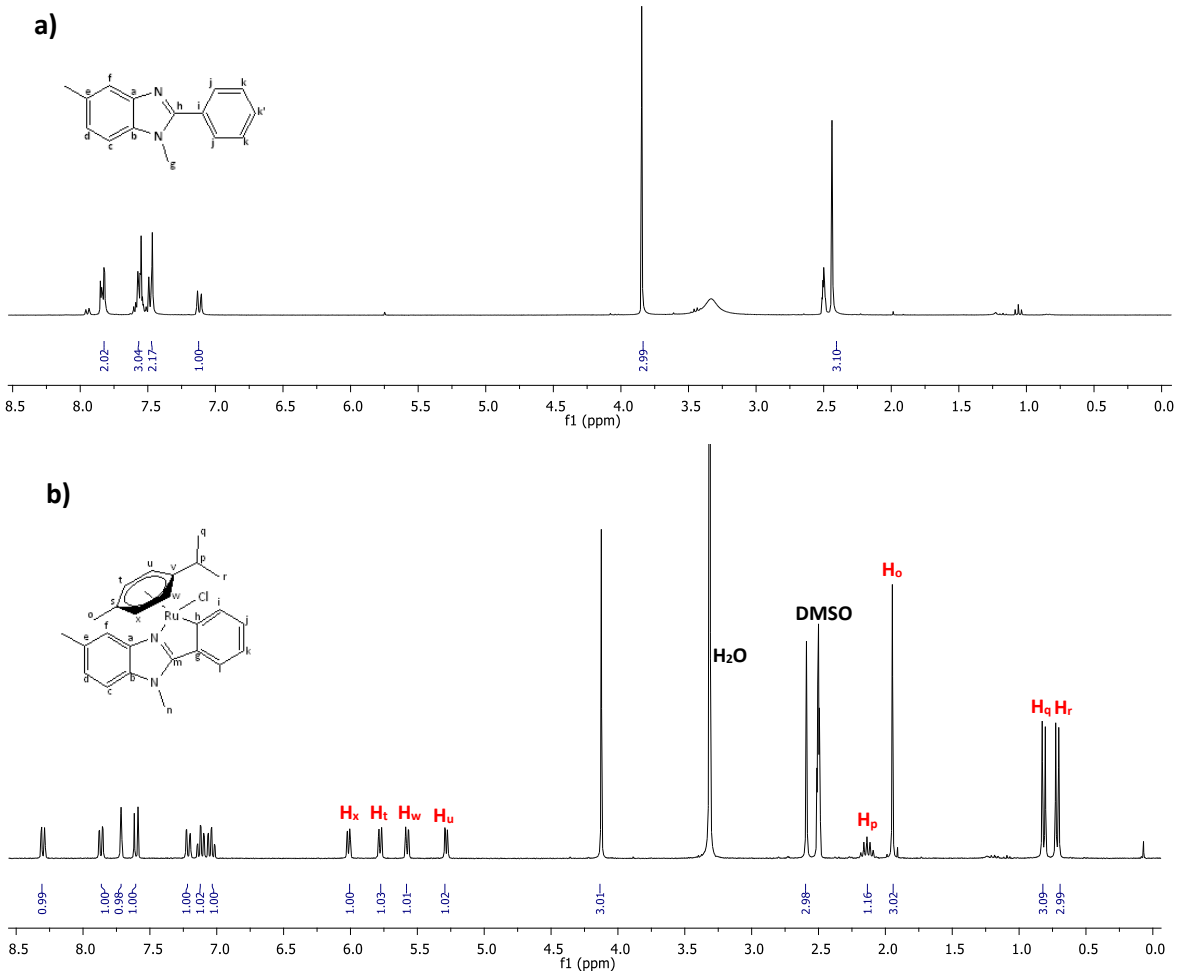

Figure 2.12: ^{1}H NMR spectra of **a)** benzimidazole ligand **39** and **b)** *N*-methyl (methyl) Ru benzimidazole complex **57** in DMSO-d_6.

From the ^{1}H NMR spectra of the ruthenium complexes, four separate doublets between 6.02 – 5.29 ppm, a multiplet at 2.15 ppm, a singlet at 1.96 ppm and two doublets between 0.82 and 0.72 ppm, are also observed (Figure 2.12b). These resonances correspond to the *p*-cymene ligand and further confirmed the formation of the ruthenium complex. Due to the

p-cymene ligand now having less freedom of rotation, the aromatic protons of the *p*-cymene moiety appear as four separate doublets (H_t, H_u, H_v, H_w) as opposed to two doublets observed in the free metal-dimer. Similarly, the methyl protons of the isopropyl group appear as two distinct doublets (H_q and H_r), due to the chirality induced by the metal centre.

In the ^{1}H NMR spectrum of the *N*-propyl (methyl substituted) Ru cyclometallated benzimidazole complex (**63**), two distinct peaks are observed at 4.45 and 4.31 ppm. These two peaks are assigned to the methylene protons adjacent to the tertiary amine. HSQC further confirmed that the two proton signals are assigned to one carbon peak. The change from an apparent triplet before complexation to two distinct signals is likely due to the methylene protons being diasterotopic, as a result of the stereogenic centre created through metal complexation.

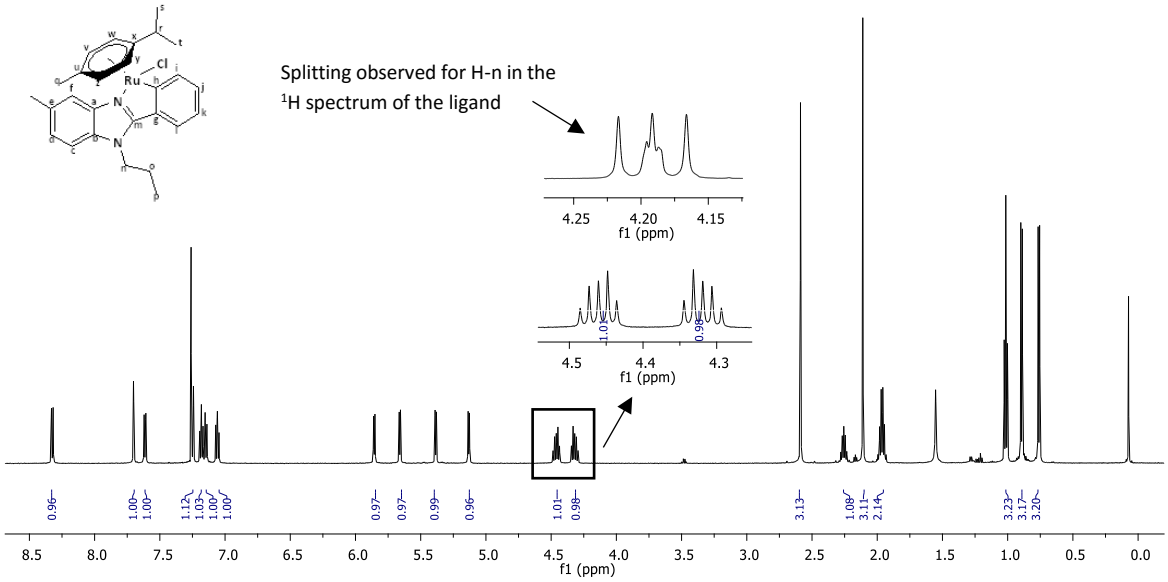

Figure 2.13: ^{1}H NMR spectrum of *N*-propyl (methyl) Ru benzimidazole complex **63** in $CDCl_3$.

The ^{1}H NMR spectrum of **62** confirmed that metal complexation was also successful. However, a second set of mirroring signals of relatively low intensity were observed. This was of concern due to the need to obtain a pure complex for biological testing. These peaks each integrated for 0.10 relative to the major signals. Interestingly, the observed peaks did not correspond to starting material (unreacted metal dimer or ligand).

The doubling of signals is generally a result of either the presence of diastereomers or conformational isomers (rotamers).[28] Since the metal centre only contains one static stereogenic element, the possibility of diastereomers, which require the presence of more than one stereogenic element, was ruled out and thus suggested that rotamers may exist. ^{1}H NMR spectroscopy was therefore performed at a higher temperature of 80 °C, the peaks which initially integrated for 0.10 integrated for 0.01 thereafter. This phenomenon provides evidence that in solution, rotamers do exist. The presence of rotamers may be due to the rotation of the *p*-cymene ligand about the metal-ligand bond.

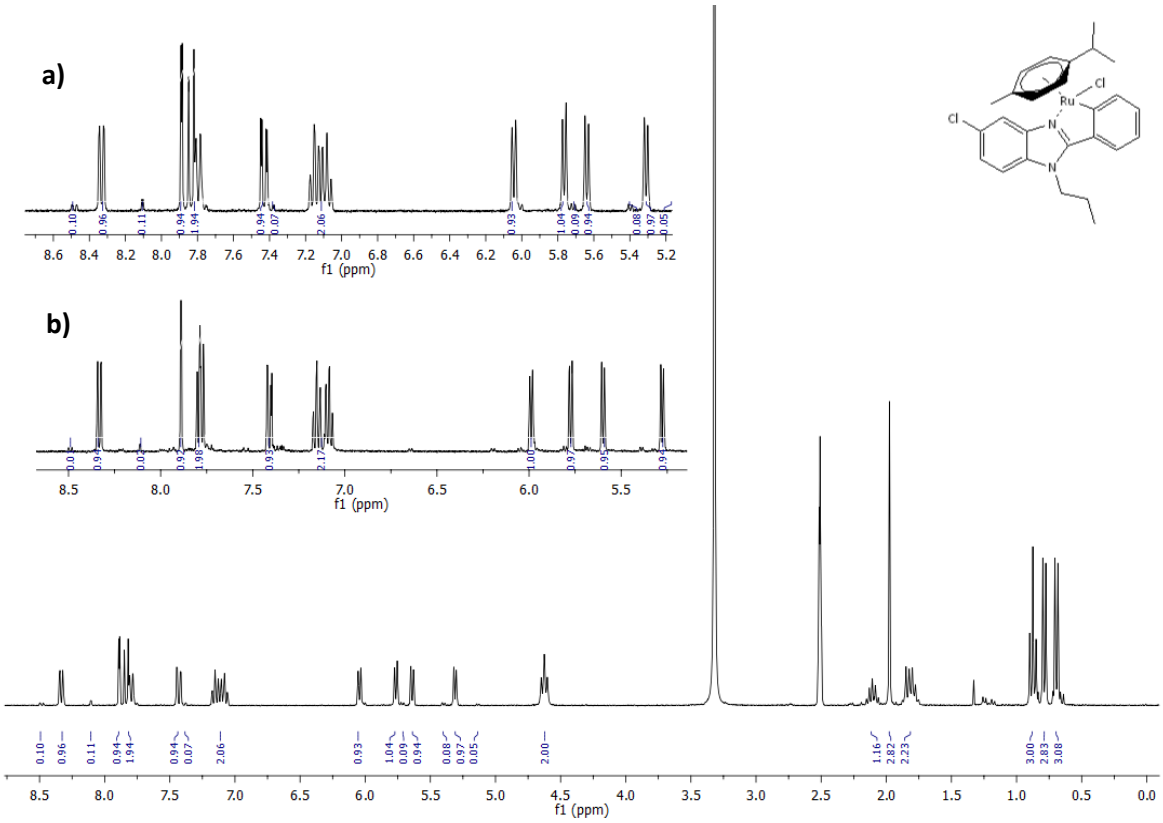

Figure 2.14: ^{1}H NMR spectrum of **62** in DMSO-d_6, where **a)** expanded region at rt and **b)** at 80 °C

^{13}C{^{1}H} NMR spectroscopy was also used to confirm that complexation had been successful. The aromatic carbon resonances for the *p*-cymene ligand is observed between 75 – 90 ppm and 2D NMR techniques such as HSQC and COSY, were used to confirm the assignments made.

The structures of the Ir(III) cyclometallated complexes were also confirmed by spectroscopic and analytical methods. Similarly, in the ^{1}H NMR spectrum of the Ir Cp* cyclometallated

benzimidazole complexes (Figure 2.15), the absence of one aromatic proton, relative to the benzimidazole starting material, supports metal complexation. Additionally, the appearance of a singlet at 1.76 ppm, which integrates for fifteen protons is assigned to the Cp* ligand and further confirmed that the metal is coordinated and that the Ir complexes were successfully synthesised.

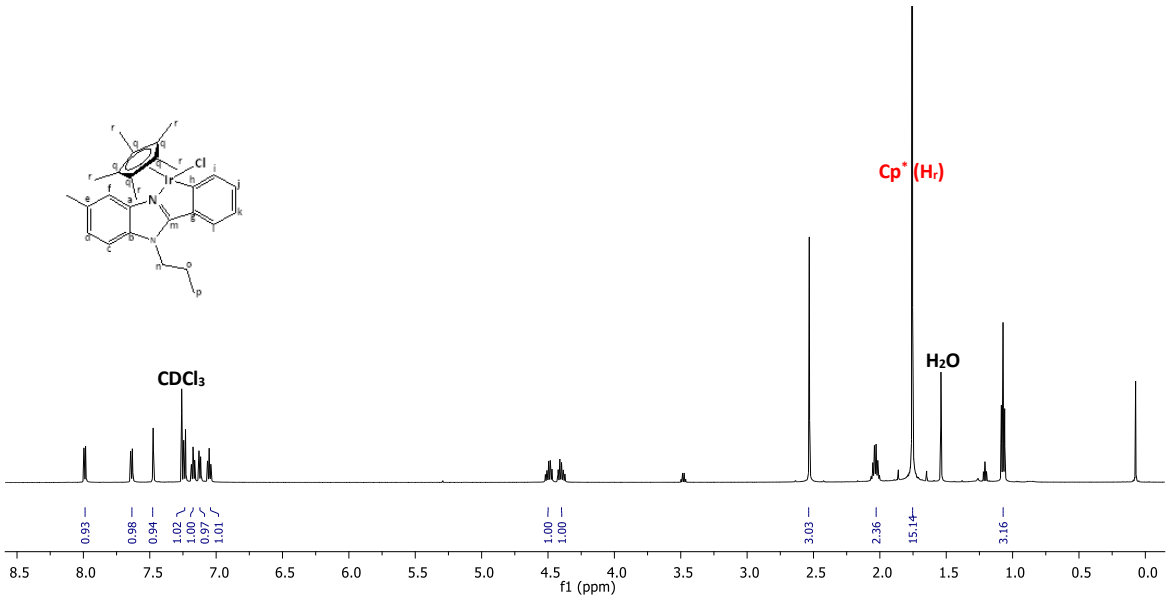

Figure 2.15: ^{1}H NMR spectrum of **67** in $CDCl_3$

In the $^{13}C\{^{1}H\}$ NMR spectra of the Ir(III) complexes, a distinct peak assigned to the methyl substituents on the Cp* moiety is observed at approximately 9.00 ppm. 2D NMR spectroscopy was used to confirm the assignments made.

In addition to ^{1}H and $^{13}C\{^{1}H\}$ NMR spectroscopy, infrared (IR) spectroscopy is also a useful technique used to substantiate successful metal complexation. IR spectroscopy data was obtained for metal complexes **55** – **68**. In the IR spectra of the complexes, a weak absorption band was observed around 1586 – 1577 cm^{-1}, which was assigned to the imine (C=N) stretching frequencies. In the IR spectra (Figure 2.16), the imine stretch for the ligand is observed at 1627 cm^{-1} and after complexation, a shift to 1586 cm^{-1} is observed.

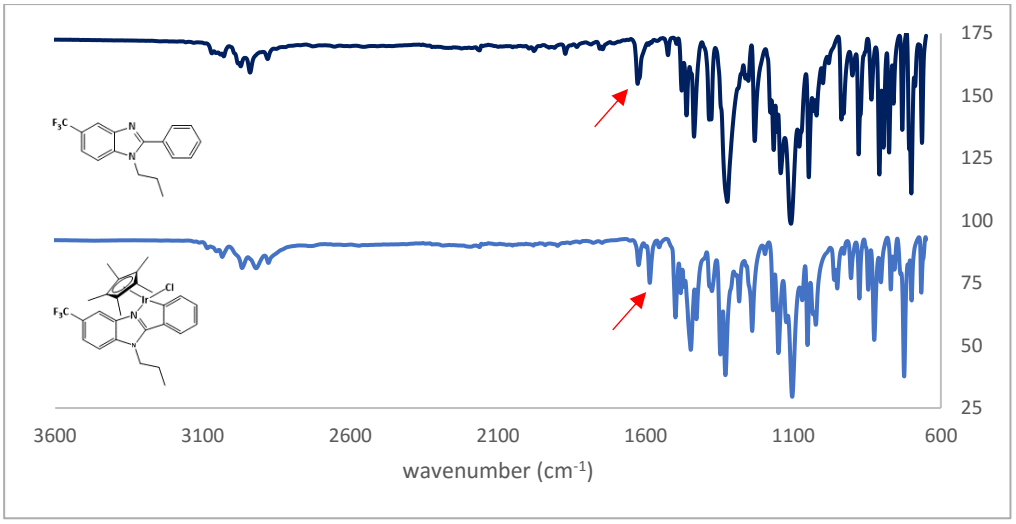

Figure 2.16: Infrared spectra of the ligand **50** (dark blue) and complex **68** (light blue).

A frequency shift of the imine absorption band observed for the corresponding benzimidazoles to lower frequencies often confirms coordination of the metal centre to the imine nitrogen. This phenomenon is explained by the synergistic effect that take place on coordination of the metal, where there is sigma donation from the benzimidazole nitrogen and subsequent back-donation of electron density from the metal (Figure 2.17). This effect results in the strengthening of the M-N bond and subsequent weakening of the C=N bond. Thus, the decrease in the wavenumber of the C=N band in the infrared spectrum is due to the weakening of the C=N bond.

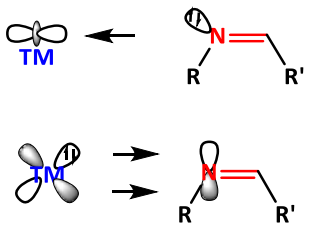

Figure 2.17: Schematic representation of the TM-N=C orbital interactions in the cyclometallated benzimidazole complexes. C=N → TM σ- donation (top) and TM → N=C π- back-donation (bottom)

All Ru(II) and Ir(III) complexes were analysed using high resolution ESI mass spectrometry, which further supported the successful synthesis of the cyclometallated benzimidazole complexes. In general, the mass spectrum of the complexes show base peaks which correspond to the molecular ion without the chloride ion, $[M\text{-}Cl]^+$. Elemental analysis of all the complexes also attested to the chemical composition for the proposed structures.

Single crystal X-ray diffraction

The molecular structures of the Ir(III) complexes **67** and **68** were elucidated by single crystal X-ray diffraction. Single crystals of each complex were obtained by the slow diffusion of a concentrated chloroform/ethyl acetate mixture. The crystal data and refinement parameters for both complexes are summarised in Table 2.1 Compound **67** crystallised as red blocks in the monoclinic space group $P2_1/c$, whereas compound **68** crystallised as orange blocks in the triclinic space group $P\bar{1}$.

Table 2.1: Crystallographic data and refinement parameters for complexes **67** and **68**.

	Complex 67	**Complex 68**
Chemical formula	$C_{27}H_{32}ClIrN_2$	$C_{27}H_{29}ClF_3IrN_2$
Formula weight	612.22	666.19
Crystal system	monoclinic	triclinic
Space group	$P2_1/c$ (No. 14)	$P\bar{1}$ (No. 2)
a, b, c (Å)	10.9895(8), 12.3159(9), 18.2121(13)	8.9926(7), 11.817(1), 12.0582(10)
α, β, γ (˚)	90, 99.465(2), 90	82.592(1), 77.641(1), 84.652(1)
V (Å^3)	2431.4(3)	1238.38(18
Z	4	2
D (g.cm^{-3})	1.673	1.787
μ (mm^{-1})	5.618	5.540
F (000)	1208	652
Crystal size (mm)	0.21 x 0.26 x 0.32	0.21 x 0.26 x 0.31
T (K)	173	173
Scan range/ ˚	1.9 < Θ < 28.4	1.7 < Θ < 28.3
Unique reflections	6077	5949
R_{int}	0.073	0.039
Reflections used [I > 2σ(I)]	5003	5248
R indices (all data)	R 0.0253, wR2 0.0532, S 1.04	R 0.0275, wR2 0.0517, S 1.02
Goodness-of-fit	1.040	1.021
Max, Min Δρ (e Å^{-3})	-0.93, 1.62	-1.30, 1.00

The ORTEP diagrams of complexes **67** and **68** are shown in Figure 2.18. The crystallographic analysis confirmed that the Ir(III) complexes adopts a “three-legged piano-stool” structure, where the pentamethylcyclopentadiene (Cp*) ligand forms the seat of the piano-stool and the three legs of the stool are formed from the chloride and chelating ligand. The piano-stool

structure is also commonly observed in many other iridium, ruthenium and rhodium half-sandwich complexes reported in literature.[29-31]

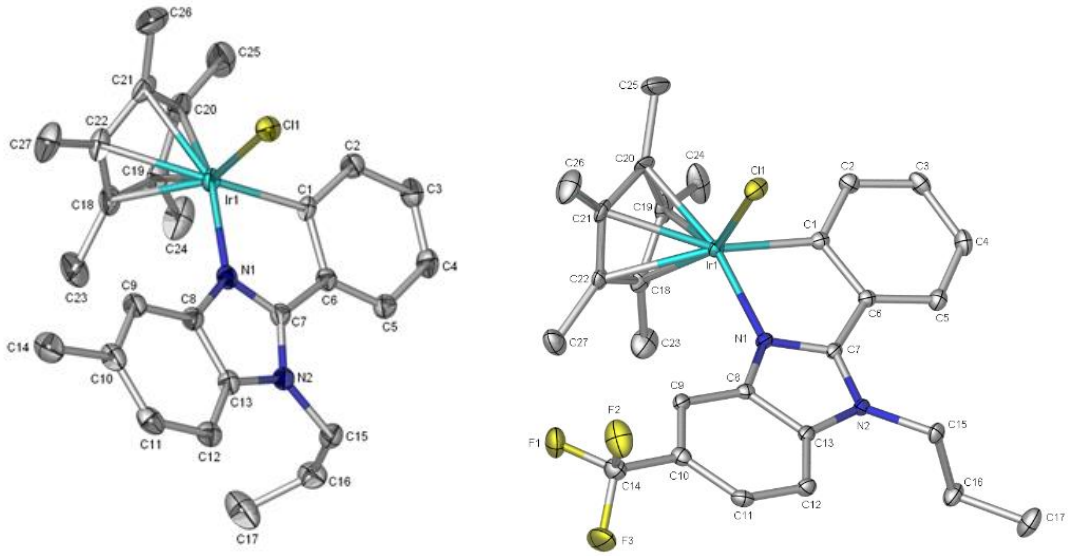

a **b**

Figure 2.18: X-ray crystallographic ORTEP diagram of Ir Cp* cyclometallated benzimidazole complexes **a) 67** and **b) 68**, where thermal ellipsoids are drawn at 50% probability level.

Selected bond distances and angles are listed in Table 2.2. The crystallographic data suggests that the geometry around the metal centre is pseudo-tetrahedral, which is typically observed in piano-stool structures. The bond angles ranging between 77 and 89˚ around the metal centre are clearly not in agreement with the angles observed for a tetrahedral (109.5˚) or a square planar (90˚) geometry. The data obtained also suggests that the benzimidazole ring and the phenyl ring are not coplanar.

The bond distances obtained for both complexes were comparable. The distance between the metal centre and the carbon atoms of the Cp* ligand ranges between 2.143 and 2.265 Å. The bond distance between the metal centre and the chloride ligand is approximately 2.4 Å, whereas the distance between the metal centre and the two chelating atoms ranges between 2.050 and 2.079 Å.

Table 2.2: Selected bond distance and bond angles.

	Complex 67	Complex 68
Selected bond distances (Å)		
Ir(1) – Cl(1)	2.4114(9)	2.4054(10)
Ir(1) – N(1)	2.072(2)	2.079(2)
Ir(1) – C(1)	2.062(3)	2.050(4)
N(1) – C(7)	1.345(4)	1.337(4)
Ir(1) – C(18)	2.173(3)	2.157(4)
Ir(1) – C(19)	2.143(3)	2.159(4)
Ir(1) – C(20)	2.177(4)	2.144(4)
Ir(1) – C(21)	2.205(4)	2.247(4)
Ir(1) – C(22)	2.257(3)	2.265(4)
Selected bond angles (˚)		
Cl(1) – Ir(1)– C(1)	89.04(9)	87.40(10)
N(1) – Ir(1) – C(1)	77.09(12)	77.05(12)
Cl(1) – Ir(1) – N(1)	88.86(7)	86.40(7)

3.3. Summary

A series of 2-phenylbenzimidazole ligands and corresponding Ru(II) and Ir(III) cyclometallated complexes were successfully synthesised. All compounds were characterised fully using standard spectroscopic and analytical techniques such as ^{1}H, $^{13}C\{^{1}H\}$, COSY, HSQC NMR spectroscopy, IR spectroscopy and ESI-mass spectrometry. Single crystal X-ray structure analysis of complexes **67** and **68**, further confirmed the molecular structure of the iridium complexes in the solid state. The purity of the target compounds was supported by elemental analysis and LC-MS data.

References

1. J. N. Dominguez, J. E. Charris, G. Lobo, N. Gamboa de Dominguez, M. a. M. Moreno, F. Riggione, E. Sanchez, J. Olson and P. J. Rosenthal, *Eur. J. Med. Chem.*, 2001, **36**, 555-560.
2. C. L. Manach, T. Paquet, D. G. l. Cabrera, Y. Younis, D. Taylor, L. Wiesner, N. Lawrence, S. Schwager, D. Waterson, M. J. Witty, S. Wittlin, L. J. Street and K. Chibale, *J. Med. Chem.*, 2014, **54**, 8839-8848.
3. R. A. Sanchez-Delgado, M. Navarro, H. Pe´rez and J. A. Urbina, *J. Med. Chem.*, 1996, **39**, 1095-1099.
4. M. Navarro, H. Perez and R. A. Sanchez-Delgado, *J. Med. Chem.*, 1997, **40**, 1937-1939.
5. M. Navarro, W. Castro, M. Madamet, R. Amalvict, N. Benoit and B. Pradines, *Malar. J.*, 2014, **13**, 1-8.
6. L. Keurulainen, M. Vahermo, M. Puente-Felipe, E. Sandoval-Izquierdo, B. Crespo-Fernández, L. Guijarro-López, L. Huertas-Valentín, L. de las Heras-Duena, T. O. Leino and A. Siiskonen, *J. Med. Chem.*, 2015, **58**, 4573-4580.
7. G. Navarrete-Vazquez, R. Cedillo, A. Hernandez-Campos, L. Yepez, F. Hernadez-Luis, J. Valdez, R. Morales, R. Cortes, M. Hernandez and R. Castillo, *Bioorg. Med. Chem. Lett.*, 2001, **11**, 187-190.
8. J. Perez-Villanueva, R. Santos, A. Hernandez-Campos, M. A. Giulianotti, R. Castillo and J. L. Medina-Franco, *Med. chem. comm.*, 2011, **2**, 44-49.
9. G. Yadav and S. Ganguly, *Eur. J. Med. Chem.*, 2015, **97**, 419-443.
10. A. J. Ndakala, R. K. Gessner, P. W. Gitari, N. October, K. L. White, A. Hudson, F. Fakorede, D. M. Shackleford, M. Kaiser, C. Yeates, S. A. Charman and K. Chibale, *J. Med. Chem.*, 2011, **54**, 4581-4589.
11. Z. J. Guo and P. J. Sadler, *Angew. Chem. Int. Ed.*, 1999, **38**, 1513-1531.
12. N. P. E. Barry and P. J. Sadler, *ACS Nano*, 2013, **7**, 5654-5659.
13. R. S. Keri, A. Hiremathad, S. Budagumpi and B. M. Nagaraja, *Chem. Biol. Drug. Des.*, 2015, **86**, 19-65.
14. L. C. R. Carvalho, E. Fernandes and M. M. B. Marques, *Chem. Eur. J.*, 2011, **17**, 12544-12555.

15. A. A. Spasov, I. N. Yozhitsa, L. I. Bugaeva and V. A. Anisimova, *Pharm. Chem. J.*, 1999, **33**, 232-243.
16. S. I. Alaqeel, *J. Saudi Chem. Soc.*, 2017, **21**, 229-237.
17. H. Sharghi, O. Asemani and R. Khalifeh, *Synth. Commun.*, 2008, **38**, 1128-1136.
18. H. Xiangming, M. Huiqiang and W. Yulu, *Arkivoc*, 2007, **13**, 150-154.
19. H. Taube, *J. Gen. Physiol.*, 1965, **1**, 39-50.
20. K. Amirbekyan, N. Duchemin, E. Benedetti, R. Joseph, A. Colon, S. A. Markarian, L. Bethge, S. Vonhoff, S. Klussmann, J. Cossy, J. Vasseur, S. Arseniyadis and M. Smietana, *ACS Catal.*, 2016, **6**, 3096-3105.
21. M. A. Bennett and A. K. Smith, *Dalton Trans.*, 1974, 233-241.
22. J. W. Kang, K. Moseley and P. M. Maitlis, *J. Am. Chem. Soc.*, 1969, **91**, 5970-5977.
23. S. Fernandez, M. Pfeffer, V. Ritleng and C. Sirlin, *Organometallics*, 1999, **18**, 2390-2394.
24. S. Attar, J. H. Nelson, J. Fischer, A. de Cian, J.-P. Sutter and M. Pfeffer, *Organometallics*, 1995, **14**, 4559-4569.
25. D. L. Davies, O. Al-Duaij, J. Fawcett, M. Giardiello, S. T. Hilton and D. R. Russell, *Dalton Trans.*, 2003, 4132-4138.
26. D. L. Davies, S. M. A. Donald and S. A. Macgregor, *J. Am. Chem. Soc.*, 2005, **127**, 13754-13755.
27. D. L. Davies, S. M. A. Donald, O. Al-Duaij, S. A. Macgregor and M. Pölleth, *J. Am. Chem. Soc.*, 2006, **128**, 4210-4211.
28. D. X. Hu, P. Grice and S. V. Ley, *J. Org. Chem.*, 2012, **77**, 5198-5202.
29. P. M. Maitlis, *Acc. Chem. Res.*, 1978, **11**, 301-307.
30. Z. Liu, A. Habtemariam, A. M. Pizarro, S. A. Fletcher, A. Kisova, O. Vrana, L. Salassa, P. C. Bruijnincx, G. J. Clarkson, V. Brabec and P. J. Sadler, *J. Med. Chem.*, 2011, **54**, 3011-3026.
31. L. C. Sudding, P. Chellan, P. Govender and G. S. Smith, *J. Inorg. Organomet. Polym.* , 2015, **25**, 457-465.

Chapter 3: Biological evaluation of 2-phenylbenzimidazoles and cyclometallated Ru(II)/Ir(III) benzimidazole complexes

3.1. Introduction

Malaria remains a highly prevalent disease, largely affecting developing countries of the sub-Saharan African region. Although there are several antimalarial drugs which have been developed over many years, the emergence of drug resistance underscores the need for researchers to search for new pharmacophores which are chemically and structurally diverse compared to current therapies.[1] This chapter is concerned with the antiplasmodial activity evaluation of the previously synthesised 2-phenybenzimidazole ligands (**35** – **54**) and the cyclometallated ruthenium(II) and iridium(III) complexes (**55** – **68**). The benzimidazole pharmacophore may be a good antimalarial drug candidate as several research articles recently demonstrate various benzimidazole derivatives with different substitution patterns, possessing potent antiplasmodial activities.[2-4]

In recent years, the synthesis and biological evaluation of cyclometallated complexes have been extensively investigated.[5-7] Literature reports suggest the synthesis of cyclometallated complexes, where the chelating ring contains a strong C-M σ bond, may help prevent biological reduction and ligand exchange reactions.[8] Moreover, structural and electronic properties can be fine-tuned by modifying the bidentate C-N ligand and/ or other ancillary ligands,[8] which may result in the enhancement of the overall activity of the compound. Therefore, the first aim of this study was to make minor structural changes to the 2-phenylbenzimidazole ligand. Since there has been reports of enhanced antiplasmodial activity upon substitution at position-5 of the benzimidazole ring,[9, 10] the effect of altering substituents at position-5 of the 2-phenylbenzimidazole scaffold with Craig plot substituents was explored. This may then lead to the identification of key structural changes which are necessary for the antiplasmodial activity of 2-phenylbenzimidazoles.

The antiplasmodial activity of the compounds was determined quantitatively using the parasite lactate dehydrogenase (pLDH) assay described by Makler.[11] There are many different

types of plasmodium strains, however since *Plasmodium falciparum* is prevalent and deadly, most drugs are generally tested against chloroquine-sensitive (CQS) and chloroquine-resistant (CQR) strains of *P. falciparum*. Thus, all of the synthesised ligands and complexes were initially screened against the CQS NF54 strain and selected complexes screened against the CQR K1 strain. This may allow us to establish if the activity of the synthesised benzimidazole compounds is comparable to chloroquine and if the compounds are cross-resistant (i.e. less active in the CQR strain compared to the CQS strain).

3.2 *In vitro* antiplasmodial evaluation against *P. falciparum*

3.2.1 Antiplasmodial activity against the chloroquine-sensitive NF54 strain

A full dose-response experiment was performed on the synthesised compounds to determine the respective IC_{50} values. An IC_{50} value is defined as the concentration of a particular drug inhibiting 50% of parasite growth. The results for the 2-phenylbenzimidazole ligands are summarised in Table 3.1 and that of the metal complexes in Table 3.2.

Table 3.1: *In vitro* antiplasmodial activity of 2-phenylbenzimidazole ligands **35** – **54** against the chloroquine-sensitive NF54 strain of *P. falciparum*.

Compound	R substituent	Structure	IC_{50} (µM) ± SD
35	H	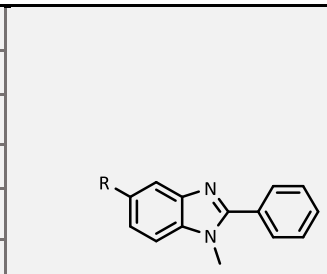	17.96 ± 0.29
36	Cl		8.23 ± 0.23
37	OCH_3		NA
38	CN		30.87 ± 0.95
39	CH_3		4.13 ± 0.11
40	CF_3		10.85 ± 1.13
41	SO_2CH_3		32.97 ± 0.35
42	$CONH_2$		NA
43	F		19.40 ± 0.44
44	H	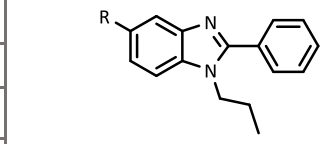	9.64 ± 0.16
45	Cl		NA
46	CH_3		NA
47	CN		21.07 ± 1.02
48	SO_2CH_3		NA
49	OCH_3		NA
50	CF_3		NA
51	CH_3	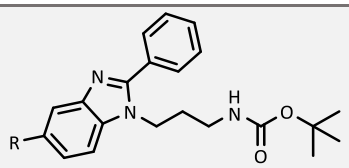	NA
52	CH_3	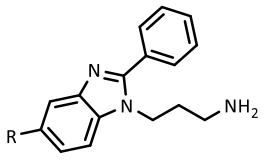	3.27 ± 0.25
53	CH_3	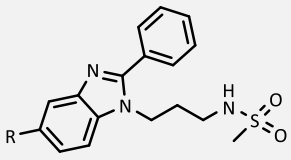	NA
54	CH_3	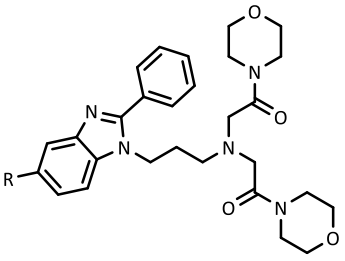	4.65 ± 1.17
CQ	-	-	0.044

NA = Not active at the tested concentration

When comparing the biological data obtained for the 2-phenylbenzimidazole ligands with a methyl linker and which were substituted at position-5 (**35** – **43**), compounds **39**, **36** and **40** (with chloro-, methyl and trifluoromethyl substituents, respectively) were found to be the most active with IC_{50} values of 4.23, 8.23 and 10.85 µM, respectively. On the other hand, compounds **38** and **41**, incorporating nitrile and methyl sulfonyl substituents were found to be significantly less active.

Figure 3.1 illustrates the Craig plot and highlights the substituents which were investigated in this study. The x- and y- axis is represented by a π- or σ- constant, respectively. As already mentioned, a positive π-constant indicates that a substituent is more hydrophobic, whereas a positive σ- constant indicates the substituent is electron-withdrawing. Thus, by relating the activity of these compounds with their relative positions in the Craig plot, it was observed that the antiplasmodial activity is generally enhanced through the incorporation of substituents positioned in the top and bottom right-hand quadrants of the Craig plot where substituents have a more positive π-constant. This suggests that more lipophilic substituents at position-5 of the benzimidazole core is important for activity in this case.

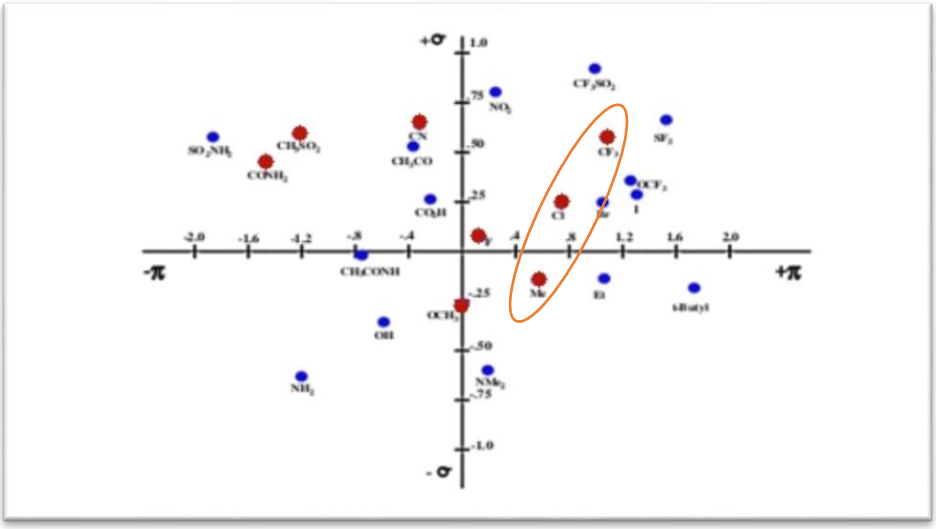

Figure 3.1: The Craig plot, highlighting the substituents chosen for this study in red.

By comparing compounds **44** and **47** (*N*-propyl) with compounds **35** and **38** (*N*-methyl), respectively, it is evident that the compounds with a propyl chain are significantly more active than the corresponding methyl analogues. Based on these two cases, the activity of the unsubstituted *N*-propyl benzimidazole ligand (**44**) and the nitrile substituted benzimidazole ligand (**47**), was increased almost two-fold compared to their corresponding *N*-methyl

analogues. However, in terms of the other 2-phenylbenzimidazole ligands containing a propyl chain, compounds **45**, **46** and **48** – **50** were found to be inactive at the tested concentration.

Due to the enhanced activity observed for the methyl-substituted compound **39**, compounds **51** – **54** were then also functionalised with a methyl group. As previously mentioned, compounds **53** and **54**, were synthesised in order to examine the overall solubility of the benzimidazole ligand and to investigate the effect of introducing a water-solubilising H-bonding moiety on antiplasmodial activity. The intermediate benzimidazole ligands **51** and **52**, functionalised with a carbamate (Boc) group and free amine moiety, respectively, were also tested. Compounds **51** and **53** were found to be inactive at the tested concentration, whereas compound **52**, functionalised with the free amine moiety proved to be more active when compared to the corresponding propyl analogue **46**. The addition of two morpholine groups, however, did not have a significant effect on the overall activity of the ligand.

In terms of the biological data obtained for the metal complexes, several trends can be observed from the results in Table 3.2 and Figure 3.2.

Table 3.2: *In vitro* antiplasmodial activity of metal complexes **55** – **68** against the NF54 strain of *P. falciparum*.

Compound	R substituent	M/ L_n	Structure	IC_{50} (µM) ± SD
55	H	Ru/ *p*-cymene	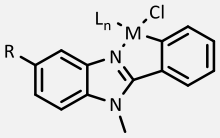	0.14 ± 0.01
56	Cl			2.69 ± 0.16
57	CH_3			2.04 ± 0.06
58	CF_3			2.31 ± 0.12
59	SO_2CH_3			NA
60	H	Ir/ Cp*		1.14 ± 0.01
61	H	Ru/ *p*-cymene	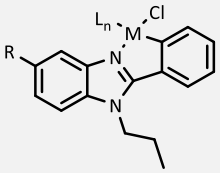	0.12 ± 0.01
62	Cl			0.59 ± 0.04
63	CH_3			1.16 ± 0.02
64	CF_3			3.02 ± 0.15
65	H	Ir/ Cp*		0.19 ± 0.01
66	Cl			1.94 ± 0.04
67	CH_3			1.73 ± 0.13
68	CF_3			1.62 ± 0.04
CQ	-	-	-	0.044

NA = Not active at the tested concentration

The potency of the most active 2-phenylbenzimidazole ligands (substituted with a methyl, chloro-, or trifluoromethyl group), is significantly enhanced upon complexation with ruthenium or iridium, which suggests that the metal moiety may play a role in activity. The enhanced activity observed upon metal complexation may be related to an increase in the overall lipophilicity of the compound, or the interaction of the metal complex with the target via an as yet unknown mechanism of action. Generally, the Ru(II) cyclometallated complexes exhibited better activity compared to the Ir(III) complexes. For example, the IC_{50} value for the unsubstituted ruthenium complex **55** was found to be 0.14 µM, whereas that for the corresponding iridium complex **60** was found to be 1.14 µM. The enhanced activity observed for the ruthenium complexes may be due to the fact that Ru(II) complexes have the ability to

mimic iron.[12] This suggests that the Ru(II) complexes may be able to bind to proteins such as serum albumin and transferrin in the plasma.[13] Moreover, the manner in which a Ru(II) compound oxidises may also be similar to an Fe(II) compound. This may give insight to the mechanism of action of these compounds, where they are perhaps involved in the generation of reactive oxygen species.

The results for the metal complexes also show a clear trend in terms of activity and chain length. In general, the activity of the *N*-propyl metal complexes (**61** – **68**) was significantly greater compared to the *N*-methyl metal complexes (**55** – **60**).

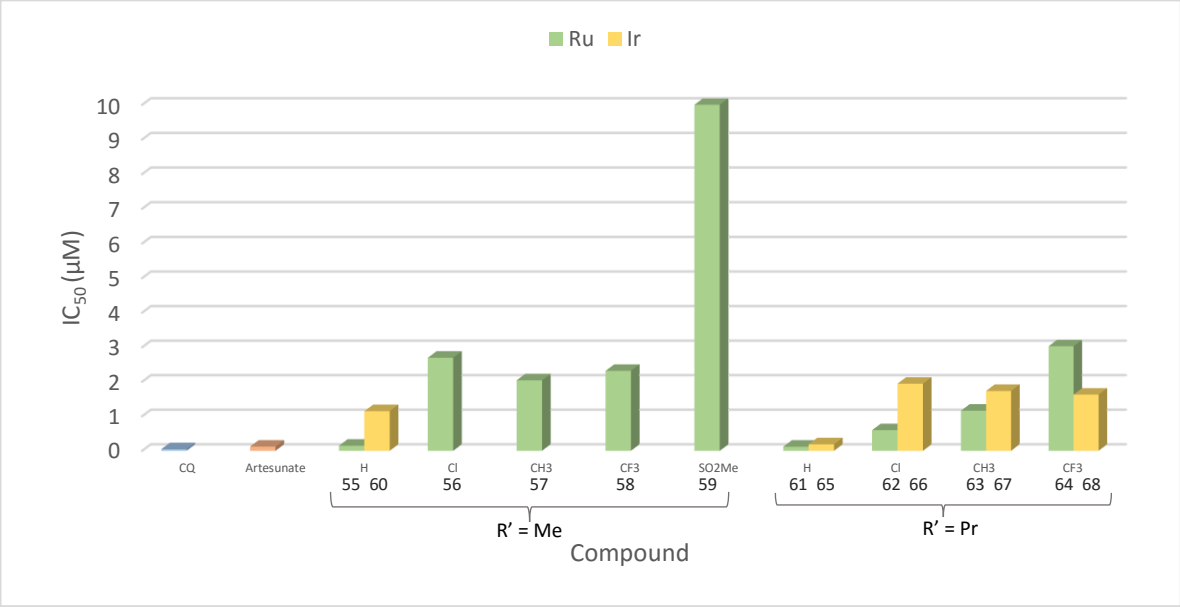

Figure 3.2: Graph depicting IC_{50} values of *N*-methyl (**55** – **60**) and *N*-propyl (**61** – **68**) Ru(II) and Ir(III) cyclometallated benzimidazole complexes.

Despite a clear trend observed for the ligands, wherein the introduction of a more lipophilic substituent enhanced the antiplasmodial activity, the substituent did not appear to significantly affect the activity. The unsubstituted metal complexes (**55**, **61** and **65**) were found to be more active compared to the substituted analogues. Trends therefore observed for the ligands were found to not necessarily be the same as that for the metal complexes.

3.2.2 Antiplasmodial activity against the chloroquine-resistant K1 strain

Since the *N*-propyl Ru(II) and Ir(III) cyclometallated benzimidazole complexes exhibited enhanced antiplasmodial activity against the chloroquine-sensitive NF54 strain compared to

their corresponding *N*-methyl analogues, compounds **61** – **68** were also tested against the chloroquine-resistant K1 strain of *P. falciparum.* The results are presented in Table 3.3 and Figure 3.3 is also shown, which graphically compares the results obtained for both strains.

Table 3.3: *In vitro* antiplasmodial activity of *N*-propyl Ru(II) and Ir(III) metal complexes **61** – **68** against CQS NF54 and CQR K1 strains of *P. falciparum*.

R substituent	Compound	IC_{50} (µM) NF54	IC_{50} (µM) ± SE K1	Resistance index[a] RI
H	**61 (Ru)**	0.12	2.68 ± 0.15	22.92
H	**65 (Ir)**	0.19	4.31 ± 0.27	22.94
Me	**63 (Ru)**	1.16	0.97 ± 0.12	0.84
Me	**67 (Ir)**	1.73	2.25 ± 0.15	1.30
CF_3	**64 (Ru)**	3.02	1.04 ± 0.14	0.34
CF_3	**68 (Ir)**	1.62	1.20 ± 0.23	0.74
Cl	**62 (Ru)**	0.59	1.85 ± 0.27	3.11
Cl	**66 (Ir)**	1.94	4.20 ± 0.18	2.16
-	**CQ**	0.04	0.29 ± 0.04	6.54

[a] *(IC_{50} K1/ IC_{50} NF54)*

From the data obtained for the K1 strain, the ruthenium complexes clearly display enhanced activity compared to the iridium complexes, a trend similarly observed in the NF54 strain.

Compound **63** displayed similar activities in both the chloroquine-sensitive and resistant strains of *P. falciparum*, whereas the activity of compounds **61**, **62**, **65** and **66** were significantly lower in the K1 strain compared to the NF54 strain. This suggests that compounds **61**, **62**, **65** and **66** may experience cross-resistance in a manner similar to that of chloroquine. Compounds **67** and **68** exhibited more or less consistent activity across both strains, while the activity of compound **64** increased significantly in the K1 strain compared to the NF54 strain.

The significant difference observed in the activity across the two strains was confirmed by the small resistance index (RI) of 0.34 calculated for compound **64**. The resistance index (RI) is a useful marker for the analysis of potential drugs and is calculated by dividing the IC_{50} value obtained in the resistant strain by the IC_{50} value obtained in the sensitive strain. A small RI value (1 or < 1) implies that the parasite is equally or more active in the resistant strain relative

to the sensitive strain. In most cases, the RI values for the compounds were significantly lower than the RI value of chloroquine. The RI value of the unsubstituted compounds **61** and **65** however, were much higher compared to CQ. This may suggest that substitution at position-5 of the benzimidazole ring is crucial for the antiplasmodial activity against the resistant strain, which may help to overcome cross-resistance. The complexes containing the trifluoromethyl- and methyl- substituents seem to exhibit the best antiplasmodial activity against the CQ-resistant K1 strain.

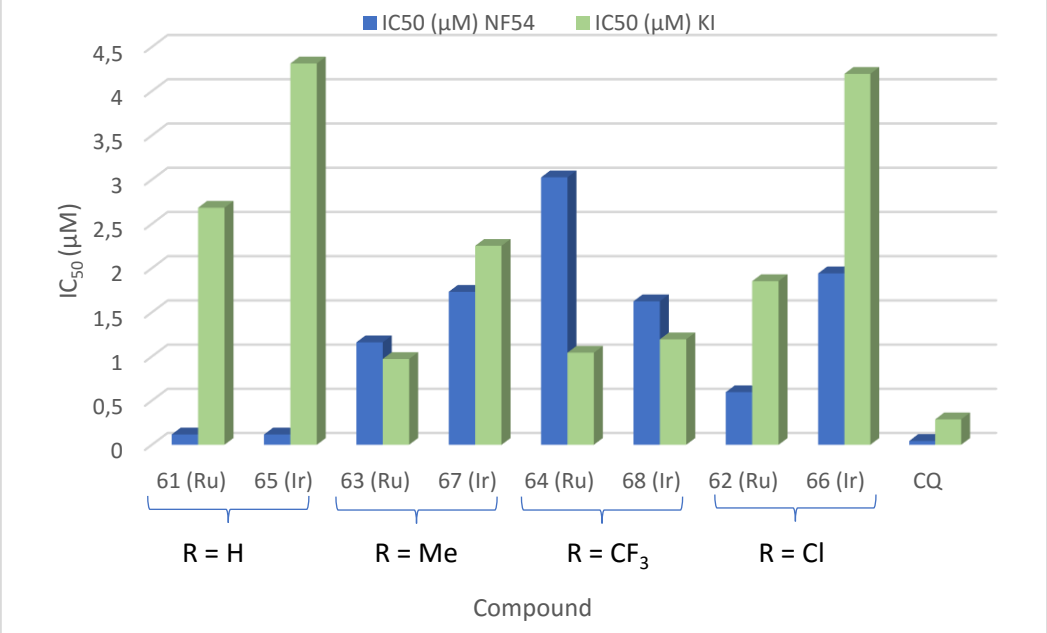

Figure 3.3: *In vitro* antiplasmodial activity of *N*-propyl Ru(II) and Ir(III) metal complexes **61** – **68** against NF54 and K1 strains of *P. falciparum*.

While the results obtained for the metal complexes (**55** – **68**) indicated that they were more active than their corresponding ligands in both CQS and CQR strains, they were not as active as chloroquine (IC_{50} = 0.044 µM) or artesunate (IC_{50} = 0.012 µM).

3.3 *In vitro* cytotoxicity studies

Since the biological data obtained indicates that the metal complexes are potent against both strains of *P. falciparum*, the most active ligand and selected metal complexes synthesised, were screened for cytotoxicity. Although there are many advantages associated with the use of metals in medicine, often the toxicity of metal complexes is of great concern. It is therefore important to evaluate the cytotoxicity of the metal complexes (or any other compound) which

display potent activity against the parasites. To determine whether the synthesised metal complexes are toxic to non-parasitic cells and to gain insight about the selectivity of the compounds towards the malaria parasites, the cytotoxicity of the compounds was tested against the mammalian Chinese Hamster Ovarian (CHO) cell-line, using the colorimetric 3-(4,5-dimethylthiazol-2-yl)-2,5-diphenyltetrazoliumbromide (MTT) assay. The results obtained are summarised in Table 3.4 below.

Table 3.4: IC_{50} values obtained for selected compounds against CHO mammalian cells.

Compound	Structure	IC_{50} (µM) ± SD	Selectivity Index[a] (SI)
39 (R = CH_3)	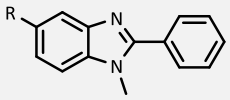	323.5 ± 4.89	78
55 (R = H, M = Ru, L_n = *p*-cymene)		74.32 ± 9.41	512
60 (R = H, M = Ir, L_n = Cp*)		92.31 ± 8.96	81
61 (R = H, M = Ru, L_n = *p*-cymene)	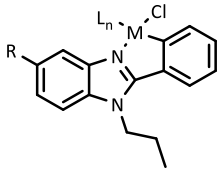	50.92 ± 0.81	434
65 (R = H, M = Ir, L_n = Cp*)		20.71 ± 0.23	110
Emetine	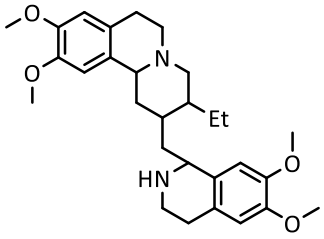	0.05 ± 0.003	-

[a] *(IC_{50} CHO/ IC_{50} NF54)*

From the results obtained it is evident that most of the compounds synthesised are not very cytotoxic compared to the standard control (Emetine). Compound **65** appears to be the most cytotoxic compared to the other synthesised metal complexes. When comparing all the metal complexes, the iridium benzimidazole complex with a methyl chain **60** appears to be the least cytotoxic with an IC_{50} value of 92.31 µM.

The selectivity index (SI) of each compound is also displayed in Table 3.4 and depicted in the graph below (Figure 3.4). As already mentioned, this value is calculated by dividing the IC_{50} value obtained for the cytotoxicity tests (CHO) by the respective *P. falciparum* strain (NF54 or K1). The selectivity index is useful in order to measure the selectivity of a compound towards

a particular cell type. A large SI value suggests selectivity towards malaria parasites as opposed to the CHO mammalian cells.

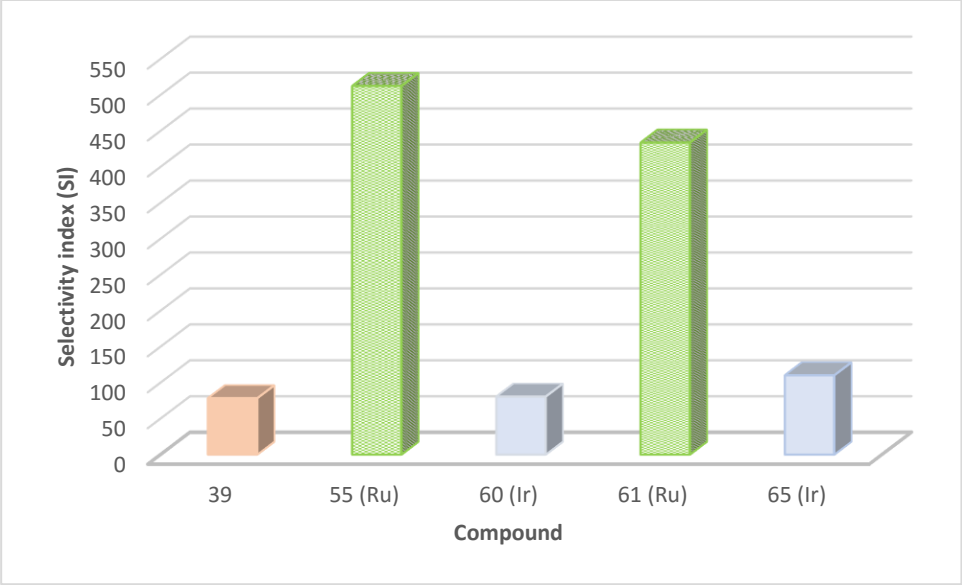

Figure 3.4: Selectivity indices

From the calculated SI values is it evident that the Ru complexes display the best selectivity, with SI values of 512 and 434, respectively. The benzimidazole ligand **39** and iridium metal complex **60** displays lower selectively as they as less active against the malaria parasite compared to the ruthenium complexes.

3.4 Aqueous solubility evaluation

A further study involved investigating the effect of improving aqueous solubility. Therefore, the apparent solubility of selected target compounds was determined in PBS buffer at the more relevant physiological pH of 6.5. The general classification of solubility ranges was analysed as follows:

- Solubility >150 µM – highly soluble
- Solubility of 50-150 µM – moderately soluble
- Solubility <50 µM – highly insoluble

Hydrocortisone (>150 µM) and Reserpine (<50 µM) were used as respective positive and negative controls. The aqueous solubility data for selected compounds are shown in Table 3.5.

Table 3.5: Aqueous solubility values determined against PBS buffer at pH 6.5.

Compound	R substituent	Structure	Solubility (µM)
37	OCH_3	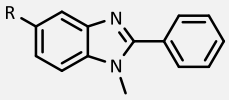	90
42	$CONH_2$		15
45	Cl	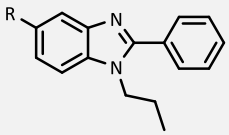	>5
48	SO_2CH_3		160
49	OCH_3		115
50	CF_3		>5
53	CH_3	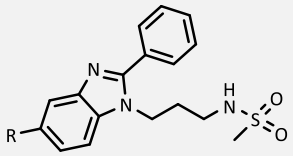	140
54	CH_3	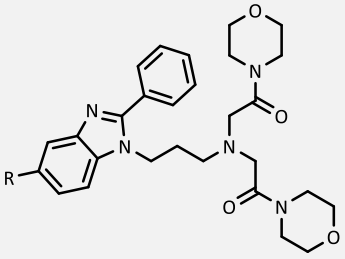	200
57	CH_3	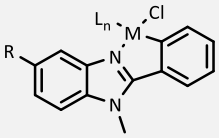	30
63	CH_3	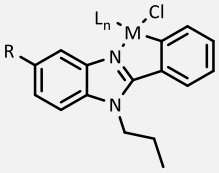	50

The strategy used to improve aqueous solubility was to introduce water-solubilising groups to the 2-phenylbenzimidazole moiety, such as a sulfonamide or morpholine functionality. The results obtained indicated that the introduction of these groups, did in fact lead to an improvement in solubility. Compound **53** showed moderately good solubility, while the dimorpholine functionalised compound (**54**) stood out with 200 µM solubility at physiological pH.

The aqueous solubility of selected *N*-propyl and *N*-methyl 2-phenylbenizmidazoles were also determined. In this case, the aqueous solubility data obtained can be related to the Craig plot, where compounds which are more lipophilic were found to have generally low aqueous solubility properties. For example, the more lipophilic chloro- and trifluoromethyl substituted

benzimidazole compounds were found to be relatively insoluble with low solubility values (>5 µM), whereas the less lipophilic methyl sulfonyl and methoxy- substituted compounds displayed relatively good aqueous solubility (160 and 115 µM, respectively).

The methyl substituted *N*-methyl (**57**) and *N*-propyl (**63**) metal complexes displayed low aqueous solubility (30 and 50 µM, respectively). The results suggest that the more lipophilic compounds are generally more active and this may be related to the compounds mechanism of action. Further modification of these metal complexes should therefore be made in order to enhance the activity and aqueous solubility of the overall compound and then assess if the activity of the compound is compromised.

3.5 β-Haematin inhibition studies

Several research articles have reported that compounds containing the benzimidazole moiety inhibit β-haematin formation. In addition, since the synthesised 2-phenylbenzimidazoles and corresponding metal complexes displayed promising antiplasmodial activity against both strains of *P. falciparum* and the mechanism of action of benzimidazoles remains unknown, β-haematin inhibition studies were also performed on selected compound in order to shed light on potential modes of action of the synthesised 2-phenylbenzimidazole compounds.

As previously mentioned, quinoline-based antimalarial drugs such as chloroquine are believed to target the erythrocytic stage of the malaria parasites life cycle. These quinoline-based drugs are considered as inhibitors of haemozoin formation, where they act by binding to haematin (a toxic product of the haemoglobin degradation process). These drugs are then able to prevent further conversion of haemozoin, resulting in the death of the parasite due to the toxic build-up of free haematin. The inhibition of the formation of haemozoin or its synthetic counterpart, β-haematin, is therefore regarded as an attractive approach in drug development. The NP40 detergent-mediated assay, developed by Sandlin *et al*, was used in this study to determine β-haematin inhibition activity.[14] This method involved the use of NP40, a neutral detergent, which mimics lipids and mediates the formation of β-haematin in this assay.

The results obtained for the 2-phenylbenzimidazole ligand (**44**) and its corresponding Ru(II) and Ir(III) metal complexes **61** and **65** are shown in Figure 3.5. The graph shows the respective

dose-response curves of the tested compounds and chloroquine (CQ), which were screened up to a concentration of 500 µM.

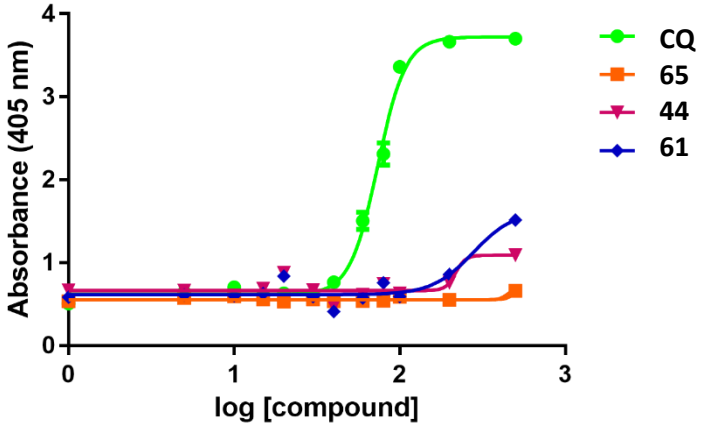

Figure 3.5: Dose response curves, depicting the β-haematin inhibition activity of **CQ**, **44**, **65** and **61**.

From the results obtained in this study, it is clear that the compounds tested did not exhibit any activity. Since the absorbance is proportional to the concentration of free haem, in the case of CQ, this compound inhibited β-haematin formation. However, in the case of the benzimidazole compounds, conversion of β-haematin was observed (low absorbance, hence no free haem present). The concentration at which the compounds are tested could be increased since there is a slight increase in absorbance at higher concentrations, however, any value obtained would not be significant. The results suggest that the compounds are not β-haematin inhibitors in this cell-free assay, which suggests that they are unlikely candidates for haemozoin inhibition in the parasite.

3.6 Summary

A series of substituted *N*-methyl and *N*-propyl 2-phenylbenzimidazole ligands as well as selected Ru(II) and Ir(III) cyclometallated benzimidazole complexes were screened *in vitro* for their antiparasitic activity against the CQS NF54 strain of *P. falciparum*. The ligands displayed moderate antiplasmodial activity and compounds substituted with lipophilic substituents (methyl, chloro- or trifluoromethyl) at position-5 of the benzimidazole core were found to be more active. The antiplasmodial activity of the benzimidazole ligands was significantly enhanced upon the incorporation of either ruthenium or iridium. The Ru(II) metal complexes were generally more active in comparison with the Ir(III) complexes and the metal complexes

with a propyl chain exhibited better activity than the metal complexes with a methyl chain. Furthermore, despite the general trend observed for the series of 2-phenylbenzimidazole ligands, where compounds substituted with more lipophilic groups showed enhanced activity, this trend was not observed for metal complexes against the CQS strain.

The metal complexes screened against the CQR strain, generally displayed low resistance index values, indicating that the complexes are not cross-resistance with chloroquine. This suggests that the compounds may have a different mode of action to CQ, which was also suggested by the β-haematin inhibition studies, where the conversion of β-haematin was not observed in the study. Aqueous solubility tests showed that although the introduction of water-solubilising groups did not have a significant effect on the antiplasmodial activity of the compounds, the aqueous solubility was greatly improved.

Cytotoxicity studies indicated that the compounds had low cytotoxicity and were selective towards the malaria parasites.

References

1. B. M. Greenwood, K. Bojang, C. J. M. Whitty and G. A. T. Targett, *The Lancet*, 2005, **365**, 1487-1498.
2. A. J. Ndakala, R. K. Gessner, P. W. Gitari, N. October, K. L. White, A. Hudson, F. Fakorede, D. M. Shackleford, M. Kaiser, C. Yeates, S. A. Charman and K. Chibale, *J. Med. Chem.*, 2011, **54**, 4581-4589.
3. K. Singh, J. Okombo, C. Brunschwig, F. Ndubi, L. Barnard, C. Wilkinson, P. M. Njogu, M. Njoroge, L. Laing, M. Machado, M. Prudêncio, J. Reader, M. Botha, S. Nondaba, L. Birkholtz, S. Lauterbach, A. Churchyard, T. L. Coetzer, J. N. Burrows, C. Yeates, P. Denti, L. Wiesner, T. J. Egan, S. Wittlin and K. Chibale, *J. Med. Chem.*, 2017, **60**, 1432-1448.
4. G. Roman, I. E. Crandall and W. A. Szarek, *ChemMedChem.*, 2013, **8**, 1795-1804.
5. Z. Liu, A. Habtemariam, A. M. Pizarro, S. A. Fletcher, A. Kisova, O. Vrana, L. Salassa, P. C. Bruijnincx, G. J. Clarkson, V. Brabec and P. J. Sadler, *J. Med. Chem.*, 2011, **54**, 3011-3026.

6. G. S. Yellol, A. Donaire, J. G. Yellol, V. Vasylyeva, C. Janiak and J. Ruiz, *Chem. Commun.*, 2013, **49**, 11533-11535.
7. L. C. Sudding, P. Chellan, P. Govender and G. S. Smith, *J. Inorg. Organomet. Polym.* , 2015, **25**, 457-465.
8. N. Cutillas, G. S. Yellol, C. de Haro, C. Vicente, V. Rodríguez and J. Ruiz, *Coord. Chem. Rev.*, 2013, **257**, 2784-2797.
9. L. Keurulainen, M. Vahermo, M. Puente-Felipe, E. Sandoval-Izquierdo, B. Crespo-Fernández, L. Guijarro-López, L. Huertas-Valentín, L. de las Heras-Duena, T. O. Leino and A. Siiskonen, *J. Med. Chem.*, 2015, **58**, 4573-4580.
10. J. Perez-Villanueva, R. Santos, A. Hernandez-Campos, M. A. Giulianotti, R. Castillo and J. L. Medina-Franco, *Med. chem. comm.*, 2011, **2**, 44-49.
11. M. T. Makler, J. M. Ries and J. A. Williams, *Am. Soc. Trop. Med. Hyg.*, 1993, **48**, 739-741.
12. C. S. Allardyce and P. J. Dyson, *Platinum Met. Rev.*, 2001, **45**, 62-69.
13. M. Pongratz, P. Schluga, M. A. Jakupec, V. B. Arion, C. G. Hartinger, G. Allmaier and B. K. Keppler, *J. Anal. At. Spectrom.*, 2004, **19**, 46-51.
14. R. D. Sandlin, M. D. Carter, P. J. Lee, J. M. Auschwitz, S. E. Leed, J. D. Johnson and D. W. Wright, *Antimicrob. Agents Chemother.*, 2011, **55**, 3363-3369.

Chapter 4: Conclusions and Future Work

4.1. Overall Summary and Conclusions

A series of substituted 2-phenylbenzimidazoles (**35** – **50**) were successfully synthesised. The 2-phenylbenzimidazoles were substituted at position-5 of the benzimidazole ring and substituents were selected from each quadrant of the Craig plot, allowing for the electronic and steric effects to be investigated. In addition, the effect of introducing water-solubilising H-bonding groups was also investigated through the synthesis of a 2-phenylbenzimidazole tethered with either a sulfonamide (**53**) or morpholine moiety (**54**), at position-1 of the benzimidazole ring. Ru(II) and Ir(III) cyclometallated benzimidazole complexes (**55** – **68**) were also successfully synthesised to introduce chemical diversity. All compounds were isolated in moderate to good yields and fully characterised using spectroscopic and analytical techniques such as 1D (^{1}H, ^{13}C{^{1}H}) and 2D (COSY, HSQC) NMR spectroscopy, IR spectroscopy and mass spectrometry (electron impact, electrospray ionisation). In addition, the molecular structure of the Ir(III) cyclometallated complexes **67** and **68** were confirmed by single crystal X-ray diffraction, corroborating a pseudo-tetrahedral geometry about the metal centre. Furthermore, the purity of the synthesised compounds were supported by elemental analysis and LC-MS data.

The synthesised 2-phenylbenzimidazole ligands (**35** – **54**) and corresponding Ru(II) and Ir(III) metal complexes (**55** – **68**) were screened *in vitro* for their potential antiplasmodial activity against the chloroquine-sensitive NF54 strain. The substituted 2-phenylbenzimidazole ligands displayed moderate activity, where compounds with lipophilic substituents (chloro-, methyl and trifluoromethyl) exhibited relatively good antiplasmodial activity when compared to the other substituted benzimidazole ligands. The antiplasmodial activity of the 2-phenylbenzimidazoles was enhanced significantly upon cyclometallation with ruthenium or iridium. The Ru(II) complexes generally displayed better antiplasmodial activity compared to the Ir(III) complexes. In addition, the *N*-propyl metal complexes (**61** – **68**) were relatively more potent than the *N*-methyl metal complexes (**55** – **60**), therefore complexes **61** – **68** were also screened against the chloroquine-resistant K1 strain. A similar trend was observed in the CQR K1 strain, where the Ru(II) complexes displayed better antiplasmodial activity. In general, the

complexes also displayed lower resistance index values relative to CQ, which suggests that they are not cross-resistant with CQ.

Since the complexes were active, they were screened against Chinese Hamster Ovarian (CHO) cells to measure selectivity. The complexes displayed low cytotoxicity and generally displayed high selectivity indices, implying that the compounds are selective towards the malaria parasites.

The apparent solubility of selected compounds were also tested in aqueous PBS buffer at a pH of 6.5. Although the introduction of a water-solubilising H-bonding group to the benzimidazole moiety did not have a significant effect on the antiplasmodial activity, solubility studies showed that through the introduction of a sulfonamide or morpholine functionality, the overall solubility of the compound increased substantially. Unfortunately, the more active compounds displayed poor solubility at the tested pH.

In terms of a potential mechanism of action, the benzimidazole compounds did not show β-haematin inhibition activity in the cell-free assay at the tested concentration of 500 µM, suggesting that the compounds are unlikely candidates for haemozoin inhibition in the parasite.

4.2. Future Work

Based on the results of this study, the benzimidazole complexes show promising antiplasmodial activity. Further mechanistic studies and structural modifications could be made in order to gain further insight to the mode(s) of action of 2-phenylbenzimidazoles and to enhance the efficacy and solubility of these compounds.

4.2.1. Further mechanistic studies

Since the benzimidazole compounds did not display β-haematin inhibition activity, it would be interesting to investigate other possible mechanisms of action. This may then result in preliminary data on how the benzimidazole compounds exerts its pharmacological effects and aid in the design and development of target-based antiplasmodial agents. Additional tests which could be performed include (but are not limited to) cysteine protease inhibition studies and DNA or mitochondrial interaction studies. The ability of the compound to produce

reactive oxygen species (ROS) could also be determined by evaluating the antiplasmodial activity of the benzimidazole compounds in the presence of an antioxidant such as *N*-acetylcysteine (NAC). Further evaluation of the electrochemistry of the compounds may help in identifying compounds which are redox active as well as those which enable ROS generation. Through the incorporation of a fluorescent tag/marker onto the benzimidazole compound, the site (in the parasite) at which the compound acts may also be established. Since this study showed that the terminal group of the *N*-propyl chain did not significantly affect the compounds overall activity, this therefore makes it an ideal site for conjugating fluorescent tags.

4.2.2. Structural modifications to enhance activity and solubility

The biological results indicate that despite the synthesised compounds exhibiting promising antiplasmodial activity, the activity was not comparable to chloroquine. Thus, further modification of the benzimidazole compound should be made to enhance the efficacy and solubility of the compounds.

Figure 4.1 below highlights suggested modifications, which may enhance the antiplasmodial activity and overall solubility of the benzimidazole pharmacophore.

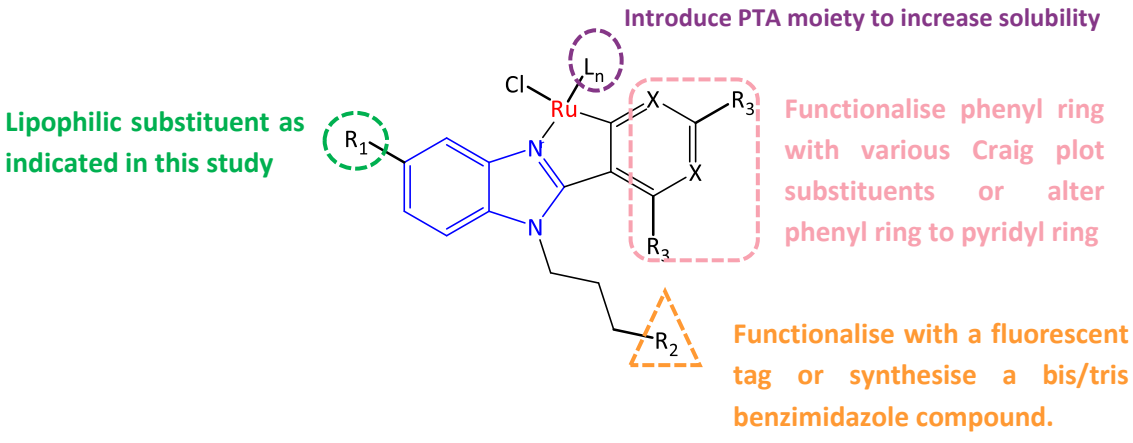

Figure 4.1: Suggested structural modifications

Further derivatisation of the phenyl ring could be evaluated as well as the replacement of the phenyl ring with a pyridyl ring, which may alter the lipophilicity of the compound. Since the

ruthenium complexes were generally more active compared to the iridium complexes, further studies could be limited to ruthenium complexes. In addition, lipophilic substituents should be maintained at position-5 of the benzimidazole ring. The aqueous solubility of the compounds may also be enhanced through the incorporation of a PTA (1,3,5-triaza-7-phosphaadamantane) moiety. The benzimidazole compound could also be functionalised with a fluorescent tag, which may help determine where the compound accumulates in the parasite. Furthermore, through the synthesis of a bis- or tris- benzimidazole compound, we could also evaluate the effects of multinuclearity.

Chapter 5: Experimental Procedures

5.1. General Remarks

All reagents and solvents were purchased from commercial sources (Sigma Aldrich or Combi blocks) and were used without further purification. All reactions were carried out under an inert nitrogen or argon atmosphere, unless otherwise stated. Reactions were monitored by TLC using aluminium-backed Merck precoated silica-gel 60 F254 plates, and compounds were visualised by ultraviolet light at 254 nm and/or were sprayed with either ninhydrin, a 2.5% solution of *p*-anisaldehyde in a mixture of sulfuric acid and ethanol (1:10 v/v), iodine vapour, or ceric ammonium sulphate solution, and then heated. Column chromatography was carried out using silica-gel (Fluka Silica Gel 60, 40-63 microns).

Nuclear Magnetic Resonance (NMR) spectra were recorded on a Bruker XR600 MHz spectrometer (^{1}H at 599.95 MHz and ^{13}C at 151.0 MHz), a Bruker XR400 MHz spectrometer (^{1}H at 399.95 MHz and ^{13}C at 100.6 MHz) or a Bruker XR300 MHz (^{1}H at 299.95 MHz) using tetramethylsilane (TMS) as the internal standard. Infrared (IR) spectroscopy was performed on a Perkin-Elmer Spectrum 100 FT-IR spectrometer using Attenuated Total Reflectance (ATR) with vibrations measured in units of cm^{-1}.

Elemental analyses for C, H, N and S were performed using a Thermo Flash 1112 series CHNS-O Analyser. Purity was determined using an analytical Agilant HPLC 1260 equipped with an Agilent infinity diode array detector (DAD) 1260 UV-Vis detector, with an absorption wavelength range of 210 – 640 nm. The compounds were eluted using a mixture of solvent A (10 mM NH_4OAc/H_2O) and solvent B (10 mM NH_4OAc/MeOH) at a flow rate of 0.9 mL min^{-1}. The gradient elution conditions were as follows: 10% solvent B between 0 and 1 min, 10 – 95% solvent B between 1 and 3 min, 95% solvent B between 3 and 5 min. Mass Spectrometry (MS) determinations were carried out using Electron Impact (EI) on a JEOL GCmateII instrument or Electrospray Ionisation (ESI) on a Waters API Quattro Micro triple quadrupole mass spectrometer with data recorded using the positive mode. Melting points were obtained using a Büchi Melting Point Apparatus B-540 and are uncorrected.

5.2. Synthesis of intermediate compounds and 2-phenylbenzimidazole ligands

5.1. General synthetic procedure for synthesis of nitroaniline derivatives (1 – 17)

Method A: Commercially available substituted nitrobenzene compounds (1 eq.) were dissolved in anhydrous DMF (5 mL) at rt. Thereafter, methylamine hydrochloride (2 eq.) and K_2CO_3 (2 eq.) were added to the solution and left to stir for 24 h. The synthesis of **3** however, required the reaction to be heated to 100 °C in a sealed vessel. After 24 h, the reaction mixture was diluted with sat. NaCl (50 mL) and the crude product extracted with ethyl acetate (3 x 50 mL). The organic extracts were combined and dried over anhydrous Na_2SO_4 and then concentrated *in vacuo*. The crude product was then purified *via* column chromatography using EtOAc:Petroleum ether as the eluent to afford the desired compounds, **1** – **3**.

Method B: Commercially available substituted nitrobenzene compounds (1 eq.) were dissolved in DCM (2 mL) at rt. Thereafter, K_2CO_3 (2 eq.) and methylamine (40% solution in H_2O, 2 mL) was added to the solution. The resulting biphasic solution was then left to stir overnight at rt. The reaction mixture was diluted with distilled H_2O (30 mL) and extracted with DCM (3 x 30 mL). The organic layers were combined and washed with sat. NaCl (30 mL). The combined organic extracts were dried over anhydrous $MgSO_4$ and concentrated *in vacuo*. The resulting residue was purified *via* flash chromatography using DCM:Petroleum ether as the eluent to afford products, **4** – **8**.[1]

Method C: Methylamine (40% solution in H_2O, 1.25 mL) was then added to 2,5- difluoronitrobenzene (0.21 mL, 1.91 mmol) at 0 °C. The solution was then left to cool to rt and allowed to stir for 2 h. The reaction mixture was then diluted with H_2O (10 mL) and the resultant orange precipitate filtered. Recrystallisation from EtOH afforded product, **9**.[2]

Method D: Commercially available substituted nitrobenzene compounds (1 eq.) were dissolved in DMF (3 mL) at rt. *N*-propylamine (2 eq.) was then added to the solution and the solution was then left to stir for 24 h. Thereafter, the reaction mixture was diluted with distilled H_2O (30 mL) and extracted with EtOAc (3 x 30 mL). The organic layers were combined and washed with sat. NaCl (30 mL). The combined organic extracts were then dried over anhydrous Na_2SO_4 and concentrated *in vacuo*. The resulting residue was purified via flash chromatography using DCM:Petroleum ether as the eluent to afford products, **10** – **12** and **14** – **16** .[3] For the synthesis of **13**, 4-chloro-3-nitrobenzonitrile (0.350 g, 1.92 mmol) was dissolved

in THF (4 mL) followed by *N*-propylamine (2 mL). The solution was left to heat at 60 °C for 4 h. Excess solvent was then concentrated *in vacuo* and upon addition of H_2O (5 mL) a yellow precipitate formed and was then filtered. Recrystallisation from EtOH afforded product, **13**.

Method E: 1-Fluoro-2-nitrotoluene (0.258 g, 1.67 mmol) was dissolved in DMF (1 mL). *tert*-Butyl *N*-(3-aminopropyl)carbamate was previously prepared according to a literature procedure,[4] whereby a solution of Boc anhydride (0.753 g, 3.43 mmol) in chloroform (30 mL) was added dropwise to 1,3-diaminopropane (g, mmol) at 0 ˚ C. The previously synthesised *tert*-Butyl *N*-(3-aminopropyl)carbamate (0.319 g, 1.83 mmol) and K_2CO_3 (0.345 g, 2.50 mmol) were then added to the reaction flask. The reaction was warmed to 100 ˚C and left to stir for 24 h. Thereafter, the reaction mixture was cooled to room temperature and diluted with water (30 mL). The aqueous layer was extracted with EtOAc (3 x 30 mL) and washed with sat. NaCl (30 mL). The organic layers were collected and dried over sat. Na_2SO_4, filtered and concentrated in vacuo. The crude residue obtained was purified by column chromatography to afford the desired product, **17**.[5]

N-Methyl-2-nitroaniline (1)

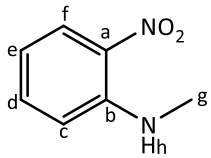

1-Fluoro-2-nitrobenzene (1.49 mL, 14.2 mmol) was diluted with DMF (15 mL). Methylamine hydrochloride (1.94 g, 28.6 mmol) and K_2CO_3 (3.80 g, 27.5 mmol) was then added to the solution. Product: Orange oil (2.00 g, 93%); $\mathbf{R_f}$ (EtOAc/Pet. Ether, 2:8): 0.70. **^{1}H-NMR (300 MHz, $CDCl_3$)** δ (ppm): 8.16 (d, $^3J_{HH}$ = 8.4 Hz, 1H, H_f), 8.04 (s, 1H, H_h), 7.46 (t, $^3J_{HH}$ = 8.4 Hz, 1H, H_d), 6.84 (d, $^3J_{HH}$ = 8.7 Hz, 1H, H_c), 6.65 (t, $^3J_{HH}$ = 8.4 Hz, 1H, H_e), 3.02 (d, $^3J_{NH}$ = 5.8 Hz, 3H, H_g). **^{13}C{^{1}H} NMR (101 MHz, $CDCl_3$)** δ (ppm): 146.49 (C_b), 136.37 (C_d), 132.17 (C_a), 126.95 (C_f), 115.32 (C_e), 113.47 (C_c), 29.83 (C_g). **Elemental Analysis** for $C_7H_8N_2O_2$ (152.15 g.mol^{-1}): Found (%) C, 55.64; H, 5.50; N, 17.83; Calcd. (%) C, 55.20; H, 5.30; N, 18.40. **MS** (EI, *m/z*): 152.0140 (100%, $[M]^+$).

4-Chloro-N-methyl-2-nitroaniline (2)

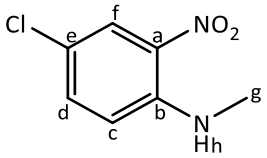

1,4-Dichloro-2-nitrobenzene (0.305 mg, 1.59 mmol) was diluted with DMF (3 mL). Methylamine hydrochloride (0.213 g, 3.15 mmol) and K_2CO_3 (0.437 g, 3.16 mmol) was then added to the solution. Product: Orange solid (0.121 g, 42%); **R_f** (EtOAc:Pet. Ether, 1:9): 0.55. **^{1}H NMR (300 MHz, $CDCl_3$)** δ (ppm): 8.17 (d, *J* = 2.5 Hz, 1H, H_f), 8.05 (s, 1H, H_h), 7.41 (dd, *J* = 9.2, 2.5 Hz, 1H, H_d), 6.81 (d, *J* = 9.2 Hz, 1H, H_c), 3.03 (d, *J* = 5.1 Hz, 3H, H_g). **^{13}C{^{1}H} NMR (101 MHz, $CDCl_3$)** δ (ppm): 145.09 (C_b), 136.53 (C_d), 126.06 (C_f), 122.74 (C_a), 120.23 (C_e), 114.94 (C_c), 42.63 (C_g).

4-Methoxy-N-methyl-2-nitroaniline (3)

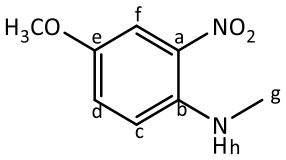

4-Chloro-3-nitroanisole (0.359 g, 1.91 mmol) and methylamine (40% solution in H_2O, 1.25 mL) was added to a sealed vessel and heated to 100 °C. Product: Red solid (0.233 g, 67%); **R_f** (EtOAc:Pet. Ether, 1:9): 0.29. **^{1}H-NMR (300 MHz, $CDCl_3$)** δ (ppm): 7.63 (d, $^4J_{HH}$ = 3.0 Hz, 1H, H_f), 7.18 (dd, $^3J_{HH}$ = 9.3 Hz and $^4J_{HH}$ = 3.0 Hz, 1H, H_d), 6.83 (d, $^3J_{HH}$ = 9.3 Hz, 1H, H_c), 3.80 (s, 3H, Ar-O$\underline{C}H_3$), 3.03 (s, 3H, H_g). **^{13}C{^{1}H} NMR (101 MHz, $CDCl_3$)** δ (ppm): 149.58 (C_e), 142.38 (C_b), 130.96 (C_a), 127.40 (C_d), 114.75 (C_c), 107.17 (C_f), 55.89 (Ar-O$\underline{C}H_3$), 29.69 (C_g). **Elemental Analysis** for $C_8H_{10}N_2O_3$ (182.07 g.mol^{-1}): Found (%) C, 53.95; H, 5.95; N, 14.64; Calcd. (%) C, 52.74; H, 5.53; N, 15.38. **MS** (EI, *m/z*): 182.0566 (100%, $[M]^+$).

4-(Methylamino)-3-nitrobenzonitrile (4)

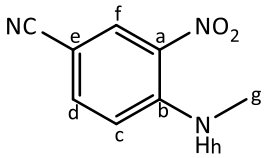

4-Chloro-3-nitrobenzonitrile (0.183 g, 1.00 mmol) was dissolved in DCM (1 mL). K_2CO_3 (0.281 g, 2.03 mmol) and $MeNH_2$ (40% solution in H_2O, 1 mL) was then added to the solution.

Product: Yellow solid (0.175 g, 98%); **R_f** (EtOAc:Pet. Ether, 1:1): 0.68. **Mp**: 160.6 - 165.8 °C. **^{1}H NMR (300 MHz, $CDCl_3$)** δ (ppm): 8.50 (d, $^4J_{HH}$ = 1.8 Hz, 1H, H_f), 8.39 (s, 1H, H_h), 7.63 (dd, $^3J_{HH}$ = 9.0 and $^4J_{HH}$ = 1.8 Hz, 1H, H_d), 6.91 (d, $^3J_{HH}$ = 9.0 Hz, 1H, H_c), 3.09 (d, $^3J_{NH}$ = 5.1 Hz, 3H, H_g). **^{13}C{^{1}H} NMR (101 MHz, $CDCl_3$)** δ (ppm): 148.12 (C_b), 137.87 (C_d), 132.23 (CN), 131.71 (C_f), 118.09 (C_a), 114.56 (C_c), 98.31 (C_e), 30.04 (C_g). **FT-IR** (ATR) *v* (cm^{-1}): = 3384.16 (sec. amine, N-H) and 2220.49 (C≡N). **Elemental Analysis** for $C_7H_8N_2O_2$ (177.16 g.mol^{-1}): Found (%) C, 53.99; H, 3.74; N, 23.42; Calcd. (%) C, 54.20; H, 4.00; N, 23.7. **MS** (EI, *m/z*): 177.0149 (100%, $[M]^+$).

N,4-Dimethyl-2-nitroaniline (5)

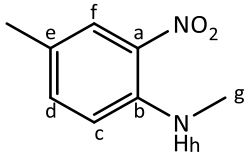

1-Fluoro-4-methyl-2-nitrobenzene (0.317 g, 2.05 mmol) was dissolved in DCM (2 mL). K_2CO_3 (0.574 g, 4.15 mmol) and methylamine (40% solution in H_2O, 2 mL) was then added to the solution. Product: Orange solid (0.338 g, 99%), **R_f** (EtOAc:Pet. Ether, 1:9): 0.59. **Mp**: 72.0 – 80.5 °C. **^{1}H-NMR (300 MHz, $CDCl_3$)** δ (ppm): 7.97 (d, $^4J_{HH}$ = 2.2 Hz, 1H, H_f), 7.29 (dd, $^3J_{HH}$ = 8.7 Hz and $^4J_{HH}$ = 2.2 Hz, 1H, H_d), 6.76 (d, $^3J_{HH}$ = 8.7 Hz, 1H, H_c), 3.01 (s, 3H, H_g), 2.27 (s, 3H, Ar-C$\underline{H_3}$). **^{13}C{^{1}H} NMR (101 MHz, $CDCl_3$)** δ (ppm): 144.64 (C_b), 137.77 (C_d), 131.62 (C_a), 126.04 (C_c), 124.73 (C_e), 113.35 (C_f), 29.75 (C_i), 19.92 (C_g). **Elemental Analysis** for $C_8H_{10}N_2O_2$ (166.18 g.mol^{-1}): Found (%) C, 57.97; H, 6.03; N, 15.82; Calcd. (%) C, 57.82; H, 6.06; N, 16.86. **MS** (EI, *m/z*): 166.0205 (100%, $[M]^+$).

N-Methyl-2-nitro-4-(trifluoromethyl)aniline (6)

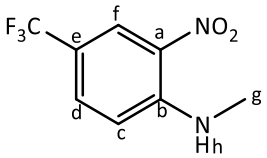

4-Chloro-3-nitrobenzotrifluoride (0.230 mL, 1.54 mmol) was dissolved in DCM (1.5 mL). K_2CO_3 (0.413 g, 2.99 mmol) and methylamine (40% solution in H_2O, 1.5 mL) was then added to the solution. Product: Yellow solid (0.336 g, 99%), **R_f** (EtOAc:Pet. Ether, 1:9): 0.29. **Mp**: 72.7 – 77.3 °C. **^{1}H-NMR (300 MHz, $CDCl_3$)** δ (ppm): 8.46 (dd, $^4J_{HH}$ = 2.1 Hz and $^4J_{HF}$ = 0.9 Hz,

1H, H_f), 8.26 (s, 1H, H_h), 7.64 (dd, $^3J_{HH}$ = 9.0 and $^4J_{HH}$ = 2.1 Hz, 1H, H_d), 6.93 (d, $^3J_{HH}$ = 9.0 Hz, 1H, H_c), 3.08 (d, $^3J_{NH}$ = 5.1 Hz, 3H, H_g). **$^{13}C\{^1H\}$ NMR (101 MHz, $CDCl_3$)** δ (ppm): 147.70 (s, C_b), 132.16 (C_d), 131.08 (s, C_a), 124.87 (C_c), 122.32 (s, C_e), 117.41 (d, $^2J_{CF}$ = 34.0 Hz, $\underline{C}F_3$), 114.04 (s, C_f), 29.85 (s, C_g). **^{19}F NMR (377 MHz, $CDCl_3$)** δ (ppm): -61.93 (s). **Elemental Analysis** for $C_8H_7F_3N_2O_2$ (220.15 g.mol^{-1}): Found (%) C, 43.61; H, 2.05; N, 12.29; Calcd. (%) C, 43.65; H, 3.21; N, 12.72. **MS** (EI, *m/z*): 219.0484 (55%, $[M-H]^+$).

N-Methyl-4-(methylsulfonyl)-2-nitroaniline (7)

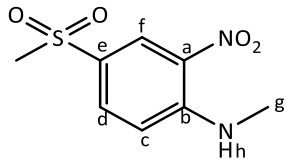

1-Fluoro-4-methanesulfonyl-2-nitrobenzene (0.326 g, 1.49 mmol) was dissolved in DCM (1.5 mL). K_2CO_3 (0.419 g, 3.03 mmol) and methylamine (40% solution in H_2O, 1.5 mL) was then added to the solution. Product: Yellow solid (0.340 g, 99%), **R_f** (EtOAc:Pet. Ether, 5:5): 0.23. **Mp**: 186.1 – 190.1 °C. **^{1}H-NMR (300 MHz, DMSO-*d_6*)** δ (ppm): 8.65 (d, $^3J_{NH}$ = 4.2 Hz, 1H, H_h), 8.51 (d, $^4J_{HH}$ = 2.1 Hz, 1H, H_f), 7.95 (dd, $^3J_{HH}$ = 9.0 and $^4J_{HH}$ = 2.1 Hz, 1H, H_d), 7.19 (d, $^3J_{HH}$ = 9.0 Hz, 1H, H_c), 3.21 (s, 3H, Ar-$SO_2C\underline{H_3}$), 3.04 (d, $^3J_{HNH}$ = 5.1 Hz, 3H, H_g). **$^{13}C\{^1H\}$ NMR (101 MHz, DMSO-*d_6*)** δ (ppm): 148.50 (C_b), 133.96 (C_d), 130.41 (C_a), 127.24 (C_f), 126.50 (C_e), 115.97 (C_c), 44.30 (C_g), 30.51 (C_h). **Elemental Analysis** for $C_8H_{10}N_2O_4S$ (230.24 g.mol^{-1}): Found (%) C, 46.98; H, 5.68; N, 10.45; S, 12.32; Calcd. (%) C, 41.73; H, 4.38; N, 12.17; S, 13.92. **MS** (EI, *m/z*): 230.0258 (100%, $[M]^+$).

4-(Methylamino)-3-nitrobenzamide (8)

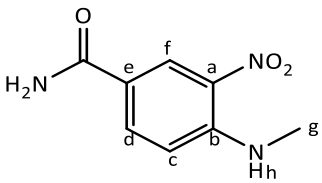

4-Chloro-3-nitrobenzamide (0.201 g, 1.00 mmol) was dissolved in DCM (1 mL). K_2CO_3 (0.283 g, 2.05 mmol) and methylamine (40% solution in H_2O, 1 mL) was then added to the solution. Product: Orange solid (0.139 g, 71%); **R_f** (EtOAc: 10): 0.56. **Mp**: 249.3 – 251.4 °C. **^{1}H NMR (300 MHz, DMSO-*d_6*)** δ (ppm): 8.66 (d, *J* = 2.1 Hz, 1H, H_f), 8.40 (d, *J* = 5.0 Hz, 1H, $CON\underline{H_2}$), 8.04 (dd,

$^{3}J_{HH}$ = 9.0 and $^{4}J_{HH}$ = 2.1 Hz, 1H, H_d), 7.98 (bs, 1H, CONH$_2$), 7.25 (bs, 1H, H_h), 7.03 (d, J_{HH} = 9.0 Hz, 1H, H_c), 3.00 (d, J_{NH} = 4.8 Hz, 3H, H_g). **^{13}C{^{1}H} NMR (101 MHz, DMSO-*d*$_6$)** δ (ppm): 166.60 (C=O), 147.65 (C_b), 135.41 (C_d), 130.83 (C_a), 126.78 (C_e), 121.00 (C_f), 114.44 (C_c), 30.31 (C_g). **Elemental Analysis** for $C_8H_9N_3O_3$ (195.18 g.mol^{-1}): Found (%) C, 51.94; H, 5.18; N, 10.45; S, 19.39; Calcd. (%) C, 49.23; H, 4.65; N, 21.53. **MS** (EI, *m/z*): 195.0549 (100%, [M]$^+$).

4-Fluoro-N-methyl-2-nitroaniline (9)

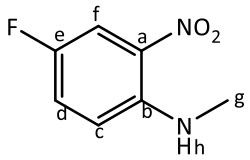

2,5-difluoronitrobenzene (0.21 mL, 1.94 mmol) was added to methylamine (40% solution in H_2O, 1.25 mL). Product: Orange solid (0.324 g, 98%), **R_f** (EtOAc:Pet. Ether, 3:7): 0.64. **Mp**: 65.5 – 72.9 °C. **^{1}H-NMR (300 MHz, DMSO-*d*$_6$)** δ (ppm): 8.11 (d, $^{3}J_{HH}$ = 3.6 Hz, 1H, H_h), 7.84 (dd, $^{3}J_{HF}$ = 9.6 and $^{4}J_{HH}$ = 3.1 Hz, 1H, H_f), 7.54 (ddd, $^{3}J_{HF}$ = 9.6, $^{3}J_{HH}$ = 7.5 and $^{4}J_{HH}$ = 4.8 Hz, 1H, H_d), 7.05 (dd, $^{3}J_{HH}$ = 9.6 and $^{4}J_{HF}$ = 4.8 Hz, 1H, H_c), 2.96 (d, *J* = 5.1 Hz, 3H, H_g). **^{13}C{^{1}H} NMR (101 MHz, CDCl$_3$)** δ (ppm): 153.62 (C_e), 151.26 (C_b), 143.48 (C_a), 124.98 (d, $^{2}J_{CF}$ = 23.8 Hz, C_d), 114.59 (d, $^{3}J_{CF}$ = 7.2 Hz, C_c), 111.97 (d, $^{2}J_{CF}$ = 26.2 Hz, C_f), 29.95 (C_g). **^{19}F NMR (377 MHz, CDCl$_3$)** δ (ppm): -128.33 (s). **Elemental Analysis** for $C_7H_7FN_2O_2$ (170.14 g.mol^{-1}): Found (%) C, 49.34; H, 3.33; N, 16.07; Calcd. (%) C, 49.42; H, 4.14; N, 16.47. **MS** (EI, *m/z*): 170.0161 (100%, [M]$^+$).

2-Nitro-N-propylaniline (10)

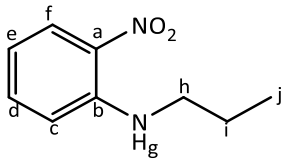

1-Fluoro-2-nitrobenzene (1.01 g, 7.16 mmol) was dissolved in DMF (15 mL). *n*-Propylamine (0.838 g, 14.2 mmol) was then added to the solution. Product: Orange oil (1.26 g; 99%); R_f (EtOAc: Pet. Ether, 1:9): 0.45. **^{1}H-NMR (400 MHz, DMSO-d$_6$)** δ (ppm): 8.10 (bs, 1H, H_g), 8.08 – 8.03 (m, 1H, H_f), 7.53 (m, 1H, H_d), 7.05 (m, 1H, H_c), 6.67 (m, 1H, H_e), 3.35 – 3.30 (t, $^{3}J_{HH}$ = 7.2 Hz, 2H, H_h), 1.72 – 1.56 (sextet, J_{HH} = 7.2 Hz, 2H, H_i), 0.95 (t, $^{3}J_{HH}$ = 7.2 Hz, 3H, H_j). **^{13}C{^{1}H} NMR (101 MHz, DMSO-*d*$_6$)** δ (ppm): 145.23 (C_b), 136.54 (C_d), 130.80 (C_a), 126.16 (C_f), 115.01 (C_e),

114.44 (C_c), 44.82 (C_h), 21.55 (C_i), 11.17 (C_j). **Elemental Analysis** for $C_9H_{12}N_2O_2$ (180.21 g.mol^{-1}): Found (%) C, 60.12; H, 6.46; N, 15.88; Calcd. (%) C, 59.9; H, 6.70; N, 15.50. **MS** (EI, *m/z*): 180.0952 (66%, $[M]^+$).

4-Chloro-2-nitro-N-propylaniline (11)

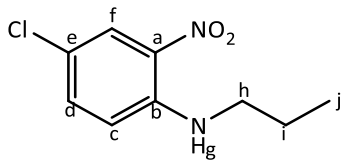

1,4-Dichloro-2-nitrobenzene (0.425 g, 2.21 mmol) was dissolved in DMSO (4 mL). *n*-Propylamine (0.36 mL, 4.38 mmol) was then added to the solution. Product: Orange solid (0.452 g, 95%); **R_f** (EtOAc: Pet. Ether, 1:9): 0.65. **Mp**: 44.5 – 46.1 °C. **^{1}H-NMR (300 MHz, $CDCl_3$)** δ (ppm): δ 8.17 (d, $^4J_{HH}$ = 2.4 Hz, 1H, H_f), 8.03 (bs, 1H, H_g), 7.37 (dd, $^3J_{HH}$ = 9.3, and $^4J_{HH}$ = 2.4 Hz, 1H, H_d), 6.81 (d, $^3J_{HH}$ = 9.3 Hz, 1H, H_c), 3.27 (m, 1H, H_h), 1.85 – 1.67 (m, 1H, H_i), 1.05 (t, *J* = 7.4 Hz, 1H, H_j). **^{13}C{^{1}H} NMR (101 MHz, $CDCl_3$)** δ (ppm): 144.41 (C_b), 136.46 (C_d), 131.75 (C_a), 126.10 (C_c), 120.00 (C_e), 115.38 (C_f), 44.09 (C_h), 22.36 (C_i), 11.66 (C_j). **Elemental Analysis** for $C_9H_{11}ClN_2O_2$ (214.65 g.mol^{-1}): Found (%) C, 52.24; H, 5.51; N, 12.04; Calcd. (%) C, 50.36; H, 5.17; N, 13.05. **MS** (EI, *m/z*): 214.0085 (75%, $[M]^+$).

4-Methyl-2-nitro-N-propylanaline (12)

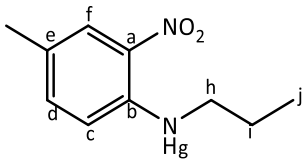

1-Fluoro-4-methyl-2-nitrobenzene (0.358 g, 2.31 mmol) was dissolved in DMF (4 mL). *n*-Propylamine (0.38 mL, 4.62 mmol) was then added to the solution. Product: Orange oil (0.442 g, 99%); **R_f** (EtOAc:Pet. Ether, 1:9): 0.76. **^{1}H-NMR (300 MHz, $CDCl_3$)** δ (ppm): 7.97 (d, $^4J_{HH}$ = 2.1 Hz, 1H, H_f), 7.30 – 7.20 (dd, $^3J_{HH}$ = 8.4 Hz and $^4J_{HH}$ = 2.1 Hz, 1H, H_d), 6.81 – 6.73 (d, $^3J_{HH}$ = 8.4 Hz, 1H, H_c), 3.26 (t, J_{HH} = 7.2 Hz, 2H, H_h), 2.26 (s, 3H, Ar-C$\underline{H}_3$), 1.85 – 1.60 (m, 2H, H_i), 1.04 (t, J_{HH} = 7.2 Hz, 3H, H_j). **^{13}C{^{1}H} NMR (101 MHz, $CDCl_3$)** δ (ppm): 139.22 (C_b), 132.97 (C_d), 126.63 (C_a), 121.32 (C_c), 119.82 (C_e), 109.07 (C_f), 40.10 (C_h), 17.57 (C_i), 15.18 (Ar-$\underline{C}H_3$), 6.81

(C_j). **Elemental Analysis** for $C_{10}H_{14}N_2O_2$ (194.23 g.mol^{-1}): Found (%) C, 62.00; H, 7.30; N, 14.16; Calcd. (%) C, 61.84; H, 7.27; N, 14.42. **MS** (EI, *m/z*): 194.1050 (75%, $[M]^+$).

3-Nitro-4-(propylamino)benzonitrile (13)

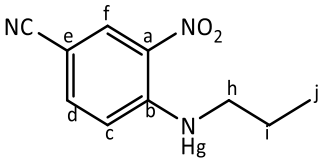

4-Chloro-3-nitrobenzonitrile (0.353 g, 1.93 mmol) was dissolved in THF (4 mL). *n*-Propylamine (2.05 mL, 24.9 mmol) was then added to the solution. Product: Yellow solid (0.181, 46%); **Mp**: 110.3 – 115.1 °C. **^{1}H-NMR (300 MHz, $CDCl_3$)** δ (ppm): 8.50 (d, $^4J_{HH}$ = 2.9 Hz, 1H, H_f), 8.40 (s, 1H, H_g), 7.59 (dd, $^3J_{HH}$ = 9.0 Hz and $^4J_{HH}$ = 2.9 Hz, 1H, H_d), 6.91 (d, $^3J_{HH}$ = 9.0 Hz, 1H, H_c), 3.33 (m, 2H, H_h), 1.90 – 1.70 (m, 2H, H_i), 1.07 (t, $^3J_{HH}$ = 7.4 Hz, 3H, H_j). **^{13}C{^{1}H} NMR (101 MHz, $CDCl_3$)** δ (ppm): 147.27 (C_b), 137.57 (C_d), 132.24 (C_f), 131.36 (C≡N), 117.98 (C_a), 114.79 (C_c), 97.95 (C_e), 44.97 (C_h), 22.06 (C_i), 11.42 (C_j). **Elemental Analysis** for $C_{10}H_{11}N_3O_2$ (205.22 g.mol^{-1}): Found (%) C, 58.52; H, 5.23; N, 20.30; Calcd. (%) C, 58.47; H, 5.36; N, 20.46. **MS** (EI, *m/z*): 205.0795 (65%, $[M]^+$).

4-(Methylsulfonyl)-2-nitro-N-propylaniline (14)

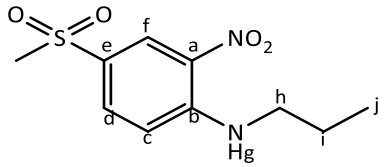

1-Fluoro-4-methanesulfonyl-2-nitrobenzene (0.708 g, 3.23 mmol) was dissolved in DMF (3 mL). *n*-Propylamine (0.53 mL, 6.48 mmol) was then added to the solution. Product: Yellow solid (0.302 g, 36%); **R_f** (EtOAc:Pet. Ether, 5:5): 0.49. **Mp**: 117.7 – 119.1 °C. **^{1}H-NMR (300 MHz, $CDCl_3$)** δ (ppm): 8.76 (d, $^4J_{HH}$ = 2.4 Hz, 1H, H_f), 8.44 (bs, 1H, H_g), 7.92 – 7.84 (dd, $^3J_{HH}$ = 9.3 Hz and $^4J_{HH}$ = 2.4 Hz, 1H, H_d), 6.97 ($^3J_{HH}$ = 9.3 Hz, 1H, H_c), 3.35 (m, 2H, H_h), 3.05 (s, 3H, Ar-$SO_2C\underline{H}_3$), 1.92 – 1.70 (m, 2H, H_i), 1.08 (t, $^3J_{HH}$ = 7.2 Hz, 3H, H_j). **^{13}C{^{1}H} NMR (101 MHz, $CDCl_3$)** δ (ppm): 148.08 (C_b), 133.72 (C_d), 131.18 (C_a), 128.29 (C_f), 126.82 (C_e), 114.78 (C_c), 45.25 (Ar-$SO_2\underline{C}H_3$), 44.91 (C_h), 22.23 (C_i), 11.57 (C_j). **MS** (EI, *m/z*) 258.9 $[M^+]$; Purity 98% by **LC** (t_R 3.68 min).

4-Methoxy-2-nitro-N-propylaniline (15)

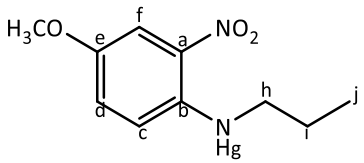

4-Chloro-3-nitroanisole (0.640 g, 3.41 mmol) was dissolved in DMF (2 mL). *n*-Propylamine (0.56 mL, 6.83 mmol) was then added to the solution and the reaction mixture was left to stir in a sealed vessel at 100 ˚C. Product: Orange oil (0.539 g, 75%); **R_f** (EtOAc:Pet. Ether, 1:9): 0.50. **^{1}H-NMR (300 MHz, $CDCl_3$)** δ (ppm): 8.02 (bs, 1H, H_g), 7.62 (d, $^4J_{HH}$ = 3.0 Hz, 1H, H_f), 7.15 (dd, $^3J_{HH}$ = 9.3 Hz and $^4J_{HH}$ = 3.0 Hz, 1H, H_d), 6.83 ($^3J_{HH}$ = 9.3 Hz, 1H, H_c), 3.79 (s, 3H, Ar-O$\underline{C}H_3$), 3.27 (t, $^3J_{HH}$ = 7.2, Hz, 2H, H_h), 1.85 – 1.65 (m, 2H, H_i), 1.05 (t, $^3J_{HH}$ = 7.2 Hz, 3H, H_j). **^{13}C{^{1}H} NMR (101 MHz, $CDCl_3$)** δ (ppm): 149.63 (C_e), 141.91 (C_b), 130.95 (C_a), 127.56 (C_d), 115.39 (C_c), 107.33 (C_f), 56.05 (Ar-O$\underline{C}H_3$), 45.20 (C_h), 22.61 (C_i), 11.69 (C_j).

2-Nitro-N-propyl-4-(trifluoromethyl)aniline (16)

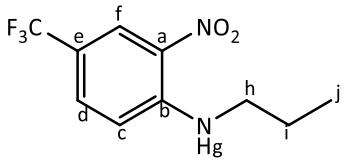

4-Chloro-3-nitrobenzotrifluoride (1.51 g, 6.71 mmol) was dissolved in DMF (3 mL). *n*-Propylamine (1.1 mL, 13.4 mmol) was then added to the solution. Product: Yellow solid (1.42 g, 85%); **R_f** (EtOAc:Pet. Ether, 1:9): 0.65. **Mp**: 54.9 – 55.8 ºC. **^{1}H-NMR (300 MHz, $CDCl_3$)** δ (ppm): 8.46 (d, $^4J_{HH}$ = 2.1 Hz, 1H, H_f), 8.28 (bs, 1H, H_g), 7.60 (dd, $^3J_{HH}$ = 9.0 Hz and $^4J_{HH}$ = 2.1 Hz, 1H, H_d), 6.94 ($^3J_{HH}$ = 9.0 Hz, 1H, H_c), 3.32 (m, 2H, H_h), 1.87 – 1.71 (m, 2H, H_i), 1.07 (t, $^3J_{HH}$ = 7.2 Hz, 3H, H_j). **^{13}C{^{1}H} NMR (101 MHz, $CDCl_3$)** δ (ppm): 147.16 (C_b), 132.21 (C_d), 131.04 (C_a), 125.16 (C_c), 122.48 ($\underline{C}F_3$) 117.38 (d, $^2J_{CF}$ = 34.2 Hz, C_e), 114.60 (C_f), 45.10 (C_h), 22.29 (C_i), 11.60 (C_j).

tert-Butyl (3-((4-methyl-2-nitrophenyl)amino)propyl)carbamate (17)

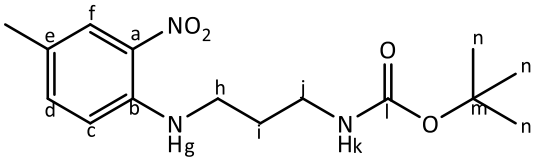

1-Fluoro-4-methyl-2-nitrobenzene (0.258 g, 1.66 mmol) was dissolved in DMF (2 mL). *N*- Boc-1,3-propanediamine (0.32 mL, 1.83 mmol) and K_2CO_3 (0.352 g, 2.55 mmol) was then added to the solution. Product: Yellow solid (0.470 g, 91%); **R_f** (EtOAc:Pet. Ether, 4:6): 0.28. **Mp**: 102.3 – 104.2 °C. **^{1}H-NMR (300 MHz, DMSO-d_6)** δ (ppm): 8.07 (s, 1H, H_g), 7.86 (d, *J* = 2.1 Hz, 1H, H_f), 7.37 (dd, $^3J_{HH}$ = 8.7 and $^4J_{HH}$ 2.1 Hz, 1H, H_d), 6.96 (d, $^3J_{HH}$ = 8.7 Hz, 1H, H_c), 6.89 (s, 1H, H_k), 3.40 – 3.32 (q, 2H, H_h), 3.01 (q, 2H, H_j), 2.22 (s, 3H, Ar-C$\underline{H_3}$), 1.70 (p, *J* = 6.6 Hz, 2H, H_i), 1.37 (s, 9H, H_n). **^{13}C{^{1}H} NMR (101 MHz, DMSO-d_6)** δ (ppm): 155.66 (C_l), 143.48 (C_b), 137.99 (C_d), 130.51 (C_a), 125.16 (C_c), 124.08 (C_e), 114.44 (C_f), 77.48 (C_m), 38.89 (C_h), 37.35 (C_j), 28.65 (C_i), 28.19 (C_n), 19.36 (Ar-$\underline{C}H_3$). **Elemental Analysis** for $C_{15}H_{23}N_3O_4$ (309.37 g.mol^{-1}): Found (%) C, 58.90; H, 7.73; N, 13.34; Calcd. (%) C, 58.24; H, 7.49; N, 13.58. **MS** (EI, *m/z*): 309.1533 (90%, $[M]^+$).

5.2. General synthetic procedure for synthesis of 1,2-diamine derivatives (18 – 34)

Nitroaniline compounds, **1** – **17** (1.eq.) were dissolved in anhydrous MeOH, under an argon atmosphere at room temperature. Ammonium chloride (10 eq.) was then added to the solution and left to stir for 5 min. Thereafter, Zinc dust (20 eq.) was added to the reaction flask. The reaction was allowed to stir vigorously for 30 – 45 min. After the reaction was complete, the reaction mixture was filtered through Celite, and washed with copious amounts of MeOH. Excess solvent was concentrated *in vacuo* and saturated $NaHCO_3$ (aq.) was added to the resultant residue and extracted with EtOAc (2 x 30 mL). The combined organic layers were collected, dried over anhydrous Na_2SO_4 and the solvent removed to afford the product or purified further *via* column chromatography using EtOAc:Petroleum ether as an eluent to afford the desired products, **18** – **34**.[6]

N-Methylbenzene-1,2-diamine (18)

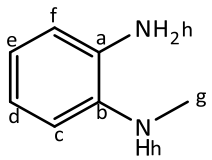

N-Methyl-2-nitroaniline **1** (1.99 g, 13.1 mmol) was dissolved in MeOH (100 mL). NH_4Cl (6.99 g, 131 mmol) and Zinc (17.1 g, 262 mmol) was then added to the solution. Product: Brown oil (1.46 g, 91%); $\mathbf{R_f}$ (EtOAc:Pet. Ether, 2:8): 0.29. **^{1}H NMR (300 MHz, $CDCl_3$)** δ (ppm): 6.95 – 6.78 (m, 1H, H_e), 6.79 – 6.57 (m, 3H, H_c, H_d, H_f), 3.59 – 2.98 (bs, 3H, H_h), 2.87 (s, 3H, H_g). **^{13}C{^{1}H} NMR (101 MHz, $CDCl_3$)** δ (ppm): 137.19 (C_b), 134.99 (C_a), 117.69 (C_d), 116.63 (C_e), 113.82 (C_c), 109.11 (C_f), 30.19 (C_g). **Elemental Analysis** for $C_7H_{10}N_2$ (122.17 g.mol^{-1}): Found (%) C, 64.05; H, 7.23; N, 21.38; Calcd. (%) C, 68.8; H, 8.30; N, 27.90. **MS** (EI, *m/z*): 122.0587 (100%, $[M]^+$).

4-Chloro-N-methylbenzene-1,2-diamine (19)

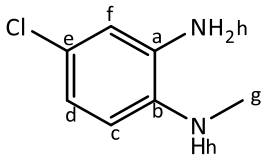

4-Chloro-*N*-methyl-2-nitroaniline **2** (2.03 g, 10.9 mmol) was dissolved in MeOH (60 mL). NH_4Cl (5.83 g, 109 mmol) and Zinc (14.0 g, 217 mmol) was then added to the solution. Product: Brown oil (0.219 g, 13%); $\mathbf{R_f}$ (EtOAc:Pet. Ether, 2:8): 0.19. **^{1}H-NMR (300 MHz, $CDCl_3$)** δ (ppm): 6.79 (dd, $^3J_{HH}$ = 8.4 and $^4J_{HH}$ = 2.3 Hz, 1H, H_d), 6.69 (d, $^4J_{HH}$ = 2.3 Hz, 1H, H_f), 6.55 (d, $^3J_{HH}$ = 8.4 Hz, 1H, H_c), 3.21 (bs, 3H, H_h), 2.84 (s, 3H, H_g). **^{13}C{^{1}H} NMR (101 MHz, $CDCl_3$)** δ (ppm): 137.38 (C_b), 135.64 (C_a), 123.55 (C_e), 120.24 (C_d), 116.13 (C_f), 112.09 (C_c), 31.23 (C_g). **Elemental Analysis** for $C_7H_{10}N_2$ (156.61 g.mol^{-1}): Found (%) C, 55.37; H, 6.01; N, 16.46; Calcd. (%) C, 53.60; H, 5.70; N, 17.90. **MS** (EI, *m/z*): 156.0301 (100%, $[M]^+$).

4-Methoxy-N^1-methylbenzene-1,2-diamine (20)

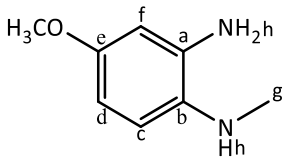

4-Methoxy-*N*-methyl-2-nitroaniline **3** (0.230 g, 1.23 mmol) was dissolved in MeOH (50 mL). NH_4Cl (0.655 g, 12.2 mmol) and Zinc (1.62 g, 24.8 mmol) was then added to the solution. Product: Dark brown solid (0.101 g, 55%); $\mathbf{R_f}$ (EtOAc:Pet. Ether, 4:6): 0.29. **^{1}H-NMR (300 MHz, $CDCl_3$)** δ (ppm): 6.62 (d, $^3J_{HH}$ = 8.6 Hz, 1H, H_c), 6.37 (m, 2H, H_d, H_f), 3.74 (s, 3H, OCH_3), 2.97 (bs, 3H, H_h), 2.82 (bs, 3H, H_g). **^{13}C{^{1}H} NMR (101 MHz, $CDCl_3$)** δ (ppm): 153.96 (C_e), 136.95 (C_a), 132.05 (C_b), 113.30 (C_c), 104.07 (C_d), 103.43 (C_f), 55.75 (OCH_3), 32.07 (C_g). **Elemental Analysis** for $C_8H_{12}N_2O$ (152.20 g.mol^{-1}): Found (%) C, 64.01; H, 7.86; N, 17.19; Calcd. (%) C, 63.13; H, 7.95; N, 18.41. **MS** (EI, *m/z*): 152.0534 (100%, $[M]^+$).

3-Amino-4-(methylamino)benzonitrile (21)

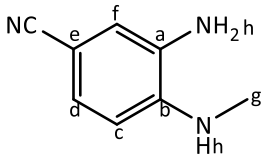

4-(Methylamino)-3-nitrobenzonitrile **4** (0.495 g, 2.79 mmol) was dissolved in MeOH (50 mL). NH_4Cl (1.50 g, 27.9 mmol) and Zinc (3.64 g, 55.9 mmol) was then added to the solution. Product: Brown solid (0.384 g, 93%); $\mathbf{R_f}$ (EtOAc:Pet. Ether, 4:10): 0.29. **Mp**: 133.6 – 140.7 °C. **^{1}H-NMR (300 MHz, $CDCl_3$)** δ (ppm): 7.18 (dd, $^3J_{HH}$ = 8.1 and $^4J_{HH}$ = 1.8 Hz, 1H, H_d), 6.92 (d, $^4J_{HH}$ = 1.8 Hz, 1H, H_f), 6.57 (d, $^3J_{HH}$ = 8.1 Hz, 1H, H_c), 3.43 (bs, 3H, H_h), 2.90 (s, 3H, H_g). **^{13}C{^{1}H} NMR (101 MHz, $CDCl_3$)** δ (ppm): 143.64 (C_b), 133.19 (C_a), 126.92 (C_d), 120.69 (C_i), 119.25 (C_f), 109.64 (C_c), 99.47 (C_e), 31.23 (C_g). **Elemental Analysis** for $C_8H_9N_3$ (147.18 g.mol^{-1}): Found (%) C, 65.24; H, 5.66; N, 29.46; Calcd. (%) C, 65.20; H, 6.10; N, 28.50. **MS** (EI, *m/z*): 147.0440 (100%, $[M]^+$).

N^1,4-dimethylbenzene-1,2-diamine (22)

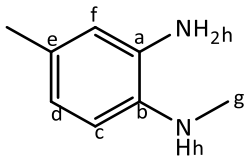

N,4-Dimethyl-2-nitroaniline **5** (0.322 g, 1.94 mmol) was dissolved in MeOH (30 mL). NH_4Cl (1.01 g, 18.8 mmol) and Zinc (2.52 g, 38.5 mmol) was then added to the solution. Product: Brown solid (0.220 g, 83%); **R_f** (EtOAc:Pet. Ether, 5:5): 0.44. **Mp**: 35.8 – 40.7 °C. **^{1}H-NMR (300 MHz, $CDCl_3$)** δ (ppm): 6.66 (m, 1H, H_d), 6.60 (d, 1H, H_c), 6.58-6.54 (m, 1H, H_f), 3.20 (s, 3H, H_h), 2.85 (s, 3H, H_g), 2.24 (s, 3H, Ar-$C\underline{H}_3$). **^{13}C{^{1}H} NMR (101 MHz, $CDCl_3$)** δ (ppm): 136.32 (C_b), 134.51 (C_a), 128.23 (C_e), 120.82 (C_d), 117.15 (C_f), 111.52 (C_c), 31.31 (Ar-CH_3), 20.58 (C_g). **Elemental Analysis** for $C_8H_{12}N_2$ (136.20 g.mol^{-1}): Found (%) C, 70.95; H, 8.59; N, 19.31; Calcd. (%) C, 70.50; H, 8.90; N, 20.60. **MS** (EI, *m/z*): 136.0467 (100%, $[M]^+$).

N^1-Methyl-4-(trifluoromethyl)benzene-1,2-diamine (23)

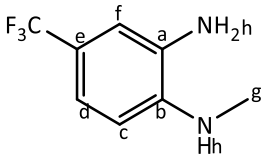

N-Methyl-2-nitro-4-(trifluoromethyl)aniline **6** (0.426 g, 1.93 mmol) was dissolved in MeOH (60 mL). NH_4Cl (1.04 g, 19.4 mmol) and Zinc (2.52 g, 38.6 mmol) was then added to the solution. Product: Brown solid (0.234 g, 64%); **R_f** (EtOAc:Pet. Ether, 2:8): 0.26. **MP**: 42.4 – 47.4 °C. **^{1}H-NMR (300 MHz, $CDCl_3$)** δ (ppm): 7.12 (dd, $^3J_{HH}$ = 8.3 and $^4J_{HH}$ = 2.0, Hz, 1H, H_d), 6.93 (d, $^4J_{HH}$ = 2.0 Hz, 1H, H_f), 6.64 (d, $^3J_{HH}$ = 8.2 Hz, 1H, H_c), 3.56 – 3.08 (bs, 3H, H_h), 2.90 (s, 3H, H_g). **^{13}C{^{1}H} NMR (101 MHz, $CDCl_3$)** δ (ppm): 141.97 (C_b), 133.26 (C_a), 124.95 (d, $^1J_{CF}$ = 268.9 Hz, Ar-$\underline{C}F_3$), 119.76 (d, $^2J_{CF}$ = 32.2 Hz, C_e), 118.47 (d, $^4J_{CF}$ = 4.1 Hz, C_c), 113.04 (C_d), 109.50 (C_f), 30.61 (C_g). **Elemental Analysis** for $C_8H_9F_3N_2$ (190.17 g.mol^{-1}): Found (%) C, 51.61; H, 4.06; N, 14.22; Calcd. (%) C, 50.53; H, 4.77; N, 14.73. **MS** (EI, *m/z*): 190.0465 (90%, $[M]^+$).

N^1-Methyl-4-(methylsulfonyl)benzene-1,2-diamine (24)

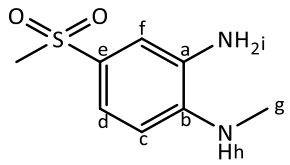

N-Methyl-4-(methylsulfonyl)-2-nitroaniline **7** (0.301 g, 1.31 mmol) was dissolved in MeOH (30 mL). NH_4Cl (0.695 g, 13.0 mmol) and Zinc (1.72 g, 26.4 mmol) was then added to the solution. Product: Brown oil (0.193 g, 74%); **R_f** (EtOAc:10) 0.63. **^{1}H-NMR (300 MHz, DMSO-d_6)** δ (ppm): 7.06 (dd, $^3J_{HH}$ = 8.4 and $^4J_{HH}$ = 2.4, Hz, 1H, H_d), 7.01 (d, $^4J_{HH}$ = 2.4 Hz, 1H, H_f), 6.47 (d, $^3J_{HH}$ = 8.4 Hz, 1H, H_c), 5.48 (bd, $^3J_{HH}$ = 5.1 Hz, 1H, H_h), 4.93 (s, 2H, H_i), 2.99 (s, 3H, Ar-$SO_2C\underline{H}_3$), 2.79 (d, $^3J_{HH}$ = 5.1 Hz, 1H, H_g). **^{13}C{^{1}H} NMR (101 MHz, DMSO-d_6)** δ (ppm): 141.72 (C_b), 135.24 (C_a), 127.35 (C_e), 118.15 (C_d), 111.08 (C_f), 107.75 (C_c), 45.17 (Ar-$SO_2\underline{C}H_3$), 30.20 (C_g). **Elemental Analysis** for $C_8H_{12}N_2O_2S$ (200.26 g.mol^{-1}): Found (%) C, 48.22; H, 6.47; N, 13.61; S, 11.64 Calcd. (%) C, 47.98; H, 6.04; N, 13.99, S, 16.01. **MS** (EI, *m/z*): 199.9416 (100%, $[M]^+$).

3-Amino-4-(methylamino)benzamide (25)

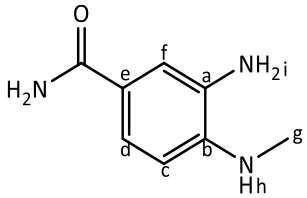

4-(Methylamino)-3-nitrobenzamide **8** (0.204 g, 1.04 mmol) was dissolved in MeOH (30 mL). NH_4Cl (0.557 g, 10.4 mmol) and Zinc (1.36 g, 20.8 mmol) was then added to the solution. Product: Brown oil (0.094 g, 54%); **R_f** (EtOAc:10) 0.14. **^{1}H-NMR (300 MHz, DMSO-d_6)** δ (ppm): 7.40 (bs, 1H, Ar-CON$\underline{H}_2$), 7.15 (dd, $^3J_{HH}$ = 8.1 and $^4J_{HH}$ = 2.1 Hz, 1H, H_d), 7.09 (d, $^4J_{HH}$ = 2.1 Hz, 1H, H_f), 6.70 (s, 1H, Ar-CON$\underline{H}_2$), 6.34 (d, $^3J_{HH}$ = 8.1 Hz, 1H, H_c), 5.08 (d, $^3J_{HNH}$ = 4.5 Hz, 1H, H_h), 4.52 (bs, 2H, H_i), 2.76 (d, $^3J_{HNH}$ = 4.5 Hz, 3H, H_g). **^{13}C{^{1}H} NMR (101 MHz, DMSO-d_6)** δ (ppm): 169.22 (C=O), 140.46 (C_b), 134.40 (C_a), 122.47 (C_e), 118.62 (C_d), 113.75 (C_c), 107.76 (C_f), 30.38 (C_g). **Elemental Analysis** for $C_8H_{11}N_3O$ (165.20 g.mol^{-1}): Found (%) C, 57.46; H, 7.21; N, 16.62; Calcd. (%) C, 58.16; H, 6.71; N, 25.42. **MS** (EI, *m/z*): 165.0466 (100%, $[M]^+$).

4-Fluoro-N^1-methylbenzene-1,2-diamine (26)

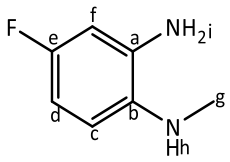

4-Fluoro-*N*-methyl-2-nitroaniline **9** (0.376 g, 2.21 mmol) was dissolved in MeOH (40 mL). NH_4Cl (1.19 g, 22.2 mmol) and Zinc (2.89 g, 44.2 mmol) was then added to the solution. Product: Brown solid (0.160 g, 52%); $\mathbf{R_f}$ (EtOAc:Pet. Ether, 2:8): 0.15. **^{1}H-NMR (300 MHz, DMSO-d_6)** δ (ppm): 6.40 – 6.33 (m, 1H, H_f), 6.33 – 6.21 (m, 2H, H_c, H_d), 4.77 (bs, 2H, H_i), 4.38 (bs, 1H, H_h), 2.68 (s, 3H, H_g). **^{13}C{^{1}H} NMR (101 MHz, DMSO-d_6)** δ (ppm): 155.92 (d, $^1J_{CF}$ = 230.0 Hz, C_e), 137.52 (d, $^3J_{CF}$ = 10.7 Hz, C_a), 133.86 (C_b), 109.55 (d, $^3J_{CF}$ = 9.6 Hz, C_c), 102.19 (d, $^2J_{CF}$ = 21.4 Hz, C_d), 100.74 (d, $^2J_{CF}$ = 25.8 Hz, C_f), 31.11 (C_g). **Elemental Analysis** for $C_7H_9FN_2$ (140.16 g.mol^{-1}): Found (%) C, 60.42; H, 6.04; N, 19.74; Calcd. (%) C, 59.99; H, 6.47; N, 19.99. **MS** (EI, *m/z*): 140.0041 (100%, $[M]^+$).

N^1-Propylbenzene-1,2-diamine (27)

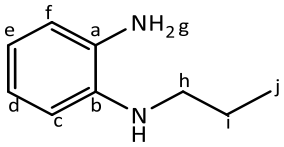

2-Nitro-*N*-propylaniline **10** (0.200 g, 1.11 mmol) was dissolved in MeOH (30 mL). NH_4Cl (0.594 g, 11.1 mmol) and Zinc (1.45 g, 22.2 mmol) was then added to the solution. Product: Brown oil (0.147 g, 88%); $\mathbf{R_f}$ (EtOAc: Pet. Ether, 1:3): 0.52. **^{1}H-NMR (400 MHz, $CDCl_3$)** δ (ppm): 6.87 – 6.82 (m, 1H, H_e), 6.75 – 6.66 (m, 3H, H_c, H_d, H_f), 3.25 (s, 2H, H_g), 3.10 (t, 2H, $^3J_{HH}$ = 7.2 Hz, H_h), 1.77 – 1.65 (m, 2H, H_i), 1.05 (t, 3H, $^3J_{HH}$ = 7.4 Hz, H_j). **^{13}C{^{1}H} NMR (101 MHz, $CDCl_3$)** δ (ppm): 138.18 (C_a), 134.06 (C_b), 120.81 (C_d), 118.35 (C_e), 116.54 (C_c), 111.71 (C_f), 46.14 (C_g), 22.91 (C_h), 11.77 (C_i). **Elemental Analysis** for $C_9H_{14}N_2$ (150.23 g.mol^{-1}): Found (%) C, 72.06; H, 9.57; N, 17.94; Calcd. (%) C, 71.80; H, 9.40; N, 18.60. **MS** (EI, *m/z*): 150.0787 (85%, $[M]^+$).

4-Chloro-N¹-propylbenzene-1,2-diamine (28)

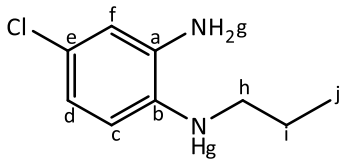

4-Chloro-2-nitro-*N*-propylaniline **11** (0.739 g, 3.44 mmol) was dissolved in MeOH (100 mL). NH_4Cl (1.84 g, 34.4 mmol) and Zinc (4.52 g, 69.1 mmol) was then added to the solution. Product: Brown oil (0.214 g, 34%); **R_f** (EtOAc: Pet. Ether, 2:8): 0.39. **^{1}H-NMR (300 MHz, $CDCl_3$)** δ (ppm): 6.76 (dd, $^3J_{HH}$ = 8.4 and $^4J_{HH}$ = 2.4 Hz, 1H, H_d), 6.69 (d, $^4J_{HH}$ = 2.4 Hz, 1H, H_f), 6.54 (d, $^3J_{HH}$ = 8.4 Hz, 1H, H_c), 3.37 (bs, 3H, H_g), 3.04 (t, $^3J_{HH}$ = 6.9 Hz, 2H H_h), 1.79 – 1.58 (m, 2H, H_i), 1.02 (t, $^3J_{HH}$ = 7.5 Hz, 3H, H_j). **^{13}C{^{1}H} NMR (101 MHz, $CDCl_3$)** δ (ppm): 136.49 (C_a), 135.46 (C_b), 123.12 (C_e), 120.03 (C_d), 116.08 (C_f), 112.56 (C_c), 46.22 (C_h), 22.78 (C_i), 11.71 (C_j). **Elemental Analysis** for $C_9H_{13}ClN_2$ (184.67 g.mol^{-1}): Found (%) C, 57.86; H, 6.78; N, 14.02; Calcd. (%) C, 58.54; H, 7.10; N, 15.17. **MS** (EI, *m/z*): 184.0871 (80%, $[M]^+$).

4-Methyl-N¹-propylbenzene-1,2-diamine (29)

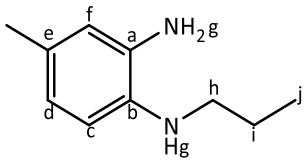

4-Methyl-2-nitro-*N*-propylaniline **12** (0.280 g, 1.44 mmol) was dissolved in MeOH (50 mL). NH_4Cl (0.773 g, 14.5 mmol) and Zinc (1.90 g, 29.1 mmol) was then added to the solution. Product: Brown oil (0.228 g, 97%); **R_f** (EtOAc:Pet. Ether, 1:9): 0.14. **^{1}H-NMR (300 MHz, $CDCl_3$)** δ (ppm): 6.67 – 6.51 (m, 3H, H_c, H_d, H_f), 3.19 (bs, 3H, H_g), 3.05 (t, $^3J_{HH}$ = 7.1 Hz, 2H, H_h), 1.77 – 1.58 (m, 2H, H_i), 1.03 (t, $^3J_{HH}$ = 7.4 Hz, 3H, H_j). **^{13}C{^{1}H} NMR (101 MHz, $CDCl_3$)** δ (ppm): 135.47 (C_a), 134.54 (C_b), 128.11 (C_e), 120.76 (C_d), 117.26 (C_f), 112.33 (C_c), 46.51 (C_h), 22.96 (C_i), 20.59 ($\underline{C}H_3$), 11.77 (C_j). **Elemental Analysis** for $C_{10}H_{16}N_2$ (164.25 g.mol^{-1}): Found (%) C, 72.91; H, 9.70; N, 16.07; Calcd. (%) C, 73.13; H, 9.82; N, 17.06. **MS** (EI, *m/z*): 164.0885 (90%, $[M]^+$).

3-Amino-4-(propylamino)benzonitrile (30)

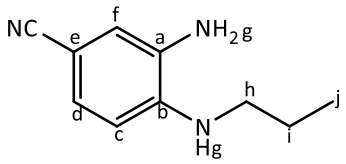

3-Nitro-4-(propylamino)benzonitrile **13** (0.371 g, 1.83 mmol) was dissolved in MeOH (30 mL). NH_4Cl (0.932 g, 17.4 mmol) and Zinc (2.31 g, 35.3 mmol) was then added to the solution. Product: Brown solid (0.299 g, 94%); $\mathbf{R_f}$ (EtOAc:Pet. Ether, 1:2): 0.74. **^{1}H-NMR (300 MHz, $CDCl_3$)** δ (ppm): 8.50 (d, $^4J_{HH}$ = 2.9 Hz, 1H, H_f), 8.41 (s, 3H, H_g), 7.59 (dd, $^3J_{HH}$ = 9.0 Hz and $^4J_{HH}$ = 2.9 Hz, 1H, H_d), 6.91 (d, $^3J_{HH}$ = 9.0 Hz, 1H, H_c), 3.40-4.23 (m, 2H, H_h), 2.89-2.70 (m, 2H, H_i), 1.07 (t, $^3J_{HH}$ = 7.4 Hz. 3H, H_j). **^{13}C{^{1}H} NMR (101 MHz, $CDCl_3$)** δ (ppm): 147.27 (C_b), 137.57 (C_d), 132.24 (C_f), 131.36 (CN), 117.98 (C_a), 114.79 (C_c), 97.95 (C_e), 44.97 (C_h), 22.06 (C_i), 11.42 (C_j). **Elemental Analysis** for $C_{10}H_{13}N_3$ (175.24 g.mol^{-1}): Found (%) C, 68.39; H, 7.15; N, 23.72; Calcd. (%) C, 68.54; H, 7.48; N, 23.98. **MS** (EI, *m/z*): 175.0765 (75%, $[M]^+$).

4-(Methylsulfonyl)-N^1-propylbenzene-1,2-diamine (31)

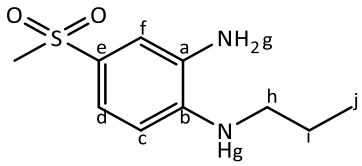

4-(Methylsulfonyl)-2-nitro-*N*-propylaniline **14** (0.283 g, 1.10 mmol) was dissolved in MeOH (50 mL). NH_4Cl (0.584 g, 10.9 mmol) and Zinc (1.46 g, 22.3 mmol) was then added to the solution. Product: Brown solid (0.247 g, 99%); $\mathbf{R_f}$ (EtOAc:Pet. Ether, 1:1): 0.33. **Mp**: 87.9 – 95.6 °C. **^{1}H-NMR (300 MHz, $CDCl_3$)** δ (ppm): 7.40 (dd, $^3J_{HH}$ = 8.4 and $^4J_{HH}$ = 2.1 Hz, 1H, H_d), 7.22 (d, $^4J_{HH}$ = 2.1 Hz, 1H, H_f), 6.64 (d, $^3J_{HH}$ = 8.4 Hz, 1H, H_c) 3.35 – 3.06 (bs, 3H, H_g), 3.14 (t, $^3J_{HH}$ = 6.9 Hz, 2H, H_h), 2.99 (s, 3H, Ar-$SO_2C\underline{H_3}$), 1.81 – 1.62 (m, 2H, H_i), 1.03 (t, $3J_{HH}$ = 7.2 Hz, 3H, H_j). **^{13}C{^{1}H} NMR (101 MHz, $CDCl_3$)** δ (ppm): 143.33 (C_b), 132.78 (C_a), 127.81 (C_e), 121.78 (C_d), 115.24 (C_f), 109.43 (C_c), 45.48 ($\underline{C}H_3$), 45.06 (C_h), 22.49 (C_i), 11.58 (C_j). Purity 98% by **LC** (t_R 2.02 min); **MS** *m/z* 228.9 (100%, $[M]^+$).

4-Methoxy-N^1-propylbenzene-1,2-diamine (32)

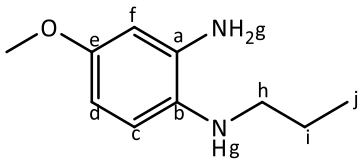

4-Methoxy-2-nitro-*N*-propylaniline **15** (0.510 g, 2.42 mmol) was dissolved in MeOH (60 mL). NH_4Cl (1.30 g, 24.3 mmol) and Zinc (3.17 g, 48.5 mmol) was then added to the solution. Product: Brown oil (0.209 g, 48%); **R_f** (EtOAc:Pet. Ether, 3:7): 0.60. **^{1}H-NMR (300 MHz, $CDCl_3$)** δ (ppm): 6.63 (d, $^3J_{HH}$ = 8.4 Hz, 1H, H_c), 6.35 – 6.28 (m, 2H, H_d, H_f) 3.76 (s, 3H, O$\underline{C}H_3$), 3.01 (bs, 2H, H_g), 3.00 (m, 2H, H_h), 1.75 – 1.59 (m, 2H, H_i), 1.02 (t, $^3J_{HH}$ = 7.5 Hz, 3H, H_j). **^{13}C{^{1}H} NMR (101 MHz, $CDCl_3$)** δ (ppm): 154.13 (C_e), 137.41 (C_a), 131.12 (C_b), 114.83 (C_c), 104.11 (C_d), 103.39 (C_f), 55.74 ($\underline{C}H_3$), 47.55 (C_h), 23.20 (C_i), 11.88 (C_j).

N^1-Propyl-4-(trifluoromethyl)benzene-1,2-diamine (33)

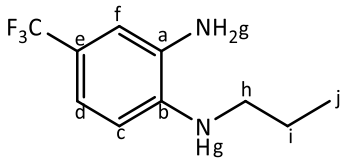

2-Nitro-*N*-propyl-4-(trifluoromethyl)aniline **16** (1.69 g, 6.79 mmol) was dissolved in MeOH (150 mL). NH_4Cl (3.63 g, 67.9 mmol) and Zinc (8.88 g, 136 mmol) was then added to the solution. Product: Brown solid (1.42 g, 96%); **R_f** (EtOAc:Pet. Ether, 2:8: 0.33. **Mp**: 41.2 – 43.1 °C. **^{1}H-NMR (300 MHz, $CDCl_3$)** δ (ppm): 7.10 (m, 1H, H_d), 6.93 (d, $^4J_{HH}$ = 2.1 Hz, 1H, H_f), 6.63 (d, $^3J_{HH}$ = 8.4 Hz, 1H, H_c) 3.42 (bs, 3H, H_g), 3.12 (t, $^3J_{HH}$ = 6.9 Hz, 2H, H_h), 1.82 – 1.64 (m, 2H, H_i), 1.04 (t, $^3J_{HH}$ = 7.2 Hz, 3H, H_j). **^{13}C{^{1}H} NMR (101 MHz, $CDCl_3$)** δ (ppm): 141.43 (C_b), 133.21 (C_a), 125.13 (d, $^1J_{CF}$ = 271.39 Hz, Ar-$\underline{C}F_3$), 119.60 (d, $^2J_{CF}$ = 32.42 Hz, C_e), 118.61 (C_c), 113.40 (C_d), 110.04 (C_f), 45.83 (C_h), 22.79 (C_i), 11.78 (C_j).

tert-Butyl (3-((2-amino-4-methylphenyl)amino)propyl)carbamate (34)

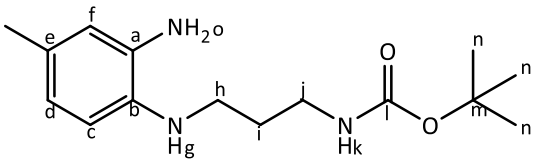

tert-Butyl (3-((4-methyl-2-nitrophenyl)amino)propyl)carbamate **17** (0.463 g, 1.50 mmol) was dissolved in MeOH (60 mL). NH_4Cl (0.801 g, 15.0 mmol) and Zinc (1.96 g, 30.0 mmol) was then added to the solution. Product: Purple solid (0.337 g, 81%); $\mathbf{R_f}$ (EtOAc:Pet Ether, 5:5): 0.58. **Mp**: 110.6 – 112.6 °C. **^{1}H-NMR (300 MHz, DMSO-*d*$_6$)** δ (ppm): 6.83 (bs, 1H, H_g), 6.37 (s, 1H, H_f), 6.35 – 6.25 (m, 2H, H_d, H_c), 4.38 (bs, 2H, H_o), 4.12 (bs, 1H, H_k), 3.00 (m, 4H, H_h, H_i), 2.08 (s, 3H, $C\underline{H}_3$), 1.83 – 1.54 (m, 2H, H_i), 1.39 (s, 9H, H_n). **^{13}C{^{1}H} NMR (101 MHz, DMSO-*d*$_6$)** δ (ppm): 155.65 (C_l), 135.34 (C_a), 133.66 (C_b), 125.18 (C_e), 117.73 (C_d), 115.03 (C_f), 110.21 (C_c), 77.37 (C_m), 41.28 (C_h), 38.02 (C_j), 29.16 (C_i), 28.24 (C_n), 20.39 ($\underline{C}H_3$). **Elemental Analysis** for $C_{15}H_{25}N_3O_2$ (279.38 g.mol^{-1}): Found (%) C, 64.35; H, 9.04; N, 14.77; Calcd. (%) C, 64.49; H, 9.02; N, 15.04. **MS** (EI, *m/z*): 279.1597 (90%, $[M]^+$).

5.3. General synthetic procedure for 2-phenylbenzimidazole ligands (35 – 53)

The synthesised 1,2-diamines (**18** – **34**) (1 eq.) were dissolved in EtOH. Benzaldehyde (1.2 eq.), TFA (0.1 eq.) and $MgSO_4$ (6 eq.) was added to the reaction flask, under an argon atmosphere at 25 °C. The reaction was then left to stir, open to air, for 24 h. The reaction mixture was filtered and the solvent reduced *in vacuo*. The resultant residue was dissolved in DCM (30 mL) and washed with H_2O (2 x 20 mL) and sat. NaCl (20 mL). The organic layers were collected, dried with anhydrous Na_2SO_4 and concentrated *in vacuo*. The crude product was then purified *via* column chromatography using EtOAc:Petroleum ether as the eluent to afford the desired compounds.[7]

1-Methyl-2-phenyl-1H-benzo[d]imidazole (35)

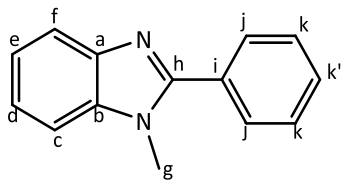

N-Methylbenzene-1,2-diamine **18** (0.410 g, 3.36 mmol) was dissolved in EtOH (30 mL). Benzaldehyde (0.41 mL, 4.03 mmol), TFA (0.026 mL, 0.336 mmol) and $MgSO_4$ (2.46 g,

20.1 mmol) was then added to the reaction flask. Product: Yellow solid (0.265 g, 38%); **R_f** (EtOAc:Pet. Ether, 5:5): 0.63. **Mp**: 94.3 – 95.4 °C. **^{1}H-NMR (300 MHz, $CDCl_3$)** δ (ppm): 7.87-7.81 (m, 1H, H_f), 7.80 – 7.73 (m, 2H, H_j), 7.58 – 7.47 (m, 3H, H_k), 7.43 – 7.36 (m, 1H, H_c), 7.35 – 7.29 (m, 2H, H_d,H_e), 3.87 (s, 3H, H_g). **^{13}C{^{1}H} NMR (101 MHz, $CDCl_3$)** δ (ppm): 153.91 (C_h), 143.06 (C_a), 136.71 (C_b), 130.36 (C_i), 129.88 ($C_{k'}$), 129.61 (C_k), 128.82 (C_j), 122.95 (C_e), 122.62 (C_d), 120.00 (C_f), 109.74 (C_c), 31.79 (C_g). **FT-IR** (ATR) ν(cm^{-1}) = 1603 (imine, C=N). **Elemental Analysis** for $C_{14}H_{12}N_2$ (208.26 g.mol^{-1}): Found (%) C, 80.26; H, 5.72; N, 13.78; Calcd. (%) C, 80.70; H, 5.80; N, 13.80. **MS** (EI, *m/z*): 208.0530 (90%, $[M]^+$).

5-Chloro-1-methyl-2-phenyl-1H-benzo[d]imidazole (36)

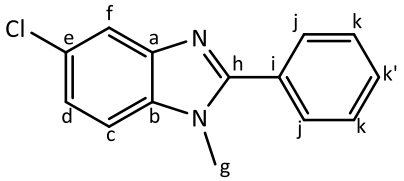

4-Chloro-*N*-methylbenzene-1,2-diamine **19** (0.201 g, 1.28 mmol) was dissolved in EtOH (15 mL). Benzaldehyde (0.16 mL, 1.57 mmol), TFA (0.015 g, 0.127 mmol) and $MgSO_4$ (0.932 g, 7.74 mmol) was then added to the reaction flask. Product: Brown solid (0.128 g, 41%); **R_f** (EtOAc:Pet. Ether, 4:6): 0.68. **Mp**: 128.4 – 134.7 °C. **^{1}H-NMR (300 MHz, $CDCl_3$)** δ (ppm): 7.81 – 7.27 (m, 1H, H_f), 7.78 – 7.27 (m, 2H, H_j), 7.57 – 7.49 (m, 3H, H_k), 7.31 – 7.27 (m, 2H, H_c, H_d), 3.85 (s, 3H, H_g). **^{13}C{^{1}H} NMR (101 MHz, $CDCl_3$)** δ (ppm): 155.05 (C_h), 143.70 (C_a), 135.32 (C_b), 130.24 ($C_{k'}$), 129.81 (C_i), 129.59 (C_k), 128.93 (C_j), 128.30 (C_e), 123.41 (C_d), 119.70 (C_c), 110.54 (C_f), 31.98 (C_g). **FT-IR** (ATR) ν(cm^{-1}) = 1610 (imine, C=N). **Elemental Analysis** for $C_{14}H_{11}ClN_2$ (242.71 g.mol^{-1}): Found (%) C, 69.01; H, 4.54; N, 11.25; Calcd. (%) C, 69.30; H, 4.60; N, 11.50. **MS** (EI, *m/z*): 241.0541 (100%, $[M-H]^+$).

5-Methoxy-1-methyl-2-phenyl-1H-benzo[d]imidazole (37)

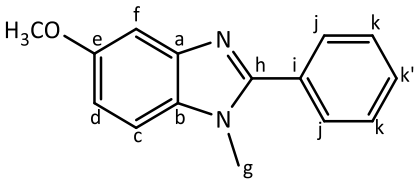

4-Methoxy-*N*^{1}-methylbenzene-1,2-diamine **20** (76.2 mg, 0.501 mmol) was dissolved in EtOH (10 mL). Benzaldehyde (0.061 mL, 0.601 mmol), TFA (5.71 mg, 0.0501 mmol) and $MgSO_4$

(0.362 g, 3.00 mmol) was then added to the reaction flask. Product: Yellow solid (0.081 g, 68%); **R_f** (EtOAc: 10): 0.67. **Mp**: 118.1 – 121.4 °C. **^{1}H-NMR (300 MHz, $CDCl_3$)** δ (ppm): 7.79 – 7.72 (m, 2H, H_j), 7.57 – 7.48 (m, 3H, H_k), 7.32 (d, $^4J_{HH}$ = 2.4 Hz, 1H, H_f), 7.27 (d, $^3J_{HH}$ = 8.7 Hz, 1H, H_c), 6.98 (dd, $^3J_{HH}$ = 8.7 and $^3J_{HH}$ = 2.4 Hz, 1H, H_d), 3.89 (s, 3H, H_g), 3.85 (s, 3H, OCH_3). **^{13}C{^{1}H} NMR (101 MHz, $CDCl_3$)** δ (ppm): 156.46 (C_e), 153.91 (C_h), 143.61 (C_a), 131.30 (C_i), 130.28 (C_b), 129.65 ($C_{k'}$), 129.37 (C_k), 128.67 (C_j), 112.91 (C_c), 109.97 (C_d), 101.98 (C_f), 55.87 (OCH_3), 31.76 (C_g). **FT-IR** (ATR) ν(cm^{-1}) = 1618 (imine, C=N). **Elemental Analysis** for $C_{15}H_{14}N_2O$ (238.29 g.mol^{-1}): Found (%) C, 74.47; H, 6.17; N, 10.71; Calcd. (%) C, 75.61; H, 5.92; N, 11.76. **MS** (EI, *m/z*): 237.9709 (100%, $[M]^+$).

1-Methyl-2-phenyl-1H-benzo[d]imidazole-5-carbonitrile (38)

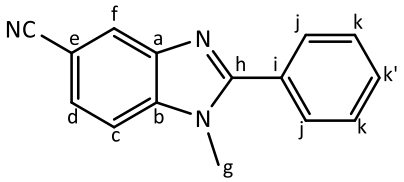

3-Amino-4-(methylamino)benzonitrile **21** (0.358 g, 2.43 mmol) was dissolved in EtOH (20 mL). Benzaldehyde (0.30 mL, 2.95 mmol), TFA (27.7 mg, 0.243 mmol) and $MgSO_4$ (1.76 g, 14.6 mmol) was then added to the reaction flask. Product: White solid (0.227 g, 40%); **R_f** (EtOAc:Pet. Ether, 4:6): 0.32. **Mp**: 185.8 – 191.3 °C. **^{1}H-NMR (300 MHz, $CDCl_3$)** δ (ppm): 8.13 (m, 1H, H_f), 7.77 (m, 2H, H_j), 7.61 – 7.53 (m, 3H, H_k), 7.46 (m, 1H, H_c), 3.91 (s, 3H, H_g). **^{13}C{^{1}H} NMR (101 MHz, $CDCl_3$)** δ (ppm): 156.45 (C_h), 142.63 (C_b), 139.37 (C_a), 130.67 ($C_{k'}$), 129.61 (C_k), 129.25 (C_i), 129.07 (C_j), 126.34 (C_d), 124.95 (C_f), 119.99 (C≡N), 110.85 (C_c), 105.94 (C_e), 32.14 (C_g). **Elemental Analysis** for $C_{15}H_{11}N_3$ (233.27 g.mol^{-1}): Found (%) C, 76.50; H, 4.68; N, 17.72; Calcd. (%) C, 77.20; H, 4.70; N, 18.08. **MS** (EI, *m/z*): 232.0766 (100%, $[M-H]^+$).

1,5-Dimethyl-2-phenyl-1H-benzo[d]imidazole (39)

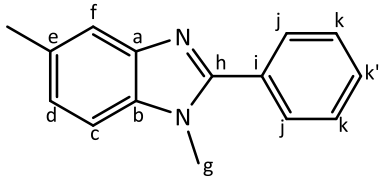

N^1,4-dimethylbenzene-1,2-diamine **22** (0.225 g, 1.65 mmol) was dissolved in EtOH (10 mL). Benzaldehyde (0.20 mL, 1.98 mmol), TFA (18.8 mg, 0.165 mmol) and $MgSO_4$ (1.19 g,

9.92 mmol) was then added to the reaction flask. Product: Orange solid (0.145 g, 51%); **R_f** (EtOAc:Pet. Ether, 4:6): 0.48. **Mp**: 114.7 – 120.7 °C. **^{1}H-NMR (300 MHz, DMSO-*d*$_6$)** δ (ppm): 7.84 (m, 1H, H_j), 7.64 – 7.52 (m, 3H, H_k, $H_{k'}$), 7.49 (m, 2H, H_c, H_d), 7.17 – 7.09 (m, 1H, H_f), 3.86 (s, 3H, H_g), 2.45 (s, 3H, Ar-C$\underline{H}_3$). **^{13}C{^{1}H} NMR (101 MHz, DMSO-*d*$_6$)** δ (ppm): 152.85 (C_h), 142.78 (C_a), 134.77 (C_b), 130.87 (C_e), 130.24 (C_i), 129.48 ($C_{k'}$), 129.20 (C_k), 128.58 (C_j), 123.73 (C_d), 118.69 (C_f), 110.03 (C_c), 31.61 (C_g), 21.18 (Ar-C$\underline{H}_3$). **FT-IR** (ATR) ν(cm^{-1}) = 1614 (imine, C=N). **Elemental Analysis** for $C_{15}H_{14}N_2$ (222.29 g.mol^{-1}): Found (%) C, 80.17; H, 6.07; N, 11.10; Calcd. (%) C, 81.65; H, 6.35; N, 12.60. **MS** (EI, *m/z*): 221.0149 (90%, $[M]^+$).

1-Methyl-2-phenyl-5-(trifluoromethyl)-1H-benzo[d]imidazole (40)

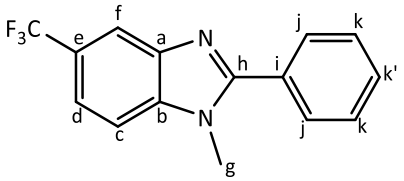

N^1-methyl-4-(trifluoromethyl)benzene-1,2-diamine **23** (0.210 g, 1.10 mmol) was dissolved in EtOH (10 mL). Benzaldehyde (0.13 mL, 1.33 mmol), TFA (12.6 mg, 0.110 mmol) and $MgSO_4$ (0.798 g, 6.63 mmol) was then added to the reaction flask. Product: Brown solid (0.145 g, 58%); **R_f** (EtOAc:Pet. Ether, 5:5): 0.47. **Mp**: 156.7 – 158.5 °C. **^{1}H-NMR (300 MHz, DMSO-*d*$_6$)** δ (ppm): 8.16 – 8.11 (m, 1H, H_d), 7.84 – 7.76 (m, 2H, H_j), 7.64 – 7.55 (m, 4H, H_k, $H_{k'}$, H_c), 7.50 (d, 1H, H_f), 3.93 (s, 3H, H_g). **^{13}C{^{1}H} NMR (101 MHz, DMSO-*d*$_6$)** δ (ppm): 150.87 (C_h), 137.37 (C_b), 133.64 (C_a), 125.59 ($C_{k'}$), 124.73 (C_k), 124.60 (C_i), 124.13 (C_j), 121.64 – 118.55 (d, $^1J_{CF}$ = 270 Hz, $\underline{C}F_3$), 120.39 (d, $^2J_{CF}$ = 32.2 Hz, C_e), 115.01 (d, $^3J_{CF}$ = 3.2 Hz, C_d), 112.72 (d, $^4J_{CF}$ = 3.8 Hz, C_c), 105.32 (C_f), 27.20 (C_g). **FT-IR** (ATR) ν(cm^{-1}) = 1621 (imine, C=N). **Elemental Analysis** for $C_{15}H_{11}F_3N_2$ (276.26 g.mol^{-1}): Found (%) C, 65.30; H, 3.64; N, 9.78; Calcd. (%) C, 65.22; H, 4.01; N, 10.14. **MS** (EI, *m/z*): 275.0554 (100%, $[M-H]^+$).

1-Methyl-5-(methylsulfonyl-2-phenyl-1H-benzo[d]imidazole (41)

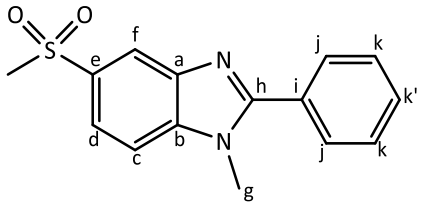

N[1]-Methyl-4-(methylsulfonyl)benzene-1,2-diamine **24** (0.168 g, 0.838 mmol) was dissolved in EtOH (10 mL). Benzaldehyde (0.10 mL, 1.01 mmol), TFA (9.56 mg, 0.0838 mmol) and $MgSO_4$ (0.606 g, 5.03 mmol) was then added to the reaction flask. Product: White solid (0.107 g, 45%); **R_f** (EtOAc:10): 0.61. **Mp**: 192.2 – 196.2 °C. **^{1}H-NMR (300 MHz, DMSO-*d*$_6$)** δ (ppm): 8.23 – 8.18 (m, 1H, H_c), 7.99 – 7.70 (m, 4H, H_j, H_d, H_f), 7.71 – 7.45 (m, 3H, H_k, $H_{k'}$), 3.95 (s, 3H, H_g), 3.24 (s, 3H, C$\underline{H_3}$). **^{13}C{^{1}H} NMR (101 MHz, DMSO-*d*$_6$)** δ (ppm): 156.45 (C_h), 142.24 (C_b), 140.12 (C_a), 135.12 (C_e), 130.72 ($C_{k'}$), 129.92 (C_k), 129.84 (C_i), 129.24 (C_j), 121.26 (C_d), 119.08 (C_c), 112.06 (C_f), 44.76 (C_l), 32.60 (C_g). **FT-IR** (ATR) *v*(cm^{-1}) = 1609 (imine, C=N). **Elemental Analysis** for $C_{15}H_{14}N_2O_2S$ (286.35 g.mol^{-1}): Found (%) C, 62.80; H, 5.12; N, 9.22; S, 10.18; Calcd. (%) C, 62.92; H, 4.93; N, 9.78; S, 11.20. **MS** (EI, *m/z*): 286.0331 (100%, $[M]^+$).

1-Methyl-2-phenyl-1H-benzo[d]imidazole-5-carboxamide (42)

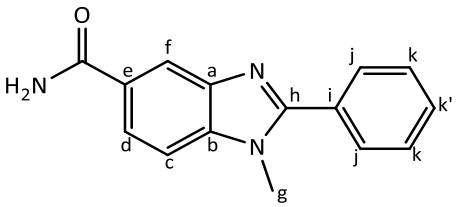

3-Amino-4-(methylamino)benzamide **25** (0.110 g, 0.666 mmol) was dissolved in EtOH (6 mL). Benzaldehyde (0.080 mL, 0.799 mmol), TFA (7.59 mg, 0.0666 mmol) and $MgSO_4$ (0.481 g, 3.99 mmol) was then added to the reaction flask. Product: Brown solid (0.0581 g, 35%); **R_f** (EtOAc:10): 0.32. **Mp**: 259.6 – 261.4 °C. **^{1}H-NMR (400 MHz, DMSO-*d*$_6$)** δ (ppm): 8.31 – 8.25 (m, 1H, H_f), 8.00 (bs, 1H, Ar-CON$\underline{H_2}$), 7.91 – 7.84 (m, 3H, H_j, H_c), 7.67 (dd, J_{HH} = 8.6, 0.6 Hz, 1H, H_d), 7.64 – 7.54 (m, 3H, H_k, $H_{k'}$), 7.26 (bs, 1H, Ar-CON$\underline{H_2}$), 3.92 (s, 3H, H_g). **^{13}C{^{1}H} NMR (101 MHz, DMSO-*d*$_6$)** δ (ppm): 168.80 (C=O), 154.93 (C_h), 142.45 (C_b), 139.06 (C_a), 130.34 ($C_{k'}$), 129.82 (C_k), 129.17 (C_j), 128.80 (C_i), 122.74 (C_d), 119.15 (C_f), 110.55 (C_c), 32.35 (C_g). **Elemental Analysis** for $C_{15}H_{13}N_3O$ (251.29 g.mol^{-1}): Found (%) C, 71.43; H, 5.53; N, 15.17; Calcd. (%) C, 71.70; H, 5.21; N, 16.72. **MS** (EI, *m/z*): 251.0960 (100%, $[M]^+$).

5-Fluoro-1-methyl-2-phenyl-1H-benzo[d]imidazole (43)

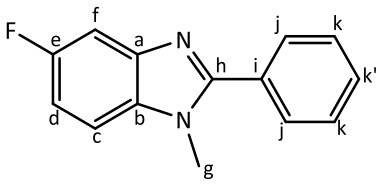

4-Fluoro-N^1-methylbenzene-1,2-diamine **26** (0.144 g, 1.027 mmol) was dissolved in EtOH (6 mL). Benzaldehyde (0.13 mL, 1.23 mmol), TFA (11.7 mg, 0.0103 mmol) and $MgSO_4$ (0.742 g, 6.16 mmol) was then added to the reaction flask. Product: Brown solid (0.127 g, 55%); **R_f** (EtOAc:Pet. Ether, 3:7): 0.38. **Mp**: 106.8 – 112.6 °C. **^{1}H-NMR (300 MHz, DMSO-d_6)** δ (ppm): 7.90 – 7.81 (m, 2H, H_j), 7.68 – 7.62 (m, 1H, H_c), 7.61 – 7.55 (m, 3H, H_k), 7.49 (m, 1H, H_f), 7.17 (m, 1H, H_d), 3.33 (s, 3H, H_g). **^{13}C{^{1}H} NMR (101 MHz, DMSO-d_6)** δ (ppm): 159.16 (d, $^1J_{CF}$ = 234.4 Hz, C_e), 155.09 (C_h), 143.21 (d, $^3J_{CF}$ = 12.9 Hz, C_a), 133.85 (C_b), 130.30 (C_i), 130.21 ($C_{k'}$), 129.75 (C_k), 129.15 (C_j), 111.87 (d, $^3J_{CF}$ = 10.4 Hz, C_c), 110.84 (d, $^2J_{CF}$ = 25.9 Hz, C_d), 104.91 (d, $^2J_{CF}$ = 23.8 Hz, C_f), 32.34 (C_g). **FT-IR** (ATR) ν(cm^{-1}) = 1623 (imine, C=N). **Elemental Analysis** for $C_{14}H_{11}FN_2$ (226.25 g.mol^{-1}): Found (%) C, 74.19; H, 4.83; N, 12.00; Calcd. (%) C, 74.32; H, 4.90; N, 12.38. **MS** (EI, *m/z*): 225.1020 (100%, $[M-H]^+$).

2-Phenyl-1-propyl-1H-benzo[d]imidazole (44)

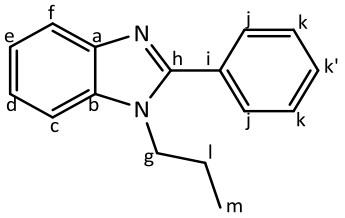

N^1-Propylbenzene-1,2-diamine **27** (96.0 mg, 0.639 mmol) was dissolved in EtOH (6 mL). Benzaldehyde (0.078 mL, 0.767 mmol), TFA (7.29 mg, 0.0639 mmol) and $MgSO_4$ (0.385 g, 3.20 mmol) was then added to the reaction flask. Product: Brown oil (0.0730 g, 49%); **R_f** (EtOAc: Pet. Ether, 2.5:7.5): 0.27. **^{1}H-NMR (400 MHz, $CDCl_3$)** δ (ppm): 7.86 – 7.81 (m, 1H, H_f), 7.74 – 7.68 (m, 2H, H_j), 7.55 – 7.48 (m, 3H, H_k, $H_{k'}$), 7.44 – 7.39 (m, 1H, H_c), 7.34 – 7.27 (m, 2H, H_d, H_e), 4.23 – 4.17 (t, 2H, *J* = 7.6 Hz, H_g), 1.90 – 1.80 (m, 2H, H_l), 0.89 – 0.85 (t, 3H, *J* = 7.2 Hz, H_m). **^{13}C{^{1}H} NMR (101 MHz, $CDCl_3$)** δ (ppm): 153.75 (C_h), 143.08 (C_a), 135.65 (C_b), 130.76 (C_i), 129.67 ($C_{k'}$), 129.36 (C_j), 128.69 (C_k), 122.66 (C_d), 122.33 (C_e), 119.98 (C_f), 110.10 (C_c), 46.35

(C_g), 23.16 (C_l), 11.21 (C_m). **FT-IR** (ATR) *v* (cm^{-1}) = 1611 (imine, C=N). **Elemental Analysis** for $C_{16}H_{16}N_2$ (236.32 $g.mol^{-1}$): Found (%) C, 78.58; H, 7.02; N, 11.41; Calcd. (%) C, 81.40; H, 6.80; N, 11.90. **MS** (EI, *m/z*): 236.1062 (100%, $[M]^+$).

5-Chloro-2-phenyl-1-propyl-1H-benzo[d]imidazole (45)

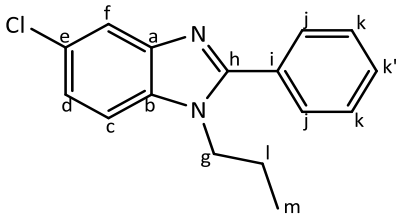

4-Chloro-N^1-propylbenzene-1,2-diamine **28** (0.190 g, 1.03 mmol) was dissolved in EtOH (10 mL). Benzaldehyde (0.13 mL, 1.23 mmol), TFA (11.7 mg, 0.103 mmol) and $MgSO_4$ (0.743 g, 6.17 mmol) was then added to the reaction flask. Product: Brown solid (0.174 g, 62%); $\mathbf{R_f}$ (EtOAc:Pet. Ether, 5:5): 0.63. **Mp**: 84.8 – 88.6 °C. **^{1}H-NMR (300 MHz, $CDCl_3$)** δ (ppm): 7.79 (d, $^4J_{HH}$ = 1.8 Hz, 1H, H_f), 7.72 – 7.65 (m, 2H, H_j), 7.56 – 7.48 (m, 3H, H_k), 7.32 (d, $^3J_{HH}$ = 8.6 Hz, 1H, H_c), 7.26 (dd, $^3J_{HH}$ = 8.6 and $^4J_{HH}$ = 1.8 Hz, 1H, H_d), 4.26 – 4.08 (m, 2H, H_g), 1.93 – 1.71 (m, 2H, H_l), 0.85 (t, $^3J_{HH}$ = 8.6 Hz, 3H, H_m). **^{13}C{^{1}H} NMR (101 MHz, $CDCl_3$)** δ (ppm): 155.12 (C_h), 144.06 (C_a), 134.43 (C_e), 130.45 (C_b), 130.09 (C_i), 129.43 ($C_{k'}$), 128.92 (C_k), 128.05 (C_j), 123.20 (C_d), 119.85 (C_f), 110.99 (C_c), 46.61 (C_g), 23.28 (C_l), 11.30 (C_m). **FT-IR** (ATR) *v* (cm^{-1}) = 1595 (imine, C=N). Purity 100% by **LC** (t_R 3.50 min); **MS** (EI, *m/z*): 270.01 (100%, $[M]^+$).

5-Methyl-2-phenyl-1-propyl-1H-benzo[d]imidazole (46)

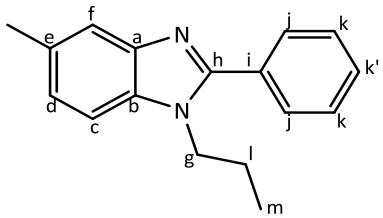

4-Methyl-N^1-propylbenzene-1,2-diamine **29** (0.206 g, 1.25 mmol) was dissolved in EtOH (10 mL). Benzaldehyde (0.15 mL, 1.50 mmol), TFA (14.3 mg, 0.125 mmol) and $MgSO_4$ (0.905 g, 7.52 mmol) was then added to the reaction flask. Product: Brown oil (0.126 g, 40%); $\mathbf{R_f}$ (EtOAc:Pet. Ether, 5:5): 0.63. **^{1}H-NMR (300 MHz, $CDCl_3$)** δ (ppm): 7.74 – 7.65 (m, 2H, H_j), 7.61 (m, 1H, H_d), 7.56 – 7.45 (m, 3H, H_k, $H_{k'}$), 7.29 (d, *J* = 8.3 Hz, 1H, H_c), 7.13 (m, 1H, H_f), 4.24 – 4.11

(m, 2H, H_g), 1.93 – 1.73 (m, 2H, H_l), 0.85 (t, *J* = 7.4 Hz, 3H, H_m). **$^{13}C\{^1H\}$ NMR (101 MHz, $CDCl_3$)** δ (ppm): 153.72 (C_h), 143.47 (C_a), 133.79 (C_e), 131.96 (C_b), 130.92 (C_i), 129.55 ($C_{k'}$), 129.34 (C_k), 128.65 (C_j), 124.10 (C_d), 119.74 (C_f), 109.62 (C_c), 46.34 (C_g), 23.16 (C_l), 21.56 ($\underline{C}H_3$), 11.21 (C_m). **FT-IR** (ATR) *v*(cm^{-1}) = 1518 (imine, C=N). **Elemental Analysis** for $C_{17}H_{18}N_2$ (250.35 $g.mol^{-1}$): Found (%) C, 77.87; H, 7.40; N, 10.34; Calcd. (%) C, 81.56; H, 7.25; N, 11.19. **MS** (EI, *m/z*): 250.1475 (100%, $[M]^+$).

2-Phenyl-1-propyl-1H-benzo[d]imidazole-5-carbonitrile (47)

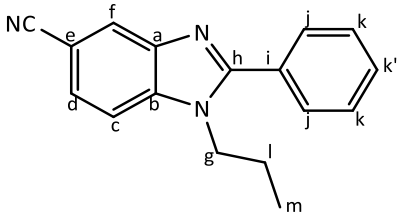

3-Amino-4-(propylamino)benzonitrile **30** (0.282 g, 1.61 mmol) was dissolved in EtOH (10 mL). Benzaldehyde (0.20 mL, 1.93 mmol), TFA (18.4 mg, 0.161 mmol) and $MgSO_4$ (1.16 g, 9.67 mmol) was then added to the reaction flask. Product: Yellow solid (0.157 g, 37%); **R_f** (EtOAc:Pet. Ether, 5:5): 0.75. **Mp**: 173.7 – 178.9 °C. **^{1}H-NMR (300 MHz, $CDCl_3$)** δ (ppm): 8.15 (dd, $^4J_{HH}$ = 1.4, 0.6 Hz, 1H, H_f), 7.80 – 7.64 (m, 2H, H_j), 7.61 – 7.52 (m, 4H, H_k, $H_{k'}$, H_d), 7.49 (dd, $^3J_{HH}$ = 8.4, 0.6 Hz, 1H, H_c), 4.35 – 4.11 (m, 2H, H_g), 1.98 – 1.73 (m, 2H, H_l), 0.87 (t, $^3J_{HH}$ = 7.4 Hz, 3H, H_m). **$^{13}C\{^1H\}$ NMR (101 MHz, $CDCl_3$)** δ (ppm): 156.30 (C_h), 142.39 (C_a), 138.39 (C_b), 130.68 ($C_{k'}$), 129.49 (C_i), 129.44 (C_k), 129.13 (C_j), 126.31 (C_d), 124.96 (C_f), 119.91 ($\underline{C}N$), 111.35 (C_c), 105.98 (C_e), 46.81 (C_g), 23.29 (C_l), 11.27 (C_m). **FT-IR** (ATR) *v*(cm^{-1}) = 1614 (imine, C=N). **Elemental Analysis** for $C_{17}H_{15}N_3$ (261.33 $g.mol^{-1}$): Found (%) C, 75.83; H, 5.52; N, 14.45; Calcd. (%) C, 78.13; H, 5.79; N, 16.08. **MS** (EI, *m/z*): 261.1180 (100%, $[M]^+$).

5-(Methylsulfonyl)-2-phenyl-1-propyl-1H-benzo[d]imidazole (48)

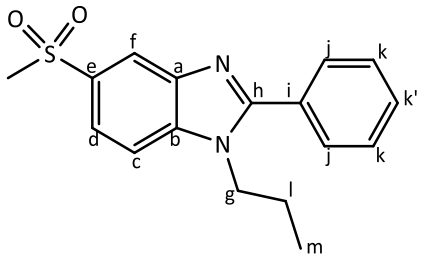

4-(Methylsulfonyl)-N^1-propylbenzene-1,2-diamine **31** (0.231 g, 1.01 mmol) was dissolved in EtOH (10 mL). Benzaldehyde (0.12 mL, 1.21 mmol), TFA (11.5 mg, 0.101 mmol) and $MgSO_4$ (0.731 g, 6.07 mmol) was then added to the reaction flask. Product: Brown solid (0.155 g, 49%); **R_f** (EtOAc:Pet. Ether, 4:6): 0.15. **Mp**: 145.8 – 148.9 °C. **^{1}H-NMR (400 MHz, $CDCl_3$)** δ (ppm): 8.42 (s, 1H, H_f), 7.89 (d, $^3J_{HH}$ = 8.8 Hz, 1H, H_c), 7.77 – 7.66 (m, 2H, H_j), 7.62 – 7.50 (m, 4H, H_d, H_k, $H_{k'}$), 4.25 (t, $^3J_{HH}$ = 7.6 Hz, 2H, H_g), 3.10 (s, 3H, CH_3), 1.94 – 1.76 (m, 2H, H_l), 0.87 (t, $^3J_{HH}$ = 7.2 Hz, 3H, H_m). **^{13}C{^{1}H} NMR (101 MHz, $CDCl_3$)** δ (ppm): 156.79 (C_h), 142.81 (C_a), 139.13 (C_b), 135.05 (C_e), 130.60 ($C_{k'}$), 129.85 (C_i), 129.49 (C_k), 129.11 (C_j), 121.66 (C_d), 120.50 (C_c), 111.02 (C_f), 46.88 (C_g), 45.27 (Ar-SO_2CH_3), 23.32 (C_l), 11.28 (C_m). **FT-IR** (ATR) ν(cm^{-1}) = 1604 (imine, C=N), 1328, 1134 (S=O). Purity 100 % by **LC** (t_R 2.52 min); **MS** (*m/z*): 314.9 (100%, $[M]^+$).

5-Methoxy-2-phenyl-1-propyl-1H-benzo[d]imidazole (49)

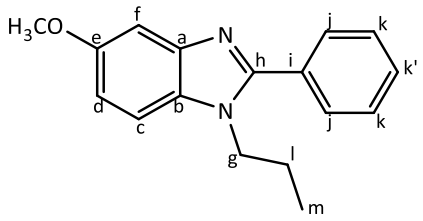

4-Methoxy-N^1-propylbenzene-1,2-diamine **32** (82.0 mg, 0.455 mmol) was dissolved in EtOH (10 mL). Benzaldehyde (0.055 mL, 0.546 mmol), TFA (5.18 mg, 0.0455 mmol) and $MgSO_4$ (0.164 g, 1.36 mmol) was then added to the reaction flask. Product: Brown oil (0.0746 g, 62%); **R_f** (EtOAc:Pet. Ether, 3:7): 0.32. **^{1}H-NMR (400 MHz, $CDCl_3$)** δ (ppm): 7.73 – 7.66 (m, 2H, H_j), 7.55 – 7.47 (m, 3H, H_k, $H_{k'}$), 7.31 (d, $^4J_{HH}$ = 2.4 Hz, 1H, H_f), 7.29 (d, $^3J_{HH}$ = 8.4 Hz, 1H, H_c), 6.96 (dd, *J* = 8.4, 2.4 Hz, 1H, H_d), 4.17 (t, $^3J_{HH}$ = 7.6 Hz, 2H, H_g), 3.88 (s, 3H, Ar-OCH_3), 1.85 – 1.75 (m, 2H, H_l), 0.86 (t, $^3J_{HH}$ = 7.2 Hz, 3H, H_m). **^{13}C{^{1}H} NMR (101 MHz, $CDCl_3$)** δ (ppm): 156.53 (C_e), 154.07 (C_h), 143.97 (C_a), 130.97 (C_i), 130.48 (C_e), 129.73 ($C_{k'}$), 129.44 (C_k), 128.82 (C_j), 112.98

(C_c), 110.62 (C_d), 102.29 (C_f), 56.02 (Ar-O<u>C</u>H$_3$), 46.60 (C_g), 23.38 (C_l), 11.32 (C_m). **FT-IR** (ATR) v(cm^{-1}) = 1620 (imine, C=N). Purity 92% by **LC** (t_R 2.66 min); **MS** (*m/z*): 267.0 (100%, $[M+H]^+$).

2-Phenyl-1-propyl-5-(trifluoromethyl)-1H-benzo[d]imidazole (50)

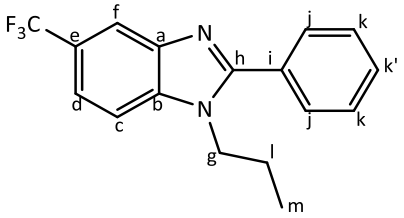

N^1-propyl-4-(trifluoromethyl)benzene-1,2-diamine **33** (1.26 g, 5.79 mmol) was dissolved in EtOH (10 mL). Benzaldehyde (0.71 mL, 6.95 mmol), TFA (65.9 mg, 0.579 mmol) and $MgSO_4$ (4.15 g, 34.7 mmol) was then added to the reaction flask. Product: Off-white solid (0.814 g, 46%); **R_f** (EtOAc:Pet. Ether, 2:8): 0.33. **Mp**: 64.7 – 66.0 °C. **^{1}H-NMR (300 MHz, $CDCl_3$)** δ (ppm): 8.12 – 8.08 (m, 1H, H_d), 7.75 – 7.66 (m, 2H, H_j), 7.60 – 7.52 (m, 4H, H_f, H_k, $H_{k'}$), 7.49 (d, $^3J_{HH}$ = 8.4 Hz, 1H, H_c), 4.27 – 4.19 (t, $^3J_{HH}$ = 7.8 Hz, 2H, H_g), 1.94 – 1.76 (m, 2H, H_l), 0.87 (t, $^3J_{HH}$ = 7.2 Hz, 3H, H_m). **^{13}C{^{1}H} NMR (101 MHz, $CDCl_3$)** δ (ppm): 155.89 (C_h), 142.78 (C_a), 136.79 (C_b), 130.32 (C_i), 130.28 ($C_{k'}$), 129.47 (C_k), 129.01 (C_j), 126.39 – 123.69 (d, $^1J_{CF}$ = 270.1 Hz, Ar-<u>C</u>F$_3$), 125.22 – 124.90 (d, $^2J_{CF}$ = 32.1 Hz, C_e), 119.66 (C_c), 117.87 (C_d), 110.60 (C_f), 46.70 (C_g), 23.31 (C_l), 11.30 (C_m). **^{19}F NMR (377 MHz, $CDCl_3$)** δ (ppm): -60.67 (s). **FT-IR** (ATR) v(cm^{-1}) = 1627 (imine, C=N), 1323 (Ar amine, C-N). Purity 100% by **LC** (t_R 3.56 min); **MS** (*m/z*): 305.1 (100%, $[M+H]^+$).

tert-Butyl (3-(5-methyl-2-phenyl-1H-benzo[d]imidazol-1-yl)propyl)carbamate (51)

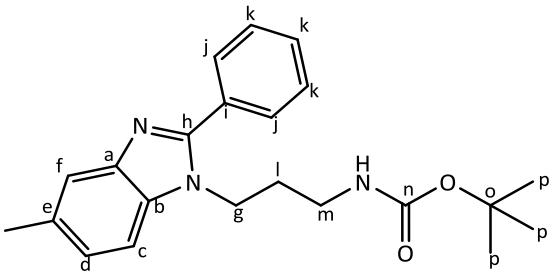

tert-Butyl (3-((2-amino-4-methylphenyl)amino)propyl)carbamate **34** (83.0 mg, 0.297 mmol) was dissolved in EtOH (10 mL). Benzaldehyde (0.036 mL, 0.357 mmol), TFA (3.39 mg, 0.0297 mmol) and $MgSO_4$ (0.215 g, 1.78 mmol) was then added to the reaction flask. Product:

White solid (56.6 mg, 52%); **R_f** (EtOAc:Pet. Ether, 5:5): 0.56. **Mp**: 84.2 – 86.8 °C. **^{1}H-NMR (300 MHz, DMSO-*d*$_6$)** δ (ppm): 7.75 (m, 2H, H_j), 7.61 – 7.55 (m, 3H, H_k), 7.55 – 7.49 (m, 1H, H_d), 7.48 (s, 1H, H_f), 7.12 (dd, $^3J_{HH}$ = 8.1, 0.9 Hz, 1H, H_c), 6.86 (bs, 1H, H_q), 4.31-4.19 (t, $^3J_{HH}$ = 7.5 Hz, 2H, H_g), 2.89 (m, 2H, H_m), 2.44 (s, 3H, CH_3), 1.92 – 1.73 (m, 2H, H_l), 1.35 (s, 9H, H_p). **^{13}C{^{1}H} NMR (101 MHz, DMSO-*d*$_6$)** δ (ppm): 156.07 (C_n), 153.19 (C_h), 143.45 (C_a), 134.26 (C_e), 131.46 (C_b), 130.96 (C_i), 130.03 ($C_{k'}$), 129.52 (C_k), 129.19 (C_j), 124.28 (C_d), 119.38 (C_f), 110.76 (C_c), 78.07 (C_o), 42.62 (C_g), 37.88 (C_m), 30.28 (C_l), 28.68 (C_p), 21.65 (CH_3). **FT-IR** (ATR) ν(cm^{-1}) = 1676 (imine, C=N), 1364 (Ar amine, C-N). **Elemental Analysis** for $C_{22}H_{27}N_3O_2$ (365.48 g.mol^{-1}): Found (%) C, 72.79; H, 7.83; N, 10.43; Calcd. (%) C, 72.30; H, 7.45; N, 11.50. **MS** (EI, *m/z*): 365.1413 (85%, $[M]^+$).

5.4. Synthetic procedure for Boc deprotection of 51

Synthesised *tert*-Butyl (3-(5-methyl-2-phenyl-*1H*-benzo[*d*]imidazol-1-yl)propyl)carbamate **51** (0.103 g, 0.274 mmol) was dissolved in DCM (3 mL). TFA (1 mL) was then added to the reaction flask under an Argon atm and the reaction was left to stir for 2 h at rt. The solvent was removed *in vacuo*. The crude material was stirred in a solution of 1M NaOH (10 mL) and thereafter extracted with EtOAc (2 x 20 mL). The organic extracts were collected, washed with sat. NaCl, dried over Na_2SO_4 and concentrated *in vacuo*.

3-(5-Methyl-2-phenyl-1H-benzo[d]imidazol-1-yl)propan-1-amine (52)

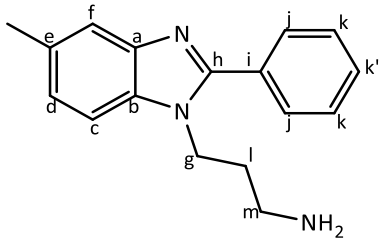

Brown oil (0.0719 g, 97%), **R_f** (EtOAc:10): 0.06. **^{1}H-NMR (400 MHz, DMSO-*d*$_6$)** δ (ppm): 7.81 – 7.73 (m, 2H, H_j), 7.61 – 7.51 (m, 4H, H_k, H_d), 7.47 (m, 1H, H_c), 7.11 (dd $^3J_{HH}$ = 8.4, 1.6, 1H, H_f), 4.39-4.20 (t, $^3J_{HH}$ = 7.2 Hz, 2H, H_g), 2.46 (t, 2H, H_l), 2.43 (s, 3H, CH_3), 1.87 – 1.67 (m, 2H, H_m). **^{13}C{^{1}H} NMR (101 MHz, DMSO-*d*$_6$)** δ (ppm): 153.28 (C_h), 143.44 (C_a), 134.37 (C_e), 131.39 (C_b), 131.09 (C_i), 130.01 ($C_{k'}$), 129.57 (C_k), 129.18 (C_j), 124.25 (C_d), 119.33 (C_f), 110.91 (C_c), 42.61

(C_g), 39.04 (C_m), 33.21 (C_l), 21.65 ($\underline{C}H_3$). **FT-IR** (ATR) ν(cm^{-1}) = 3158 (primary amine, N-H), 1618 (imine, C=N), 1327 (Ar amine, C-N). **MS** (EI, *m/z*): 265.0131 (85%, $[M]^+$).

5.5. Synthetic procedure for nucleophilic acyl substitution of 53

52 (0.0720 g, 0.271 mmol) was dissolved in DCM (3 mL). Triethylamine (0.04 mL, 1.1 eq.) and methanesulfonyl chloride (0.02 mL, 0.271 mmol) was added dropwise to the reaction mixture at 0 ˚C. The reaction allowed to stir for 2 h at rt. Thereafter it was then warmed to rt and left to stir for 24 h at rt. Thereafter, the crude material obtained was purified *via* column chromatography using EtOAc (100%) as an eluent to afford the desired product.[8]

N-(3-(5-Methyl-2-phenyl-1H-benzo[d]imidazol-1-yl)propyl)methanesulfonamide (53)

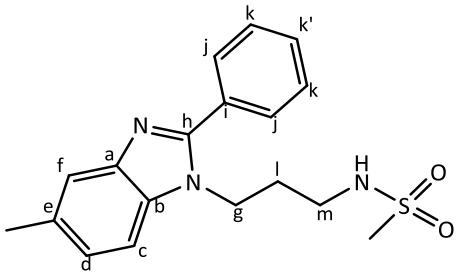

Brown oil (5.51 mg, 6.0%); $\mathbf{R_f}$ (EtOAc:10): 0.47. **^{1}H-NMR (400 MHz, $CDCl_3$)** δ (ppm): 7.71 (m, 2H, H_j), 7.63 (s, 1H, H_f), 7.58 – 7.48 (m, 3H, H_k, $H_{k'}$), 7.31 (d, $^3J_{HH}$ = 8.4 Hz, 1H, H_c), 7.17 (dd, *J* = 8.4, 1.2 Hz, 1H, H_d), 4.43 – 4.32 (t, $^3J_{HH}$ = 7.2 Hz, 2H, H_g), 4.18 (bs, 1H, N$\underline{H}$), 2.97 (m, 2H, H_l), 2.82 (s, 3H, $SO_2C\underline{H_3}$), 2.50 (s, 3H, Ar-$C\underline{H_3}$) 2.00 (m, 2H, H_m). **^{13}C{^{1}H} NMR (101 MHz, $CDCl_3$)** δ (ppm): 153.19 (C_h), 142.76 (C_a), 133.36 (C_e), 133.05 (C_b), 130.39 ($C_{k'}$), 129.98 (C_i), 129.48 (C_k), 129.26 (C_j), 125.04 (C_d), 119.83 (C_f), 109.67 (C_c), 41.90 (C_g), 40.41 ($SO_2\underline{C}H_3$) 30.42 (C_m), 29.85 (C_l), 21.69 (Ar-$\underline{C}H_3$). Purity 100% by **LC** (t_R 2.36 min); **MS** (*m/z*): 343.9 (100%, $[M]^+$).

5.6. Synthetic procedure for *N*-alkylation of 52

52 (0.101 g, 0.380 mmol) was dissolved in anhydrous acetonitrile (2 mL). Potassium carbonate (0.0551 g, 1 eq.) was added to the brown solution and was allowed to stir for 5 min. 4-(Chloroacetyl)morpholine (0.0653 g, 0.399 mmol) was then added dropwise to the reaction mixture at 0˚C and left to stir for a further 4 h. After 4h, the reaction was warmed to rt and

the crude material was concentrated *in vacuo* and purified *via* column chromatography using MeOH:EtOAc (1:9) as an eluent to afford the desired product.

2,2'-((3-(5-Methyl-2-phenyl-1H-benzo[d]imidazol-1-yl)propyl)azanediyl)bis(1-morpholinoethan-1-one) (54)

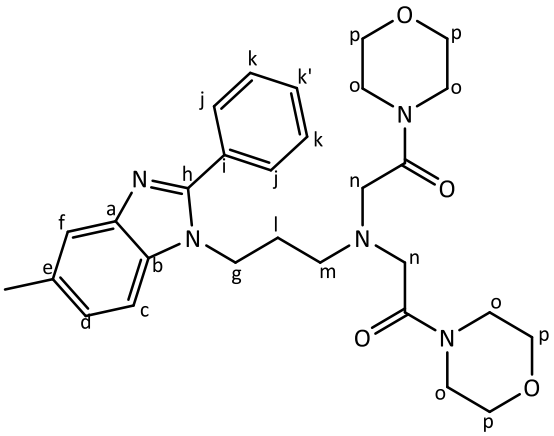

Brown solid (0.0741 g, 38%); **R_f** (MeOH:EtOAc, 1:9): 042. **Mp**: 62.2 – 68.3 °C. **^{1}H-NMR (400 MHz, $CDCl_3$)** δ (ppm): 7.72 (m, 2H, H_j), 7.62 (s, 1H, H_f), 7.55 – 7.46 (m, 3H, H_k, $H_{k'}$), 7.35 (d, $^3J_{HH}$ = 8.4 Hz, 1H, H_c), 7.13 (dd, $^3J_{HH}$ = 8.4, 1.6 Hz, 1H, H_d), 4.40 – 4.28 (t, $^3J_{HH}$ = 7.2 Hz, 2H, H_g), 3.59 (m, 12H, $H_{o/p}$), 3.43 (m, 4H, $H_{o/p}$), 3.37 (s, 4H, H_n), 2.64 (t, $^3J_{HH}$ = 6.8 Hz, 2H, H_m) 2.50 (s, 3H, Ar-C$\underline{H}_3$), 1.87 (m, 2H, H_l). **^{13}C{^{1}H} NMR (101 MHz, $CDCl_3$)** δ (ppm): 168.88 (C=O), 153.44 (C_h), 143.17 (C_a), 133.83 (C_e), 132.47 (C_b), 130.69 (C_i), 129.90 ($C_{k'}$), 129.46 (C_k), 128.95 (C_j), 124.52 (C_d), 119.82 (C_f), 109.90 (C_c), 67.00 ($C_{o/p}$), 66.75 ($C_{o/p}$), 55.40 (C_n), 51.89 (C_m), 45.63($C_{o/p}$), 42.85 (C_g), 42.07 ($C_{o/p}$), 27.57 (C_l), 21.69 (C$\underline{H}_3$). **FT-IR** (ATR) ν(cm^{-1}) = 2920 (C-H), 1635 (imine, C=N). Purity 94% by **LC** (t_R 2.71 min); **MS** (*m/z*): 520.3 (100%, $[M+H]^+$).

5.3. Synthesis of cyclometallated benzimidazole complexes (55 – 68)

5.3.1. General synthetic procedure for Ru and Ir cyclometallated complexes

The selected 2-phenylbenzimidazole (1 eq.) was dissolved in dry DCM (6 mL) under argon. Sodium acetate (1.2 eq.) was then added, and the reaction mixture left to stir at rt for 10 min. Thereafter, the appropriate metal dimer (2 eq.) was added, in one portion. The reaction mixture was allowed to stir at rt, under argon, for 24 h, after which the reaction mixture was filtered through Celite and washed with DCM. The solvent was concentrated and diethyl ether

(10 mL) was added to the residue. The mixture was then cooled to 0 °C and left to stir for 10 min. The precipitate that formed was filtered by suction and dried under vacuum.[7]

N-Methyl Ru benzimidazole complex (55)

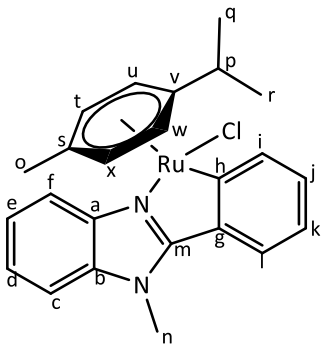

1-Methyl-2-phenyl-*1H*-benzo[*d*]imidazole **35** (81.6 mg, 0.392 mmol) was dissolved in DCM (5 mL). Sodium acetate (38.6 mg, 0.470 mmol) and dichloro(*p*-cymene)ruthenium(II) dimer (120 mg, 0.195 mmol) was then added to the solution. Product: Green solid (0.101 g, 54%); **Mp**: 250.9 – 257.9 °C. **^{1}H-NMR (300 MHz, $CDCl_3$)** δ (ppm): 8.34 (d, $^{3}J_{HH}$ = 7.6 Hz, 1H, H_i), 7.92 (d, $^{3}J_{HH}$ = 8.0 Hz, 1H, H_f), 7.73 (d, $^{3}J_{HH}$ = 7.8 Hz, 1H, H_l), 7.45 – 7.27 (m, 3H, H_c, H_d, H_e), 7.20 (td, $^{3}J_{HH}$ = 7.4, 1.3 Hz, 1H, H_k), 7.04 (td, $^{3}J_{HH}$ = 7.7, 1.2 Hz, 1H, H_j), 5.85 (d, $^{3}J_{HH}$ = 5.7 Hz, 1H, H_x), 5.71 (d, $^{3}J_{HH}$ = 5.8 Hz, 1H, H_t), 5.38(d, $^{3}J_{HH}$ = 5.9 Hz, 1H, H_w), 5.15 (d, $^{3}J_{HH}$ = 5.8 Hz, 1H, H_u), 3.99 (s, 3H, H_n), 2.29 (m, 1H, H_p), 2.08 (s, 3H, H_o), 0.93 (d, $^{3}J_{HH}$ = 6.9 Hz, 3H, H_q), 0.79 (d, $^{3}J_{HH}$ = 6.9 Hz, 3H, H_r). **^{13}C{^{1}H} NMR (101 MHz, $CDCl_3$)** δ (ppm): 183.22 (C_h), 157.41 (C_m), 141.41 (C_g), 140.53 (C_i), 136.30 (C_x), 134.19 (C_u), 128.86 (C_k), 124.36 (C_l), 123.13 (C_d), 123.01 (C_e), 122.43 (C_j), 117.00 (C_f), 109.88 (C_c), 101.07 (C_a), 99.02 (C_b), 89.30 (C_t), 88.81 (C_x), 81.76 (C_u), 81.31 (C_w), 31.93 (C_n), 30.89 (C_p), 22.60 (C_r), 21.91 (C_q), 18.95 (C_o). **FT-IR** (ATR) *v* (cm^{-1}) = 1577 (imine, C=N). **Elemental Analysis** for $C_{24}H_{25}ClN_2Ru$ (478.07 g.mol^{-1}): Found (%) C, 59.26; H, 5.41; N, 5.57; Calcd. (%) C, 60.31; H, 5.27; N, 5.86. **MS** (HR-ESI, *m/z*): 478.0753 (100%, $[M]^+$), requires 478.0749.

N- Methyl (chloro-) Ru benzimidazole complex (56)

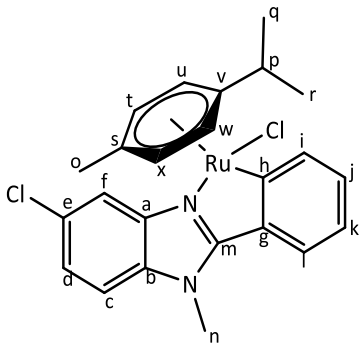

5-Chloro-1-methyl-2-phenyl-*1H*-benzo[*d*]imidazole **36** (60.3 mg, 0.248 mmol) was dissolved in DCM (4 mL). Sodium acetate (24.5 mg, 0.298 mmol) and dichloro(*p*-cymene)ruthenium(II) dimer (76.1 mg, 0.124 mmol) was then added to the solution. Product: Yellow solid (0.061 g, 48%); **Mp**: Decomp. 251.9 – 259.0 °C. **^{1}H-NMR (300 MHz, $CDCl_3$)** δ (ppm): 8.34 (d, *J* = 7.5 Hz, 1H, H_i), 7.86 (s, 1H, H_f), 7.73 (d, $^{3}J_{HH}$ = 7.8 Hz, 1H, H_l), 7.27 (d, *J* = 1.2 Hz, 2H, H_d, H_c), 7.22 (td, $^{3}J_{HH}$ = 7.5 and $^{4}J_{HH}$ 1.2 Hz, 1H, H_j), 7.06 (td, $^{3}J_{HH}$ = 7.5, 1.2 Hz, 1H, H_k), 5.85 (d, $^{3}J_{HH}$ = 6.0 Hz, 1H, H_x), 5.72 (d, $^{3}J_{HH}$ = 5.7 Hz, 1H, H_t), 5.39 (d, $^{3}J_{HH}$ = 6.0 Hz, 1H, H_w), 5.15 (d, $^{3}J_{HH}$ = 5.7 Hz, 1H, H_u), 3.99 (s, 3H, H_n), 2.30 (m, 1H, H_p), 2.09 (s, 3H, H_o), 0.93 (d, $^{3}J_{HH}$ = 6.9 Hz, 3H, H_q), 0.81 (d, $^{3}J_{HH}$ = 6.9 Hz, 3H, H_r). **^{13}C{^{1}H} NMR (101 MHz, $CDCl_3$)** δ (ppm): 183.57 (C_h), 159.56 (C_m), 142.20 (C_g), 140.64 (C_i), 134.97, 133.70, 129.25 (C_j), 128.99, 124.57 (C_l), 123.43 (C_c), 122.58 (C_k), 116.80 (C_f), 110.77 (C_d), 101.50, 98.98, 89.60 (C_t), 88.68 (C_x), 81.94 (C_w), 81.19 (C_u), 32.25 (C_n), 30.93 (C_p), 22.60 (C_q), 21.93 (C_r), 18.99 (C_o). **FT-IR** (ATR) *v* (cm^{-1}) = 1577 (imine, C=N). **Elemental Analysis** for $C_{24}H_{24}Cl_2N_2Ru \cdot H_2O$: Found (%) C, 53.26; H, 4.97; N, 4.51; Calcd. (%) C, 54.34; H, 4.94; N, 5.28. **MS** (HR-ESI, *m/z*): 557.0809 (80%, $[M+2Na-H]^+$), requires 557.0809.

N- Methyl (methyl-) Ru benzimidazole complex (57)

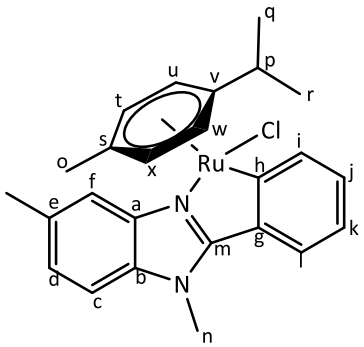

1,5-Dimethyl-2-phenyl-*1H*-benzo[*d*]imidazole **39** (54.5 mg, 0.245 mmol) was dissolved in DCM (3 mL). Sodium acetate (24.1 mg, 0.294 mmol) and dichloro(*p*-cymene)ruthenium(II) dimer (75.1 mg, 0.123 mmol) was then added to the solution. Product: Green solid (0.0301 g, 25%); **Mp**: 222.8 – 225.1 °C. **^{1}H-NMR (300 MHz, DMSO-*d*$_6$)** δ (ppm): 8.31 (dd, $^3J_{HH}$ = 7.5, 1.2 Hz, 1H, H_i), 7.87 (dd, $^3J_{HH}$ = 7.8, 1.2 Hz, 1H, H_l), 7.72 (s, 1H, H_f), 7.61 (d, $^3J_{HH}$ = 8.4 Hz, 1H, H_d), 7.22 (d, $^3J_{HH}$ = 8.4 Hz, 1H, H_c), 7.13 (td, $^3J_{HH}$ = 7.5, 1.2 Hz, H_j), 7.05 (td, $^3J_{HH}$ = 7.8, 1.2 Hz, 1H, H_k), 6.02 (d, $^3J_{HH}$ = 5.7 Hz, 1H, H_x), 5.79 (d, $^3J_{HH}$ = 5.7 Hz, 1H, H_t), 5.59 (d, $^3J_{HH}$ = 5.7 Hz, 1H, H_w), 5.29 (d, $^3J_{HH}$ = 5.7 Hz, 1H, H_u), 4.13 (s, 1H, H_n), 2.60 (s, 3H, Ar-C$\underline{H}_3$), 2.15 (m, 1H, H_p), 1.96 (s, 3H, H_o), 0.82 (d, $^3J_{HH}$ = 6.9 Hz, 3H, H_q), 0.72 (d, $^3J_{HH}$ = 6.9 Hz, 3H, H_r). **^{13}C{^{1}H} NMR (101 MHz, DMSO-*d*$_6$)** δ (ppm): 183.68 (C_h), 158.24 (C_m), 141.63 (C_g), 141.13 (C_i), 134.78, 134.64, 132.71, 128.18 (C_j), 124.72 (C_l), 124.65 (C_c), 122.34 (C_k), 117.22 (C_f), 110.82 (C_d), 101.31, 97.56, 89.74 (C_t), 88.75 (C_x), 82.81 (C_w), 81.13 (C_u), 32.40 (C_n), 30.96 (C_p), 22.67 (C_q), 22.07 (C_r), 21.81 (Ar-$\underline{C}H_3$), 19.01 (C_o). **FT-IR** (ATR) *v* (cm^{-1}) = 1579 (imine, C=N). **Elemental Analysis** for $C_{25}H_{27}ClN_2Ru \cdot CH_2Cl_2$: Found (%) C, 54.13; H, 4.73; N, 4.90; Calcd. (%) C, 54.13; H, 5.07; N, 4.86. **MS** (HR-ESI, *m/z*): 457.1218 (60%, $[M\text{-}Cl]^+$), requires 457.1218.

N- Methyl (trifluoromethane-) Ru benzimidazole complex (58)

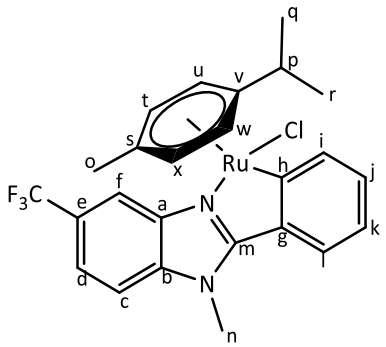

1-Methyl-2-phenyl-5-(trifluoromethyl)-*1H*-benzo[*d*]imidazole **40** (66.9 mg, 0.242 mmol) was dissolved in DCM (3 mL). Sodium acetate (23.8 mg, 0.291 mmol) and dichloro(*p*-cymene)ruthenium(II) dimer (74.2 mg, 0.121 mmol) was then added to the solution. Product: Yellow solid (0.0548 g, 41%); **Mp**: Decomp. 248.5 °C. **^{1}H-NMR (300 MHz, $CDCl_3$)** δ (ppm): 8.36 (dd, $^{3}J_{HH}$ = 7.5, 0.9 Hz, 1H, H_i), 8.18 (s, 1H, H_f), 7.76 (dd, $^{3}J_{HH}$ = 7.8, 0.9 Hz, 1H, H_l), 7.56 (d, $^{3}J_{HH}$ = 8.7 Hz, 1H, H_d), 7.44 (d, $^{3}J_{HH}$ = 8.7 Hz, 1H, H_c), 7.23 (m, 1H, H_j), 7.12 – 7.04 (m, 1H, H_k), 5.85 (d, $^{3}J_{HH}$ = 5.7 Hz, 1H, H_x), 5.77 (d, $^{3}J_{HH}$ = 5.7 Hz, 1H, H_t), 5.34 (d, $^{3}J_{HH}$ = 5.7 Hz, 1H, H_w), 5.16 – 5.10 (d, $^{3}J_{HH}$ = 5.7 Hz, 1H, H_u), 4.04 (s, 1H, H_n), 2.36 (m, 1H, H_p), 2.08 (s, 3H, H_o), 0.98 (d, $^{3}J_{HH}$ = 6.9 Hz, 3H, H_q), 0.83 (d, $^{3}J_{HH}$ = 6.9 Hz, 3H, H_r). **^{13}C{^{1}H} NMR (101 MHz, $CDCl_3$)** δ (ppm): 184.14, 160.43, 140.91, 140.70, 138.29, 133.46, 129.51, 125.79 – 125.46 (d, $^{2}J_{CF}$ = 32.7 Hz, C_e), 124.83, 122.66, 120.03, 114.30, 110.43, 100.91, 100.43, 89.52, 88.88, 81.66, 81.21, 32.31, 30.95, 22.47, 21.97, 18.93. **FT-IR** (ATR) *v* (cm^{-1}) = 1581 (imine, C=N). **Elemental Analysis** for $C_{25}H_{24}ClF_3N_2Ru$ (546.00 $g.mol^{-1}$): Found (%) C, 63.55; H, 5.84; N, 6.34; Calcd. (%) C, 55.00; H, 4.43; N, 5.13. **MS** (HR-ESI, *m/z*): 591.1100 (60%, $[M+2Na-H]^+$), requires 591.1100.

N- Methyl (methylsulfonyl-) Ru benzimidazole complex (59)

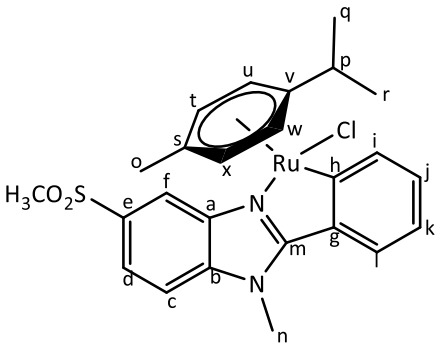

1-Methyl-2-phenyl-*1H*-benzo[*d*]imidazole **41** (70.1 mg, 0.245 mmol) was dissolved in DCM (4 mL). Sodium acetate (24.1 mg, 0.294 mmol) and dichloro(*p*-cymene)ruthenium(II) dimer (75.0 mg, 0.122 mmol) was then added to the solution. Product: Yellow solid (0.0531 g, 39%); **Mp**: Decomp. 258.0 °C. **^{1}H-NMR (400 MHz, $CDCl_3$)** δ (ppm): 8.53 (d, $^4J_{HH}$ = 2.0 Hz, 1H, H_i), 8.37 (dd, $^3J_{HH}$ = 7.6, 0.8 Hz, 1H, H_f), 7.90 – 7.86 (dd, $^3J_{HH}$ = 8.4, 1.6 Hz, 1H, H_j), 7.81 – 7.78 (dd, $^3J_{HH}$ = 8.4, 1.2 Hz, 1H, H_d), 7.52 (d, $^3J_{HH}$ = 8.4 Hz, 1H, H_c), 7.24 (m, 1H, H_k), 7.11 – 7.06 (m, 1H, H_l), 5.89 (dd, $^3J_{HH}$ = 6.0, 0.4 Hz, 1H, H_x), 5.79 (dd, $^3J_{HH}$ = 5.6, 0.8 Hz, 1H, H_t), 5.39 (dd, $^3J_{HH}$ = 6.0, 0.8 Hz, 1H, H_w), 5.15 (dd, $^3J_{HH}$ = 6.0, 1.2 Hz, 1H, H_u), 4.10 (s, 3H, H_n), 3.18 (s, 3H, Ar-$SO_2C\underline{H_3}$) 2.35 (m, 1H, H_p), 2.08 (s, 3H, H_o), 0.98 (d, $^3J_{HH}$ = 6.8 Hz, 3H, H_q), 0.83 (d, $^3J_{HH}$ = 6.8 Hz, 3H, H_r). **^{13}C{^{1}H} NMR (101 MHz, $CDCl_3$)** δ (ppm): 184.81 (C_h), 161.36 (C_m), 141.14 (C_g), 140.82 (C_i), 139.62, 135.60, 133.20, 129.74 (C_j), 129.49, 128.92, 125.03 (C_l), 122.75 (C_c), 121.82 (C_k), 121.56, 117.17 (C_f), 110.75 (C_d), 101.21, 100.57, 89.66 (C_t), 89.05 (C_x), 81.98 (C_w), 81.30 (C_u), 45.06 ($SO_2\underline{C}H_3$), 32.52 (C_n), 31.00 (C_p), 22.46 (C_q), 21.99 (C_r), 18.93 (C_o). **FT-IR** (ATR) *v* (cm^{-1}) = 1580 (imine, C=N). **Elemental Analysis** for $C_{25}H_{27}ClN_2O_2RuS$ (556.08 $g.mol^{-1}$): Found (%) C, 59.72; H, 5.17; N, 6.05; Calcd. (%) C, 54.00; H, 4.89; N, 5.04. **MS** (HR-ESI, *m/z*): 601.0997 (60%, $[M+2Na-H]^+$), requires 601.0242.

N-Methyl Ir benzimidazole complex (60)

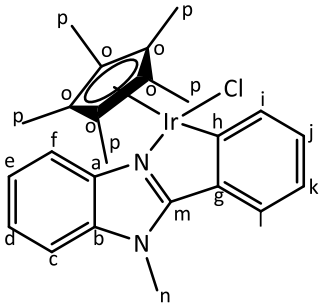

1-Methyl-2-phenyl-*1H*-benzo[*d*]imidazole **35** (62.7 mg, 0.301 mmol) was dissolved in DCM (6 mL). Sodium acetate (29.7 mg, 0.362 mmol) and pentamethylcyclopentadienyliridium(III) chloride dimer (120 mg, 0.151 mmol) was then added to the solution. Product: Yellow solid (0.130 g, 76%); **Mp**: Decomp. 339.2 – 342.9 °C. **^{1}H-NMR (300 MHz, $CDCl_3$)** δ (ppm): 8.01 (d, $^{3}J_{HH}$ = 7.6 Hz, 1H, H_i), 7.80 (d, $^{3}J_{HH}$ = 7.7 Hz 1H, H_f), 7.69 (m, 1H, H_l), 7.41 – 7.28 (m, 3H, H_c, H_d, H_e), 7.20 (t, $^{3}J_{HH}$ = 7.1 Hz, 1H, H_k), 7.05 (t, $^{3}J_{HH}$ = 7.6 Hz, 1H, H_j), 4.14 (s, 3H, H_n), 1.77 (s, 15H, H_p). **^{13}C{^{1}H} NMR (101 MHz, $CDCl_3$)** δ (ppm): 165.48, 139.85, 137.24, 136.50, 134.64, 130.73, 129.18, 124.19, 123.22, 123.08, 122.02, 116.79, 110.00, 88.14 (C_q), 31.88 (C_n), 9.87 (C_r). **FT-IR** (ATR) *v* (cm^{-1}) = 1580 (imine, C=N). **Elemental Analysis** for $C_{24}H_{26}ClIrN_2$ (570.15 $g.mol^{-1}$): Found (%) C, 49.96; H, 4.66; N, 4.54; Calcd. (%) C, 50.56; H, 4.60; N, 4.91. **MS** (HR-ESI, *m/z*): 535.1729 (100%, $[M-Cl]^+$), requires 535.1725.

N- Propyl Ru benzimidazole complex (61)

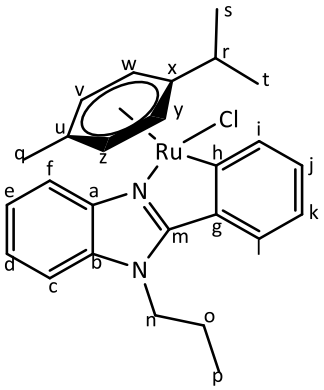

2-Phenyl-1-propyl-*1H*-benzo[*d*]imidazole **44** (77.2 mg, 0.327 mmol) was dissolved in DCM (6 mL). Sodium acetate (32.1 mg, 0.392 mmol) and dichloro(*p*-cymene)ruthenium(II) dimer (100 mg, 0.0.163 mmol) was then added to the solution. Product: Green solid (77.0 mg, 46%). **Mp:** 239.3 – 247.7 °C. **^{1}H-NMR (300 MHz,$CDCl_3$)** δ (ppm): 8.34 (d, $^{3}J_{HH}$ = 7.5 Hz, 1H, H_i), 7.93

(d, $^3J_{HH}$ = 7.8 Hz, 1H, H_f), 7.63 (d, $^3J_{HH}$ = 7.8 Hz, 1H, H_l), 7.45 – 7.29 (m, 3H, H_c, H_d, H_e), 7.20 (td, $^3J_{HH}$ = 7.2, 1.2 Hz, 1H, H_k), 7.12 – 7.03 (td, $^3J_{HH}$ = 7.8, 1.2 Hz, 1H, H_j), 5.86 (d, $^3J_{HH}$ = 5.7 Hz, 1H, H_z), 5.67 (d, $^3J_{HH}$ = 5.4 Hz, 1H, H_v), 5.37 (d, $^3J_{HH}$ = 6.0 Hz, 1H, H_y), 5.14 (d, $^3J_{HH}$ = 5.7 Hz, 1H, H_w), 4.49 (m, 1H, H_n), 4.36 (m, 1H, $H_{n'}$), 2.33 – 2.21 (m, 1H, H_r), 2.10 (s, 3H, H_q), 1.98 (m, 2H, H_o), 1.03 (t, $^3J_{HH}$ = 7.5 Hz, 3H, H_p), 0.90 (d, $^3J_{HH}$ = 6.9 Hz, 3H, H_s), 0.76 (d, $^3J_{HH}$ = 6.9 Hz, 3H, H_t). **$^{13}C\{^1H\}$-NMR (101 MHz, $CDCl_3$)** δ (ppm): 183.78 (C_h), 157.85 (C_m), 141.46 (C_g), 140.66 (C_i), 136.08 (C_x), 133.91 (C_u), 128.77 (C_k), 123.95 (C_l), 123.15 (C_d), 123.00 (C_e), 122.49(C_j), 117.20 (C_f), 109.97 (C_c), 101.52 (C_a), 98.49 (C_b), 89.30 (C_v), 89.10 (C_z), 81.96 (C_w), 81.30 (C_y), 46.22 (C_n), 31.24 (C_r), 23.07 (C_o), 22.59 (C_t), 21.72 (C_s), 18.94 (C_q), 11.24 (C_p). **FT-IR** (ATR) *v* (cm^{-1}) = 1577 (imine, C=N). **Elemental Analysis** for $C_{26}H_{29}ClN_2Ru$ (506.054 $g.mol^{-1}$): Found (%) C, 60.73; H, 5.46; N, 5.78; Calcd. (%) C, 61.70; H, 5.20; N, 5.50. **MS** (HR-ESI, *m/z*): 471.1377 (100%, $[M\text{-}Cl]^+$), requires 471.1374.

N- Propyl (chloro-) Ru benzimidazole complex (62)

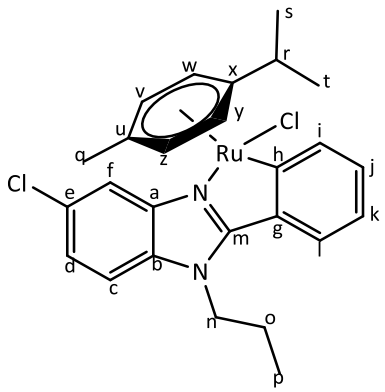

5-Chloro-2-phenyl-1-propyl-*1H*-benzo[*d*]imidazole **45** (93.5 mg, 0.345 mmol) was dissolved in DCM (6 mL). Sodium acetate (33.9 mg, 0.414 mmol) and dichloro(*p*-cymene)ruthenium(II) dimer (106 mg, 0.173 mmol) was then added to the solution. Product: Orange solid (77.5 mg, 42%). **Mp**: Decomp. 197.7 °C. **^{1}H-NMR (300 MHz, DMSO-d_6)** δ (ppm): 8.32 (d, $^3J_{HH}$ = 7.2 Hz, 1H, H_i), 7.88 (d, $^4J_{HH}$ = 1.8 Hz, 1H, H_f), 7.83 (d, $^3J_{HH}$ = 8.7 Hz, 1H, H_l), 7.79 (d, $^3J_{HH}$ = 8.7 Hz, 1H, H_c), 7.42 (d, $^3J_{HH}$ = 8.7, 1.8 Hz, 1H, H_d), 7.11 (m, 2H, H_j, H_k), 6.04 (d, $^3J_{HH}$ = 6.0 Hz, 1H, H_v), 5.76 (d, $^3J_{HH}$ = 6.0 Hz, 1H, H_z), 5.63 (d, $^3J_{HH}$ = 6.0 Hz, 1H, H_y), 5.30 (d, $^3J_{HH}$ = 6.0 Hz, 1H, H_w), 4.62 (t, $^3J_{HH}$ = 6.9 Hz 2H, H_n), 2.19 – 2.04 (m, 1H, H_r), 1.97 (s, 3H, H_q), 1.80 (m, 2H, H_o), 0.87 (t, $^3J_{HH}$ = 7.2 Hz, 3H, H_p), 0.78 (d, $^3J_{HH}$ = 6.9 Hz, 3H, H_s), 0.69 (t, $^3J_{HH}$ = 6.9 Hz, 3H, H_t). **$^{13}C\{^1H\}$ NMR (101 MHz, $CDCl_3$)** δ (ppm): 184.22 (C_h), 159.06 (C_m), 142.34 (C_g), 140.86 (C_i), 134.89 (C_{Ar}), 133.57,

129.25 (C_d), 129.08 (C_{Ar}), 124.33 (C_j), 123.56 (C_l), 122.78 (C_k), 117.01 (C_f), 111.10 (C_c), 102.00 (C_{Ar}), 98.52 (C_{Ar}), 89.70 (C_v), 89.10 (C_z), 82.34 (C_w), 81.34 (C_y), 46.47 (C_n), 31.05 (C_r), 23.12 (C_o), 22.72 (C_t), 21.88 (C_s), 19.12 (C_q), 11.31 (C_p). **FT-IR** (ATR) *v* (cm^{-1}) = 1578 (imine, C=N). **Elemental Analysis** for $C_{26}H_{28}Cl_2N_2Ru$ (540.49 $g.mol^{-1}$): Found (%) C, 57.18; H, 5.32; N, 5.12; Calcd. (%) C, 57.78; H, 5.22; N, 5.18. **MS** (HR-ESI, *m/z*): 541.0596 (50%, $[M+H]^+$), requires 541.0751.

N- Propyl (methyl-) Ru benzimidazole complex (63)

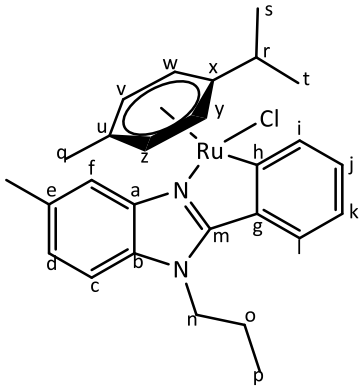

5-Methyl-2-phenyl-1-propyl-*1H*-benzo[*d*]imidazole **46** (102 mg, 0.406 mmol) was dissolved in DCM (6 mL). Sodium acetate (39.0 mg, 0.487 mmol) and dichloro(*p*-cymene)ruthenium(II) dimer (124 mg, 0.202 mmol) was then added to the solution. Product: Green solid (0.101 g, 48%). **Mp**: Decomp. 212.0 – 214.9 °C. **^{1}H-NMR (400 MHz, $CDCl_3$)** δ (ppm): 8.33 (d, $^3J_{HH}$ = 7.6 Hz, 1H, H_i), 7.70 (s, 1H, H_f), 7.62 (d,^{3} J_{HH} = 8.0 Hz, 1H, H_l), 7.24 (d, ^3J = 8.4 Hz, 1H, H_c), 7.22 – 7.13 (m, 2H, $H_{d,}$ H_j), 7.06 (t, $^3J_{HH}$ = 7.6 Hz 1H, H_k), 5.86 (d, $^3J_{HH}$ = 5.6 Hz, 1H, H_v), 5.66 (d, $^3J_{HH}$ = 6.0 Hz, 1H, H_z), 5.39 (d, $^3J_{HH}$ = 6.0 Hz, 1H, H_y), 5.13 (d, $^3J_{HH}$ = 5.6 Hz, 1H, H_w), 4.47 (m, 1H, H_n), 4.32 (m, 1H, $H_{n'}$), 2.59 (s, 3H, C$\underline{H}_3$), 2.26 (m, 1H, H_r), 2.11 (s, 3H, H_q), 1.96 (m, 2H, H_o), 1.02 (t, $^3J_{HH}$ = 7.6 Hz, 3H, H_p), 0.89 (d, $^3J_{HH}$ = 7.2 Hz, 3H, H_s), 0.76 (d, $^3J_{HH}$ = 6.8 Hz, 3H, H_t). **^{13}C{^{1}H} NMR (101 MHz, $CDCl_3$)** δ (ppm): 183.48 (C_h), 157.61 (C_m), 141.71 (C_g), 140.61 (C_i), 134.23 (C_a), 134.02 (C_{Ar}), 132.96 (C_b), 128.64 (C_d), 124.49 (C_j), 123.81 (C_l), 122.47 (C_k), 117.04 (C_f), 109.60 (C_c), 101.70 (C_{Ar}), 98.05 (C_{Ar}), 89.46 (C_z), 88.90 (C_v), 82.15 (C_y), 81.11 (C_w), 46.23 (C_n), 30.88 (C_r), 29.70 (C_o), 22.58 (C_s), 21.90 ($\underline{C}H_3$), 21.77 (C_t), 18.98 (C_q), 11.26 C_p). **Elemental Analysis** for $C_{27}H_{31}ClN_2Ru$ (520.08 $g.mol^{-1}$): Found (%) C, 62.01; H, 6.04; N, 5.37; Calcd. (%) C, 62.36; H, 6.01; N, 5.39. **MS** (HR-ESI, *m/z*): 485.1545 (70%, $[M-Cl]^+$), requires 485.1530.

N- Propyl (trifluoromethane-) Ru benzimidazole complex (64)

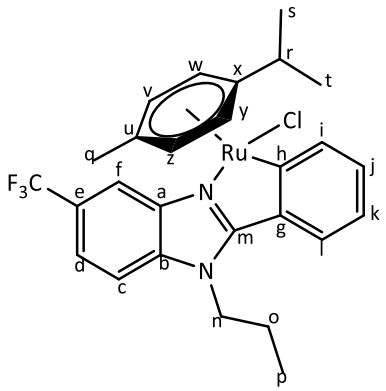

2-Phenyl-1-propyl-5-(trifluoromethyl)-*1H*-benzo[*d*]imidazole **50** (95.0 mg, 0.312 mmol) was dissolved in DCM (6 mL). Sodium acetate (38.1 mg, 0.464 mmol) and dichloro(*p*-cymene)ruthenium(II) dimer (95.6 mg, 0.156 mmol) was then added to the solution. Product: Green solid (71.2 mg, 40%). **Mp**: Decomp. 214.4 – 218.7 °C. **^{1}H-NMR (400 MHz, $CDCl_3$)** δ (ppm): 8.36 (m, 1H, H_i), 8.19 (s, 1H, H_f), 7.63 (m, 1H, H_l), 7.55 (dd, $^3J_{HH}$ = 8.8, 1.2 Hz, 1H, H_d), 7.44 (d, $^3J_{HH}$ = 8.4 Hz, 1H, H_c), 7.23 (td, $^3J_{HH}$ = 7.6, 1.2 Hz 1H, H_j), 7.09 (td, $^3J_{HH}$ = 7.2, 1.2 Hz, 1H, H_k), 5.86 (dd, $^3J_{HH}$ = 6.0, 0.8 Hz, 1H, H_v), 5.73 (dd, $^3J_{HH}$ = 6.0, 1.2 Hz, 1H, H_z), 5.33 (dd, $^3J_{HH}$ = 6.0, 1.2 Hz, 1H, H_y), 5.12 (dd, $^3J_{HH}$ = 6.0, 1.2 Hz, 1H, H_w), 4.50 – 4.26 (m, 2H, H_n, $H_{n'}$), 2.31 (m, 1H, H_r), 2.10 (s, 3H, H_q), 1.96 (m, 2H, H_o), 1.01 (t, $^3J_{HH}$ = 7.6 Hz, 3H, H_p), 0.95 (d, $^3J_{HH}$ = 7.2 Hz, 3H, H_s), 0.79 (d, $^3J_{HH}$ = 7.2 Hz, 3H, H_t). **^{13}C{^{1}H} NMR (101 MHz, $CDCl_3$)** δ (ppm): 184.85 (C_{Ar}), 160.04 (C_{Ar}), 141.12 (C_{Ar}), 140.96 (C_i), 138.27 (C_a), 133.37 (C_b), 129.52 (C_j), 126.18, 125.95, 125.64, 124.59 (C_l), 122.87 (C_k), 120.13 (C_d), 114.62 (C_f), 110.75 (C_c), 101.45 (C_u), 100.12 (C_x), 89.65 (C_z), 89.35 (C_v), 82.03 (C_y), 81.40 (C_w), 46.65 (C_n), 31.10 (C_r), 23.14 (C_o), 22.61 (C_s), 21.94 (C_t), 19.06 (C_q), 11.30 C_p). **FT-IR** (ATR) *v* (cm^{-1}) = 1580 (imine, C=N). **Elemental Analysis** for $C_{27}H_{28}ClF_3N_2Ru$ (574.05 $g.mol^{-1}$): Found (%) C, 56.32; H, 5.15; N, 4.94; Calcd. (%) C, 56.49; H, 4.92; N, 4.88. **MS** (HR-ESI, *m/z*): 539.1236 (100%, $[M\text{-}Cl]^+$), requires 539.1248.

N- Propyl Ir benzimidazole complex (65)

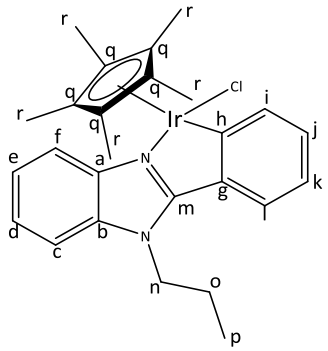

2-Phenyl-1-propyl-*1H*-benzo[*d*]imidazole **44** (59.3 mg, 0.251 mmol) was dissolved in DCM (6 mL). Sodium acetate (24.7 mg, 0.301 mmol) and pentamethylcyclopentadienyliridium(III) chloride dimer (100 mg, 0.126 mmol) was then added to the solution. Product: Yellow solid (76.0 mg, 51%). **Mp**: 312.2 – 315.9 °C. **^{1}H-NMR (300 MHz, $CDCl_3$)** δ (ppm): 8.00 (dd, $^{3}J_{HH}$ = 7.5, 0.9 Hz, 1H, H_i), 7.71 – 7.62 (m, 2H, H_f, H_l), 7.40 – 7.27 (m, 3H, H_c, H_d, H_e), 7.19 (td, $^{3}J_{HH}$ = 7.5, 1.2 Hz, 1H, H_k), 7.06 (td, $^{3}J_{HH}$ = 7.5, 1.2 Hz, 1H, H_j), 4.60 – 4.35 (m, 2H, H_n, $H_{n'}$), 2.14 – 1.95 (m, 2H, H_o), 1.76 (s, 15H, H_r), 1.09 (t, $^{3}J_{HH}$ = 7.5 Hz, 3H, H_p). **^{13}C{^{1}H}-NMR (101 MHz, $CDCl_3$)** δ (ppm): 165.80 (C_h), 161.91 (C_m), 139.78 (C_g), 137.36 (C_i), 136.25(C_a), 134.26 C_b), 130.63 (C_k), 123.76 (C_f), 123.17 (C_e), 123.04 (C_d), 122.04 (C_j), 116.89 (C_l), 110.19 (C_c), 46.36 (C_n), 23.37 (C_o), 11.47 (C_p), 9.84 (C_r). **FT-IR** (ATR) *v* (cm^{-1}) = 1578 (imine, C=N). **Elemental Analysis** for $C_{26}H_{30}ClIrN_2$ (598.212 $g.mol^{-1}$): Found (%) C, 51.73; H, 4.51; N, 4.21; Calcd. (%) C, 52.20; H, 5.05; N, 4.73. **MS** (HR-ESI, *m/z*): 563.2047 (100%, $[M-Cl]^+$), requires 563.2038.

N- Propyl (chloro-) Ir benzimidazole complex (66)

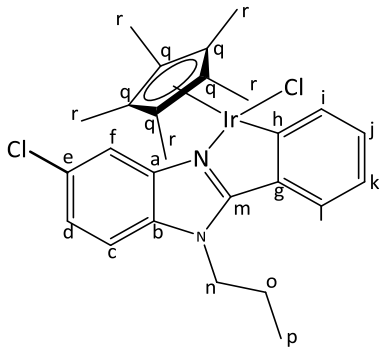

5-Chloro-2-phenyl-1-propyl-*1H*-benzo[*d*]imidazole **45** (93.7 mg, 0.346 mmol) was dissolved in DCM (6 mL). Sodium acetate (36.5 mg, 0.445 mmol) and pentamethylcyclopentadienyliridium(III) chloride dimer (138 mg, 0.173 mmol) was then

added to the solution. Product: Yellow solid (0.198 g, 90%). **Mp**: 304.2 – 305.3 °C. **^{1}H-NMR (600 MHz, $CDCl_3$)** δ (ppm): 8.00 (dd, $^{3}J_{HH}$ = 7.8, 1.2 Hz, 1H, H_i), 7.67 – 7.65 (m, 1H, H_f), 7.63 (dd, $^{3}J_{HH}$ = 7.8, 0.6 Hz, 1H, H_l), 7.28 – 7.25 (m, 1H, H_c), 7.24 (m, 1H, H_d), 7.20 (td, $^{3}J_{HH}$ = 7.8, 1.2 Hz, 1H, H_j), 7.10 – 7.03 (td, $^{3}J_{HH}$ = 7.8, 1.2 Hz, 1H, H_k), 4.48 – 4.40 (m, 1H, H_n), 4.36 (m, 1H, $H_{n'}$), 2.06 – 1.97 (m, 2H, H_o), 1.76 (s, 15H, H_r), 1.06 (t, $^{3}J_{HH}$ = 7.8 Hz, 3H, H_p). **^{13}C{^{1}H} NMR (151 MHz, $CDCl_3$)** δ (ppm): 166.28 (C_h), 163.08 (C_m), 140.53 (C_g), 137.39 (C_i), 134.92 (C_a), 133.71 C_b), 131.01 (C_j), 129.08 (C_e), 124.01 (C_l), 123.41 (C_d), 122.21 (C_k), 116.70 (C_f), 111.16 (C_c), 88.30 (C_q), 46.53 (C_n), 23.30 (C_o), 11.42 (C_p), 9.84 (C_r). **FT-IR** (ATR) *v* (cm^{-1}) = 1579 (imine, C=N). **Elemental Analysis** for $C_{27}H_{32}Cl_2IrN_2 \cdot H_2O$: Found (%) C, 48.21; H, 4.58; N, 4.41; Calcd. (%) C, 48.71; H, 5.15; N, 4.21. **MS** (HR-ESI, *m/z*): 670.1050 (10%, $[M\text{-}Na]^+$), requires 670.1470.

N- Propyl (methyl-) Ir benzimidazole complex (67)

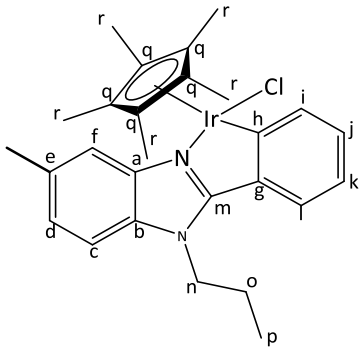

5-Methyl-2-phenyl-1-propyl-*1H*-benzo[*d*]imidazole **46** (62.8 mg, 0.251 mmol) was dissolved in DCM (6 mL). Sodium acetate (26.8 mg, 0.327 mmol) and pentamethylcyclopentadienyliridium(III) chloride dimer (100 mg, 0.126 mmol) was then added to the solution. Product: Yellow solid (0.126 g, 80%). **Mp**: 280.1 – 281.5 °C. **^{1}H-NMR (600 MHz, $CDCl_3$)** δ (ppm): 7.99 (dd, $^{3}J_{HH}$ = 7.8, 1.2 Hz, 1H, H_i), 7.64 (d, $^{3}J_{HH}$ = 7.8 Hz, 1H, H_l), 7.48 (s, 1H, H_f), 7.24 (d, $^{3}J_{HH}$ = 8.4 Hz, 1H, H_c), 7.17 (td, $^{3}J_{HH}$ = 7.2, 0.6 Hz, 1H, H_j), 7.14 – 7.10 (dd, , $^{3}J_{HH}$ = 7.8, 1.2 Hz, 1H, H_d), 7.08 – 7.01 (td, $^{3}J_{HH}$ = 7.8, 1.2 Hz, 1H, H_k), 4.50 (m, 1H, H_n), 4.40 (m, 1H, $H_{n'}$), 2.53 (s, 3H, Ar-C$\underline{H}_3$), 2.04 (m, 2H, H_o), 1.76 (s, 15H, H_r), 1.07 (t, $^{3}J_{HH}$ = 7.8 Hz, 3H, H_p). **^{13}C{^{1}H} NMR (151 MHz, $CDCl_3$)** δ (ppm): 165.50 (C_h), 161.65 (C_m), 140.01 (C_g), 137.29 (C_i), 134.37 (C_a), 132.96 C_b), 130.48 (C_j), 124.43 (C_d), 123.61 (C_l), 122.02 (C_k), 116.84 (C_f), 109.82 (C_c), 88.07 (C_q), 46.36 (C_n), 23.38 (C_o), 21.77 (Ar-$\underline{C}H_3$), 11.47 (C_p), 9.85 (C_r). **FT-IR** (ATR) *v* (cm^{-1}) = 1580 (imine, C=N). **Elemental Analysis** for $C_{28}H_{35}ClIrN_2$ (627.27 $g.mol^{-1}$): Found (%)

C, 53.29; H, 5.31; N, 4.68; Calcd. (%) C, 53.61; H, 5.62; N, 4.47. **MS** (HR-ESI, *m/z*): 577.2216 (100%, $[M\text{-}Cl\text{-}CH_3]^+$), requires 577.2195.

N- Propyl (trifluoromethane-) Ir benzimidazole complex (68)

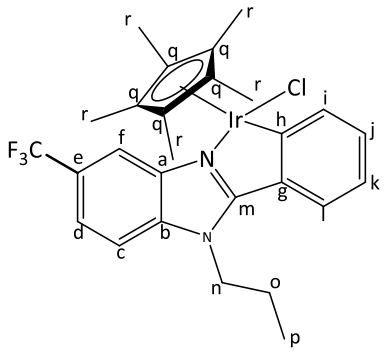

2-Phenyl-1-propyl-5-(trifluoromethyl)-*1H*-benzo[*d*]imidazole **50** (76.5 mg, 0.251 mmol) was dissolved in DCM (6 mL). Sodium acetate (25.3 mg, 0.308 mmol) and pentamethylcyclopentadienyliridium(III) chloride dimer (100 mg, 0.126 mmol) was then added to the solution. Product: Yellow solid (0.112 g, 67%). **Mp**: 309.4 – 310.2 °C. **^{1}H-NMR (300 MHz, $CDCl_3$)** δ (ppm): 8.03 (dd, $^3J_{HH}$ = 7.8, 0.9 Hz, 1H, H_i), 7.99 (s, 1H, H_f), 7.65 (dd, $^3J_{HH}$ = 8.1, 1.2 Hz, 1H, H_l), 7.50 (dd, $^3J_{HH}$ = 8.7, 1.2 Hz, 1H, H_d), 7.43 (d, $^3J_{HH}$ = 8.7 Hz, 1H, H_c), 7.23 (td, $^3J_{HH}$ = 7.5, 1.2 Hz, 1H, H_k), 7.13 – 7.05 (td, $^3J_{HH}$ = 7.8, 1.2 Hz, 1H, H_j), 4.40 (m, 2H, H_n), 2.14 – 1.91 (m, 2H, H_o), 1.77 (s, 15H, H_r), 1.06 (t, $^3J_{HH}$ = 7.5 Hz, 3H, H_p). **^{13}C{^{1}H} NMR (101 MHz, $CDCl_3$)** δ (ppm): 166.63 (C_g), 164.07 (C_m), 139.36 (C_b), 138.24 (C_a), 137.37(C_i), 133.51 C_h), 131.27 (C_k), 126.13 (C_{Ar}), 125.81 (C_{Ar}), 125.49 (C_e), 124.33 (C_l), 122.30 (C_j), 119.98 (C_d), 114.44 (C_f), 110.87 (C_c), 88.45 (C_q), 46.59 (C_n), 23.28 (C_o), 11.37 (C_p), 9.79 (C_r). **FT-IR** (ATR) *v* (cm^{-1}) = 1586 (imine, C=N). **Elemental Analysis** for $C_{28}H_{32}Cl_2F_3IrN_2$ (681.24 $g.mol^{-1}$): Found (%) C, 49.05; H, 4.48; N, 4.26; Calcd. (%) C, 49.37; H, 4.73; N, 4.11. **MS** (HR-ESI, *m/z*): 707.2049 (45%, $[M\text{-}Cl\text{+}IsoProp\text{+}H]^+$), requires 707.2800.

5.4. Single-crystal X-ray crystallography

Suitable single crystals of iridium complexes **67** and **68** were grown from a mixture of chloroform and EtOAc which were allowed to evaporate over 3 – 5 days. Single-crystal X-ray data were collected on a Bruker KAPPA APEX II DUO diffractometer using graphite-monochromated Mo-Kα radiation (χ = 0.71073 Å). Data collection was carried out at 173(2)

K. Temperature was controlled by an Oxford Cryostream cooling system (Oxford Cryostat). Cell refinement and data reduction were performed using the program SAINT.[9] The data were scaled and absorption correction performed using SADABS.[10] The structure was solved by direct methods using SHELXS-97 and refined by full-matrix least-squares methods based on F using SHELXL-2014 and using the graphics interface program X-Seed.[10, 11] The programs X-Seed and POV-Ray were both used to prepare molecular graphic images.

5.5. Pharmacological activity and solubility testing protocols

5.5.1. *In vitro* antiplasmodial activity

The test samples were tested in triplicate on one or two separate occasions against chloroquine-sensitive (NF54) strain of *P. falciparum*. Continuous *in vitro* cultures of asexual erythrocyte stages of *P. falciparum* were maintained using a modified method of Trager and Jensen.[12] Quantitative assessment of antiplasmodial activity *in vitro* was determined *via* the parasite lactate dehydrogenase assay using a modified method described by Makler.[13] The test samples were prepared to a 20 mg/mL stock solution in 100% DMSO. Samples were tested as a suspension if not completely dissolved. Stock solutions were stored at -20 °C. Further dilutions were prepared on the day of the experiment. Chloroquine (CQ) was used as the reference drug in all experiments. A full dose-response was performed for all compounds to determine the concentration inhibiting 50% of parasite growth (IC_{50} value). Test samples were tested at a starting concentration of 100 µg/mL, which was then serially diluted 2-fold in complete medium to give 10 concentrations; with the lowest concentration being 0.2 µg/mL. The same dilution technique was used for all samples. The IC_{50} values were obtained using a non-linear dose response curve fitting analysis via Graph Pad Prism v.4.0 software.

5.5.2. Cytotoxicity

Compounds were tested for *in vitro* cytotoxicity against the mammalian cell-line, Chinese Hamster Ovarian (CHO), using the 3-(4,5-dimethylthiazol-2-yl)-2,5-diphenyltetrazoliumbromide (MTT) assay. The MTT assay is used as a colorimetric assay for cellular growth and survival, and compares well with other available assays.[14, 15] The test samples were tested in triplicate on one occasion. The test samples were prepared to a 2 mg/mL stock solution in 10% MeOH or 10% DMSO and were tested as a suspension if not

completely dissolved. Test compounds were stored at -20 °C until use. Emetine was used as the reference drug in all experiments. The initial concentration of emetine was 100 µg/mL, which was serially diluted in complete medium with 10-fold dilutions to give 6 concentrations, the lowest being 0.001 µg/mL. The same dilution technique was applied to all the test samples. The highest concentration of solvent to which the cells were exposed had no measurable effect on cell viability. IC_{50} values were obtained from full dose-response curves using a non-linear dose-response curve fitting analysis via GraphPad Prism V.4 software.

5.5.3. Beta-hematin inhibition assay

The β-haematin formation assay was modified from the method described by Sandlin *et al*.[16] The stock solutions of the compounds tested were prepared at 10 mM in DMSO. The compounds were delivered to a 96-well plate in triplicate and were tested at a starting concentration of 500 µM, where the lowest drug concentration was 5 µM. The stock solution was serially diluted to give 12 concentrations in the 96-well flat-bottom assay plate. NP-40 detergent was then added to mediate the formation of β-haematin (30.55 µM, final concentration). A 25 mM stock solution of haematin was prepared by dissolving hemin (16.3 mg) in dimethyl sulfoxide (1 mL). A 177.76 µL aliquot of haematin stock was suspended in 20 mL of a 2 M acetate buffer, pH 4.7. The haematin suspension was then added to the plate to give a final haematin concentration of 100 µM. The plate was then incubated for 16 h at 37 °C. The compounds were analysed using the pyridineferrochrome method developed by Ncokazi and Egan.[17] 32 µL of a solution of 50% pyridine, 20% acetone, 20% water, and 10% 2 M HEPES buffer (pH 7.4) was added to each well. To this, 60 µL acetone was then added to each well and mixed. The UV-Vis absorbance of the resulting complex was measured at 405 nm on a SpectraMax 340PC plate reader. The IC_{50} values were obtained using a non-linear dose-response curve fitting analysis *via* Graph Pad Prism v.5.0 software.[18]

5.5.4. Kinetic solubility assay

The kinetic solubility assay was performed using a miniaturised shake flask method.[19] 10 mM stock solutions of each of the test compounds were used to prepare calibration standards (10 – 220 µM) in DMSO, and to spike (1:50) duplicate aqueous samples of phosphate buffered saline (pH 6.5), 0.01 M HCl (pH 2) and FaSSIF (simulating fasting state biorelevant media, pH 6.5), with a final DMSO concentration of 2%. After shaking for 2 hours at 25 ˚C, the solutions

were filtered and analysed by means of HPLC-DAD (Agilent 1200 Rapid Resolution HPLC with a diode array detector). Best fit calibration curves were constructed using the calibration standards, which were used to determine the aqueous samples' solubility.

References

1. P. P. Seth, D. E. Robinson, E. A. Jefferson and E. E. Swayze, *Tetrahedron Lett.*, 2002, **43**, 7303-7306.
2. P. Nicholaus, *United States Pat.,* US 8877758 B2, 2014.
3. P. Zhang, E. A. Terefenko, J. Bray, D. Deecher, A. Fensome, J. Harrison, C. Kim, E. Koury, L. Mark, C. C. McComas, C. A. Mugford, E. J. Trybulski, A. T. Vu, G. T. Whiteside and P. E. Mahaney, *J. Med. Chem.*, 2009, **52**, 5703-5711.
4. K. Amirbekyan, N. Duchemin, E. Benedetti, R. Joseph, A. Colon, S. A. Markarian, L. Bethge, S. Vonhoff, S. Klussmann, J. Cossy, J.-J. Vasseur, S. Arseniyadis and M. Smietana, *ACS Catal.*, 2016, **6**, 3096-3105.
5. G. Lelais, R. Epple, T. H. Marsilje, Y. O. Long, M. McNeill, B. Chen, W. Lu, J. Anumolu, S. Badiger, B. Bursulaya, M. DiDonato, R. Fong, J. Juarez, J. Li, M. Manuia, D. E. Mason, P. Gordon, T. Groessl, K. Johnson, Y. Jia, S. Kasibhatla, C. Li, J. Isbell, G. Spraggon, S. Bender and P.-Y. Michellys, *J. Med. Chem.*, 2016, **59**, 6671-6689.
6. D. C. McCutcheon, W. B. Porterfield and J. A. Prescher, *Org. Biomol. Chem.*, 2015, **13**, 2117-2121.
7. G. S. Yellol, A. Donaire, J. G. Yellol, V. Vasylyeva, C. Janiak and J. Ruiz, *Chem. Commun.*, 2013, **49**, 11533-11535.
8. R. Bersot and P. Humphries, *United states Pat.,* US 9265772 B2, 2013.
9. A. Bruker and A. X. S. Saint, *Acta Crystallogr., Sect.A: Fundam.Crystallogr*, 2008, **64**, 112-122.
10. G. M. Sheldrick, *SHELXL-97, program for X-ray crystal structure refinement*, 1997.
11. J. L. Atwood, L. J. Barbour, M. W. Heaven and C. L. Raston, *Angew. Chem. Int. Ed. Engl.*, 2003, **42**, 3254-3257.
12. W. Trager and J. B. Jensen, *Science*, 1976, **193**, 673-675.
13. M. T. Makler, J. M. Ries and J. A. Williams, *Am. Soc. Trop. Med. Hyg.*, 1993, **48**, 739-741.

14. T. Mosmann, *J. Immunol. Methods*, 1983, **65**, 55-63.
15. L. V. Rubinstein, R. H. Shoemaker, K. D. Paull, R. M. Simon, S. Tosini, P. Skehan, D. A. Scudiero, A. Monks and M. R. Boyd, *J. Natl. Cancer I.*, 1990, **82**, 1113-1118.
16. R. D. Sandlin, M. D. Carter, P. J. Lee, J. M. Auschwitz, S. E. Leed, J. D. Johnson and D. W. Wright, *Antimicrob. Agents Chemother.*, 2011, **55**, 3363-3369.
17. K. K. Ncokazi and T. J. Egan, *Anal. Biochem.*, 2005, **338**, 306-319.
18. T. Stringer, R. Seldon, N. Liu, D. F. Warner, C. Tam, L. W. Cheng, K. M. Land, P. J. Smith, K. Chibale and G. S. Smith, *Dalton Trans.*, 2017, **46**, 9875-9885.
19. P. A. Hill and R. J. Young, *Drug Discov. Today*, 2010, 648.